

DISSERTATION

Titel der Dissertation

Quantum violation of macroscopic realism
and the transition to classical physics

Verfasser

Johannes Kofler

angestrebter akademischer Grad

Doktor der Naturwissenschaften

Wien, im Juni 2008

Studienkennzahl laut Studienblatt: A 091 411

Dissertationsgebiet laut Studienblatt: Physik

Betreuer: ao. Univ.-Prof. Časlav Brukner

Ich weiß ehrlich nicht, was die Leute meinen, wenn sie von der Freiheit des menschlichen Willens sprechen. Ich habe zum Beispiel das Gefühl, daß ich irgend etwas will; aber was das mit Freiheit zu tun hat, kann ich überhaupt nicht verstehen. Ich spüre, daß ich meine Pfeife anzünden will und tue das auch; aber wie kann ich das mit der Idee der Freiheit verbinden? Was liegt hinter dem Willensakt, daß ich meine Pfeife anzünden will? Ein anderer Willensakt? Schopenhauer hat einmal gesagt: "Der Mensch kann tun was er will; er kann aber nicht wollen was er will."

[Honestly I cannot understand what people mean when they talk about the freedom of the human will. I have a feeling, for instance, that I will something or other; but what relation this has with freedom I cannot understand at all. I feel that I will to light my pipe and I do it; but how can I connect that up with the idea of freedom? What is behind the act of willing to light the pipe? Another act of willing? Schopenhauer once said: "Man can do what he wills but he cannot will what he wills."]

Albert Einstein

Contents

Abstract	7
Zusammenfassung	9
Acknowledgement	11
List of publications	13
0 Introduction	17
1 Classical world emerging from quantum physics	21
1.1 The Leggett-Garg inequality	23
1.2 Violation of the Leggett-Garg inequality for arbitrarily large spins	24
1.3 The quantum-to-classical transition for a spin-coherent state	26
1.4 The quantum-to-classical transition for an arbitrary spin state	30
1.5 An alternative derivation	33
2 General conditions for quantum violation of macroscopic realism	37
2.1 Violation of the Leggett-Garg inequality for arbitrary Hamiltonians	39
2.2 Macrorealism per se	40
2.3 Non-invasive measurability	43
2.4 The sufficient condition for macrorealism	45
2.5 An oscillating Schrödinger cat	46
2.6 Continuous monitoring by an environment	48
2.7 Non-classical Hamiltonians are complex	52
2.8 Information and randomness	54
3 Entanglement between macroscopic observables	57
3.1 The linear harmonic chain	59
3.1.1 Defining collective operators	61
3.1.2 Quantifying entanglement between collective operators	63
3.1.3 Collective operators for scalar quantum fields	68
3.2 Spin ensembles	69

3.2.1	Bipartite entanglement	70
3.2.2	Multi-partite entanglement	77
4	Mathematical undecidability and quantum randomness	81
4.1	Logical complementarity and mathematical undecidability	83
4.2	Physical implementation and quantum randomness	84
4.3	Generalization to many qubits	89
	Conclusions and outlook	95
	Bibliography	97
	Curriculum vitae	103

Abstract

The descriptions of the quantum realm and the macroscopic classical world differ significantly not only in their mathematical formulations but also in their foundational concepts and philosophical consequences. The assumptions of a genuine classical world—local realism and macroscopic realism (macrorealism)—are at variance with quantum mechanical predictions as characterized by the violation of the Bell and the Leggett-Garg inequality, respectively. When and how physical systems stop to behave quantumly and begin to behave classically is still heavily debated in the physics community and subject to theoretical and experimental research.

The first chapter of this dissertation puts forward a novel approach to the quantum-to-classical transition fully within quantum theory and conceptually different from already existing models. It neither needs to refer to the uncontrollable environment of a system (decoherence) nor to change the quantum laws itself (collapse models), but puts the stress on the limits of observability of quantum phenomena due to imprecisions of our measurement apparatuses. Naively, one would say that the predictions of quantum mechanics reduce to those of classical physics merely by going to large quantum numbers. Using a quantum spin as a model object, we first demonstrate that for unrestricted measurement accuracy the system’s time evolution cannot be described classically and is conflict with macrorealism through violation of the Leggett-Garg inequality, no matter how large the spin is. How then does the classical world arise? Under realistic conditions in every-day life, we are only able to perform coarse-grained measurements and do not resolve individual quantum levels of the macroscopic system. We show that for some “classical” Hamiltonians it is this mere restriction to fuzzy measurements which is sufficient to see the natural emergence of macrorealism and the classical Newtonian laws out of the full quantum formalism. This resolves the apparent impossibility of how classical realism and deterministic laws can emerge out of fundamentally random quantum events.

In the second chapter, we find that the restriction of coarse-grained measurements usually allows to describe the time evolution of any quantum spin state by a time evolution of a statistical mixture. However, we demonstrate that there exist “non-classical” Hamiltonians for which the time evolution of this mixture cannot be understood classically, leading to a violation of macrorealism. We derive the necessary condition for these non-classical time evolutions and illustrate it with the example of an oscillating Schrödinger cat-like state. Constant interaction of the system with an environment establishes macrorealism but cannot account for a continuous spatiotemporal description of the system’s non-classical time evolution in terms of classical laws of motion. We argue that non-classical Hamiltonians are unlikely to appear in nature because they require interactions between a large number of particles or are of high computational complexity.

The third chapter investigates entanglement between collective operators in two specific physical systems, namely in a linear chain of harmonic oscillators and in ensembles of spin- $\frac{1}{2}$ particles. We show that under certain conditions entanglement between macroscopic observables can persist for

large system sizes. However, since this analysis uses sharp measurements, it is not in disagreement with our quantum-to-classical approach.

The last chapter addresses the question of the origin of quantum randomness and proposes a link with mathematical undecidability. We demonstrate that the states of elementary quantum systems are capable of encoding a set of mathematical axioms. Quantum measurements reveal whether a given proposition is decidable or undecidable within this set. We theoretically find and experimentally confirm that whenever a mathematical proposition is undecidable within the axiomatic set encoded in the state, the measurement associated to the proposition has random outcomes. This supports the view that quantum randomness is irreducible and a manifestation of mathematical undecidability.

Zusammenfassung

Die Beschreibungen der quantenmechanischen und der klassischen Welt unterscheiden sich nicht nur signifikant in ihren mathematischen Formulierungen sondern auch in ihren grundsätzlichen Konzepten und philosophischen Implikationen. Die Annahmen einer klassischen Welt – lokaler und makroskopischer Realismus (Makrorealismus) – widersprechen den Vorhersagen der Quantenphysik, was durch die Verletzung der Bell- und der Leggett-Garg-Ungleichung charakterisiert wird. Die Frage, wann und wie physikalische Systeme aufhören sich quantenmechanisch und anfangen sich klassisch zu verhalten, wird in der wissenschaftlichen Gemeinschaft noch immer heftig diskutiert und ist Gegenstand experimenteller und theoretischer Forschung.

Das erste Kapitel der vorliegenden Dissertation entwickelt einen neuen Zugang zum Übergang der Quanten- zur klassischen Physik, und zwar vollkommen innerhalb der Quantentheorie und konzeptionell verschieden von bereits bestehenden Modellen. Dieser Zugang muss sich weder auf die unkontrollierbare Umgebung von Systemen beziehen (Dekohärenz) noch die Gesetze der Quantenmechanik selbst abändern (Kollaps-Modelle). Er fokussiert sich vielmehr auf die Limitierung der Beobachtbarkeit von Quantenphänomen aufgrund der Ungenauigkeit unserer Messapparate. Naiverweise würde man annehmen, dass sich die Vorhersagen der Quantenmechanik auf jene der klassischen Physik allein dadurch reduzieren, indem man zu großen Quantenzahlen geht. Wir verwenden einen Quantenspin als Modellobjekt und zeigen zunächst, dass bei uneingeschränkter Messgenauigkeit die Zeitevolution des Systems nicht klassisch verstanden werden kann und aufgrund der Verletzung der Leggett-Garg-Ungleichung im Widerspruch zu Makrorealismus steht, selbst wenn der Spin beliebig groß ist. Wie entsteht dann die klassische Welt? Unter realistischen alltäglichen Bedingungen sind wir nur in der Lage, grobkörnige Messungen durchzuführen, die die einzelnen Quantenniveaus des makroskopischen Systems nicht auflösen können. Wir zeigen, dass für bestimmte “klassische” Hamilton-Operatoren diese bloße Einschränkung zu unscharfen Messungen ausreicht, um die natürliche Emergenz von Makrorealismus und klassischer Newtonscher Gesetze aus dem vollen quantenmechanischen Formalismus zu sehen. Dies löst die scheinbare Unmöglichkeit auf, wie klassischer Realismus und deterministische Gesetze aus fundamental zufälligen Quantenergebnissen entstehen können.

Im zweiten Kapitel zeigen wir, dass die Einschränkung grobkörniger Messungen es üblicherweise erlaubt, die zeitliche Evolution jedes beliebigen quantenmechanischen Spinzustands durch die zeitliche Evolution einer statistischen Mischung zu beschreiben. Ungeachtet dessen demonstrieren wir, dass es “nicht-klassische” Hamilton-Operatoren gibt, für die die Zeitentwicklung dieser Mischung nicht klassisch verstanden werden kann. Wir leiten die allgemeine Bedingung für solche nicht-klassischen Zeitentwicklungen her und veranschaulichen sie anhand des Beispiels einer oszillierenden Schrödinger-Katze. Andauernde Interaktion des Systems mit einer Umgebung etabliert Makrorealismus, kann aber keine kontinuierliche raumzeitliche Beschreibung der nicht-klassischen Zeitevolution des Systems durch klassische Bewegungsgleichungen liefern. Wir argumen-

tieren, dass nicht-klassische Hamilton-Operatoren in der Natur wahrscheinlich nicht vorkommen, weil sie Vielteilchen-Wechselwirkungen benötigen oder von hoher Komplexität sind.

Das dritte Kapitel untersucht Verschränkung zwischen kollektiven Operatoren in zwei spezifischen physikalischen Systemen, nämlich in einer linearen Kette von harmonischen Oszillatoren und in Ensembles von Spin- $\frac{1}{2}$ -Teilchen. Wir zeigen, dass Verschränkung zwischen makroskopischen Observablen für große Systeme bestehen bleiben kann. Zumal diese Analyse scharfe Messungen verwendet, steht sie nicht im Widerspruch zu unserem Zugang zum Übergang von der Quanten- zur klassischen Physik.

Das letzte Kapitel beschäftigt sich mit der Frage nach dem Ursprung von quantenmechanischem Zufall und schlägt eine Verbindung mit mathematischer Unentscheidbarkeit vor. Wir demonstrieren, dass Zustände elementarer Quantensysteme einen Satz von mathematischen Axiomen kodieren können. Quantenmechanische Messungen bringen zum Vorschein, ob eine gegebene Proposition innerhalb dieses Satzes entscheidbar oder unentscheidbar ist. Wir finden theoretisch und bestätigen experimentell, dass Messungen, die mit innerhalb des vom Quantenzustand kodierten Axiomensatzes unentscheidbaren mathematischen Propositionen assoziiert sind, zu zufälligen Resultaten führen. Dies unterstützt die Sichtweise, dass quantenmechanischer Zufall irreduzibel und eine Manifestation von mathematischer Unentscheidbarkeit ist.

Acknowledgement

When I was writing my diploma thesis at the University of Linz in summer 2004, I applied for a PhD position in Vienna because of a strong interest in quantum physics and foundational questions. In retrospect, this was likely one of the best decisions that I could have made—both from a professional and a private perspective.

A few days after my arrival in Vienna in January 2005, I was the first person to move into the building of the Institute for Quantum Optics and Quantum Information of the Austrian Academy of Sciences. I did not yet know how great the pleasure would be to learn and work in this extremely inspiring and challenging environment during the following years. Now is the time to thank:

First and foremost Časlav Brukner for his perfect scientific and personal support. I am sincerely grateful for all the time and effort he has put into our joint research, and without exaggeration, I could not have wished for a better supervision. His vast knowledge and insight into quantum theory as well as the true joy and interest with which he is doing science have been an enduring inspiration through my whole doctoral studies.

Nikita Arnold and Urbaan M. Titulaer for their objective advice on my interest to go to Vienna after my graduate studies.

Anton Zeilinger for advocating my application for a theoretical PhD position, for his open-minded way of leading the institute, and for integrating me into experimental activities.

Markus Aspelmeyer, Tomasz Paterek, and Rupert Ursin for many fascinating discussions, not only on quantum mechanics.

Simon Gröblacher and Robert Prevedel for forcing me every now and then to have a glass of wine. Katharina Gugler for sharing with me the disbelief in free will.

The whole Vienna quantum group—Academy and University—for creating a very pleasant atmosphere.

The Austrian Academy of Sciences for a doctoral fellowship that allowed me to pursue the second half of my research in a fully independent way.

And last but not least my family for their unconditional support and interest in my work throughout the years, and my friends for all the hiking trips, cinema evenings, and discussions on Life, the Universe, and Everything.

Johannes Kofler

Vienna, June 2008

List of publications

The titles of publications that are directly relevant for this dissertation are written in bold face.

Articles in refereed journals

- J. Kofler and Č. Brukner
The conditions for quantum violation of macroscopic realism
Phys. Rev. Lett. (accepted); arXiv:0706.0668 [quant-ph].
- J. Kofler and Č. Brukner
Classical world arising out of quantum physics under the restriction of coarse-grained measurements
Phys. Rev. Lett. **99**, 180403 (2007).
- J. Kofler and Č. Brukner
Entanglement distribution revealed by macroscopic observations
Phys. Rev. A **74**, 050304(R) (2006).
- M. Lindenthal and J. Kofler
Measuring the absolute photo detection efficiency using photon number correlations
Appl. Opt. **45**, 6059 (2006).
- J. Kofler and N. Arnold
Axially symmetric focusing as a cuspid diffraction catastrophe: Scalar and vector cases and comparison with the theory of Mie
Phys. Rev. B **73**, 235401 (2006).
- J. Kofler, V. Vedral, M. S. Kim, and Č. Brukner
Entanglement between collective operators in a linear harmonic chain
Phys. Rev. A **73**, 052107 (2006).
- J. Kofler, T. Paterek, and Č. Brukner
Experimenter's freedom in Bell's theorem and quantum cryptography
Phys. Rev. A **73**, 022104 (2006).

Submitted or in preparation

- J. Kofler and Č. Brukner
The conditions for quantum violation of macroscopic realism
arXiv:0706.0668 [quant-ph] (submitted).

- X. Ma, A. Qarry, J. Kofler, T. Jennewein, and A. Zeilinger
Experimental violation of a Bell inequality with two different degrees of freedom
In preparation (2008).
- X. Ma, A. Qarry, N. Tetik, J. Kofler, T. Jennewein, and A. Zeilinger
Entanglement-assisted delayed-choice experiment
In preparation (2008).
- J. Kofler and Č. Brukner
Fundamental limits on observing quantum phenomena from within quantum theory
In preparation (2008).

Contributions in books

- J. Kofler and Č. Brukner
A coarse-grained Schrödinger cat
In: *Quantum Communication and Security*, ed. M. Żukowski, S. Kilin, and J. Kowalik (IOS Press 2007).
- J. Kofler and N. Arnold
Axially symmetric focusing of light in dry laser cleaning and nanopatterning
In: *Laser Cleaning II*, ed. D. M. Kane (World Scientific Publishing, 2006).
- D. Bäuerle, T. Gumpenberger, D. Brodoceanu, G. Langer, J. Kofler, J. Heitz, and K. Piglmayer
Laser cleaning and surface modifications: Applications in nano- and biotechnology
In: *Laser Cleaning II*, ed. D. M. Kane (World Scientific Publishing, 2006).

Contributions in proceedings

- R. Ursin, T. Jennewein, J. Kofler, J. Perdigues, L. Cacciapuoti, C. J. de Matos, M. Aspelmeyer, A. Valencia, T. Scheidl, A. Fedrizzi, A. Acin, C. Barbieri, G. Bianco, Č. Brukner, J. Capmany, S. Cova, D. Gigenbach, W. Leeb, R. H. Hadfield, R. Laflamme, N. Lütkenhaus, G. Milburn, M. Peev, T. Ralph, J. Rarity, R. Renner, E. Samain, N. Solomos, W. Tittel, J. P. Torres, M. Toyoshima, A. Ortigosa-Blanch, V. Pruneri, P. Villoresi, I. Walmsley, G. Weihs, H. Weinfurter, M. Żukowski, and A. Zeilinger
Space-QUEST: Experiments with quantum entanglement in space
Accepted for the 59th International Astronautical Congress (2008); arXiv:0806.0945v1 [quant-ph].
- D. Bäuerle, L. Landström, J. Kofler, N. Arnold, and K. Piglmayer
Laser-processing with colloid monolayers
Proc. SPIE 5339, **20** (2004).

Articles in popular journals

- A. Zeilinger and J. Kofler
La dissolution du paradoxe
Sciences et Avenir Hors-Série **148**, 54 (2006).

Theses

- J. Kofler
Focusing of light in axially symmetric systems within the wave optics approximation
Diploma Thesis, Johannes Kepler University Linz, Austria (2004).

Chapter 0

Introduction

Since the birth of quantum theory in the 1920s, *quantum entanglement* and *quantum superposition* have been used to highlight a number of counter-intuitive phenomena. They lie at the heart of the Einstein-Podolsky-Rosen [30] and the Schrödinger cat paradox [83] (Figure 1). The corresponding conflicts between quantum mechanics on one side and a classical world—*local realism* and *macroscopic realism* (macrorealism)—on the other, are quantitatively expressed by the violation of Bell’s [9] and the Leggett-Garg inequality [60], respectively. The quantum violation of local realism shows that the view is untenable that space-like separated events do not influence each other *and* that objects have their properties prior to and independent of measurement. The quantum violation of macrorealism means that it is wrong to believe that a macroscopic object has definite properties at any time *and* that it can be measured without effecting them or their subsequent dynamics.

The importance of this incongruousness today exceeds the realm of the foundations of quantum physics and has become an important conceptual tool for developing new quantum information technology. Entanglement and superposition allow to perform certain computation and communication tasks such as quantum cryptography [10, 38], teleportation [11, 14] or quantum computation [28, 67], which are not possible classically. Experiments in the near future will be realized with increasingly complex objects, either by entangling more and more systems with each other, or by entangling systems with a very large number of degrees of freedom. Eventually, all these developments will push the realm of quantum physics well into the macroscopic world. Moreover, implications on society in a cultural sense may manifest themselves, for the characteristics and peculiarities of the quantum world—in particular quantum entanglement and quantum superposition—could eventually become part of the every-day experience.

However, the macroscopic classical world that we perceive around us does not show any characteristics of the quantum realm. The question “Why do classical systems stop to show quantum features?” is still answered in radically different ways within the physics community. Since classical apparatuses are needed for performing measurements on quantum systems, this question is also related to the so called “measurement problem” and the various interpretations of quantum mechanics, ranging from the Copenhagen over the Bohmian to the many-worlds interpretation [46].

On the one hand, there exist a number of so-called collapse models [36, 73] which try to explain

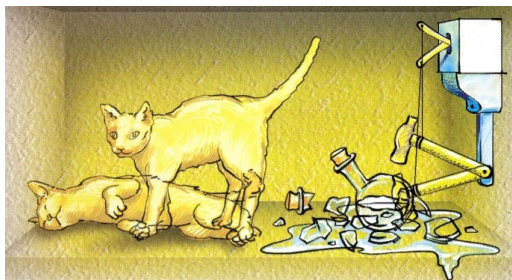


Figure 1: In 1935, Schrödinger put forward the “burlesque” *Gedankenexperiment* of a “hell machine” to illustrate that, according to quantum physics, it is possible to prepare a cat in a superposition of ‘dead’ and ‘alive’ [83]. [Picture taken from *Sciences et Avenir Hors-Série* 148, 54 (2006).]

the discrepancy between the quantum and the classical world by introducing a fundamental breakdown of quantum superpositions at some quantum-classical border. On the other, the decoherence program [103, 104] demonstrates that the states of complex systems interacting with an environment, which cannot be accessed and controlled in detail, rapidly evolve into statistical mixtures and lose their quantum character.

While neither of these approaches can give a definite or already experimentally settled answer, the understanding of the quantum-to-classical transition is not only of prior importance for the future development towards macroscopic superpositions and entanglement but also necessary for a consistent description of the physical world. Collapse models make assumptions about inherently non-quantum mechanical background fields or gravitational mechanisms which are still to be tested experimentally. The decoherence program is inherently quantum mechanical and can give good explanations for many observations though it has to rely on the assumption of a preferred pointer basis. However, the effects of decoherence can in principle be always reduced and the experimental progress of the last years has already demonstrated quantum interference of (Schrödinger-cat like) macroscopic superpositions, e.g., interference fringes with large molecules of $\sim 10^3$ atomic mass units [4], entanglement between clouds of $\sim 10^{12}$ atoms [47], or superpositions of macroscopically distinct flux states in superconducting rings corresponding to $\sim 10^{-6}$ amperes of current flowing clock- or anticlockwise [32]. These experiments circumvent the problem of decoherence but did not yet come into the region where they could exclude collapse models.

Until today there exists no definite answer to the problem of the quantum-to-classical transition. Hence, certainly one of the most fundamental and interesting questions in modern physics still remains unanswered:

How does the classical physical world emerge out of the quantum realm?

Chapter 1 of this dissertation addresses this question from a novel perspective and develops an approach to the *quantum-to-classical transition* fully within quantum theory and conceptually different from already existing models. It neither needs to refer to the environment of a system (decoherence) nor to change the quantum laws itself (collapse models) but puts the stress on the limits of observability of quantum phenomena due to our measurement apparatuses. Using a



Figure 2: Under the magnifying glass of sharp measurements Albert Einstein sees a strange and colorful quantum picture of the face next to him. Its abstractness is symbolized by Pablo Picasso’s “Head of a Reading Woman”. Under an every-day coarse-grained view the classical appearance of Charlie Chaplin emerges.

quantum spin as a model object, we first demonstrate that for unrestricted measurement accuracy the system’s time evolution cannot be described classically and is in conflict with macrorealism through violation of the Leggett-Garg inequality. This conflict remains even if the spin is arbitrarily large and macroscopic.

Under realistic conditions in every-day life, however, we are only able to perform *coarse-grained measurements* and do not resolve individual quantum levels of the macroscopic system. As we show, it is this mere restriction to fuzzy measurements which is sufficient to see the natural emergence of macrorealism and the classical Newtonian laws out of the full quantum formalism: the system’s time evolution governed by the Schrödinger equation and the state projection induced by measurements. This resolves the apparent impossibility of how classical realism and deterministic laws can emerge out of fundamentally random quantum events. Figure 2 presents an illustration of this approach.

Chapter 2 first shows that a violation of the Leggett-Garg inequality itself is possible for arbitrary Hamiltonians given the ability to perform sharp quantum measurements. Apparatus decoherence or the restriction of coarse-grained measurements usually allow to describe the time evolution of any quantum spin state by a time evolution of a statistical mixture. However, we demonstrate that there are “*non-classical*” *Hamiltonians* for which the time evolution of this mixture cannot be understood classically, leading to a violation of macrorealism. We derive the necessary condition for these non-classical time evolutions and illustrate it with the example of an oscillating Schrödinger cat-like state. System decoherence, i.e. the continuous monitoring of the system by an environment, leads to macrorealism but a dynamical description of non-classical time evolutions in terms of classical laws of motion remains impossible.

In the last part we argue that non-classical Hamiltonians either require interactions between a large number of particles or are of high *computational complexity*. This might be understood as the reason why they are unlikely to appear in nature.

Chapter 3 investigates *entanglement between collective operators* in two specific physical sys-

tems, namely in a linear chain of harmonic oscillators and in ensembles of spin- $\frac{1}{2}$ particles. We demonstrate that under certain conditions entanglement between macroscopic observables can indeed persist for large system sizes. However, since this analysis uses sharp measurements, it is not in disagreement with our quantum-to-classical approach.

Chapter 4 addresses the question of the *origin of quantum randomness*. In our view, classical physics emerges out of the quantum world but the randomness in the classical mixture is still irreducible and of quantum nature. We propose to link quantum randomness with *mathematical undecidability* in the sense of Chaitin's version of Gödel's theorem. It states that given a set of axioms that contains a certain amount of information, it is impossible to deduce the truth value of a proposition which, together with the axioms, contains more information than the set of axioms itself.

First, we demonstrate that the states of elementary quantum systems are capable of encoding mathematical axioms. Quantum mechanics imposes an upper limit on how much information can be carried by a quantum state, thus limiting the information content of the set of axioms. Then, we show that quantum measurements are capable of revealing whether a given proposition is decidable or undecidable within this set. This allows for an experimental test of mathematical undecidability by realizing in the laboratory the actual quantum states and operations required. We theoretically find and experimentally confirm that whenever a mathematical proposition is undecidable within the system of axioms encoded in the state, the measurement associated to the proposition gives random outcomes. Our results support the view that quantum randomness is irreducible and a manifestation of mathematical undecidability.

Chapter 1

Classical world emerging from quantum physics

Summary:

Inspired by the thoughts of Peres on the classical limit [74]—we present a *novel theoretical approach to macroscopic realism and classical physics within quantum theory*. While our approach is not at variance with the decoherence program [103, 104], it differs conceptually from it. It is not dynamical and puts the stress on the limits of observability of quantum effects of macroscopic objects, i.e. on the required precision of our measurement apparatuses such that quantum phenomena can still be observed. The term “macroscopic” is used here to denote a system with a high dimensionality rather than a low-dimensional system with a large parameter such as mass or size. Furthermore, there is no need to change the quantum laws itself like in collapse models [36, 73].

Using a quantum spin as a model system, we first show that, if consecutive eigenvalues of a spin component can be experimentally resolved in sharp quantum measurements, the Leggett-Garg inequality is violated for arbitrary spin lengths and the violation persists even in the limit of infinitely large spins. This contradicts the naive assumption that the predictions of quantum mechanics reduce to those of classical physics merely due to the fact that a system becomes “large”. For local realism this persistence of quantum features was demonstrated by Garg and Mermin [33], and the violation even increases with the systems’ dimensionality [48, 25].

In every-day life, however, one not only encounters very high-dimensional systems but is experimentally restricted to *coarse-grained measurements*. They only distinguish between eigenvalues which are separated by much more than the intrinsic quantum uncertainty. We show for arbitrary spin states that, given a certain time evolution, the macroscopically distinct outcomes obey the classical Newtonian laws which emerge out of the Schrödinger equation and the projection postulate.

This suggests that *classical physics can be seen as implied by quantum mechanics under the restriction of fuzzy measurements* and resolves the apparent impossibility of how classical realism and deterministic laws can emerge out of fundamentally random quantum events.

This chapter mainly bases on and also uses parts of Reference [56]:

- J. Kofler and Č. Brukner
Classical world arising out of quantum physics under the restriction of coarse-grained measurements
Phys. Rev. Lett. **99**, 180403 (2007).

1.1 The Leggett-Garg inequality

In this section we introduce the concept of *macroscopic realism* (macrorealism) and show how to derive a Leggett-Garg inequality, which can be used as a tool to indicate whether or not a system's time evolution can be understood in classical terms. In agreement with this, we then briefly demonstrate explicitly that the inequality can always be violated for genuine quantum systems but always satisfied for classical objects.

Macrorealism is defined by the conjunction of the following three postulates [62]:

- (1) *Macrorealism per se.* A macroscopic object which has available to it two or more macroscopically distinct states is at any given time in a definite one of those states.
- (2) *Non-invasive measurability.* It is possible in principle to determine which of these states the system is in without any effect on the state itself or on the subsequent system dynamics.
- (3) *Induction.* The properties of ensembles are determined exclusively by initial conditions (and in particular not by final conditions).

The last two postulates can be phrased into the single assumption that the object's state is independent of past and future measurements [61]. Classical (Newtonian) physics belongs to the class of macrorealistic theories.

Now consider a macroscopic physical system and a dichotomic quantity A , which whenever measured is found to take one of the values ± 1 only. Further consider a series of runs starting from identical initial conditions at time $t = 0$ such that on the first set of runs A is measured only at times t_1 and t_2 , only at t_2 and t_3 on the second, at t_3 and t_4 on the third, and at t_1 and t_4 on the fourth ($0 \leq t_1 < t_2 < t_3 < t_4$). Let A_i denote the value of A at time t_i (see Figure 1.1). Consider the algebraic combination of the Clauser-Horne-Shimony-Holt (CHSH) type [23]:

$$A_1 (A_2 - A_4) + A_3 (A_2 + A_4) = \pm 2. \quad (1.1)$$

It can only have the values $+2$ or -2 for one of the two brackets has to vanish and the other is $+2$ or -2 and then multiplied with $+1$ or -1 . *Macrorealism per se* is reflected by the objective existence of unambiguous values of A_i at all times, and *non-invasive measurability* together with *induction* is reflected by the fact that the A_i 's are the same, independent in which combination they appear. E.g., A_4 is independent of previous measurements, i.e. whether it appears in a run

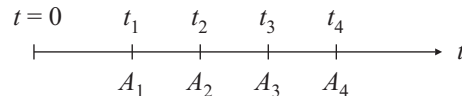


Figure 1.1: In a macrorealistic theory *macrorealism per se* implies that a time-dependent quantity $A(t)$ of a macroscopic object has a well defined unambiguous value $A_i = A(t_i)$ at every time t_i . *Non-invasive measurability* (together with *induction*) is reflected by the fact that the A_i 's do not depend on whether the system was or was not measured at earlier times.

together with A_1 or A_3 . Repeating the experimental runs many times, we introduce the temporal correlation functions

$$C_{ij} \equiv \langle A_i A_j \rangle. \quad (1.2)$$

By averaging (1.1) it follows that any macrorealistic theory has to satisfy the *Leggett-Garg inequality* [60]

$$\boxed{K \equiv C_{12} + C_{23} + C_{34} - C_{14} \leq 2.} \quad (1.3)$$

Its violation implies that the object's time evolution cannot be understood classically.

Let us briefly analyze the quantum evolution of a *microscopic* quantum object, say the precession of a spin- $\frac{1}{2}$ particle with the Hamiltonian $\hat{H} = \frac{1}{2} \omega \hat{\sigma}_x$, where ω is the angular precession frequency and $\hat{\sigma}_x$ is the Pauli x -matrix.¹ If we measure the spin along the z -direction, then we obtain the temporal correlations $C_{ij} = \langle \hat{\sigma}_z(t_i) \hat{\sigma}_z(t_j) \rangle = \cos[\omega(t_j - t_i)]$. Choosing the four possible measurement times as equidistant, with time distance $\Delta t = t_2 - t_1 = t_3 - t_2 = t_4 - t_3$, the Leggett-Garg inequality becomes

$$K = 3 \cos(\omega \Delta t) - \cos(3\omega \Delta t) \leq 2. \quad (1.4)$$

This is maximally violated for the time distance $\Delta t = \frac{\pi}{4\omega}$ for which $K = 2\sqrt{2}$ (see red line in Figure 1.2). The violation is not surprising as a spin- $\frac{1}{2}$ particle is a genuine quantum system and cannot have the objective properties tentatively attributed to macroscopic objects prior to and independent of measurements. In contrast, we consider an arbitrarily sized uniformly rotating classical spin vector, again precessing around x and pointing along z at time t_1 . As dichotomic observable quantity we use $A(t_i) = \text{sgn}(\cos \omega t_i)$ such that $A = +1$ (-1) if the spin is pointing upwards (downwards) along z . As expected, the inequality (1.3) is always satisfied (see blue line in Figure 1.2).

1.2 Violation of the Leggett-Garg inequality for arbitrarily large spins

In this section, we demonstrate that the Leggett-Garg inequality (1.3) is violated for arbitrarily large (macroscopic) spin lengths j as long as accurate measurements can be performed. In any run, the first of the two measurements acts as a preparation of the state for the subsequent measurement. Therefore, the initial state of the spin is not decisive and it is sufficient for us to consider as initial state the maximally mixed one:

$$\hat{\rho}(0) \equiv \frac{1}{2j+1} \sum_m |m\rangle \langle m| = \frac{\mathbb{1}}{2j+1}. \quad (1.5)$$

Here, $\mathbb{1}$ is the identity operator and $|m\rangle$ are the \hat{J}_z (spin z -component) eigenstates with the possible eigenvalues $m = -j, -j+1, \dots, +j$. We consider the Hamiltonian

$$\hat{H} = \frac{\hat{\mathbf{J}}^2}{2I} + \omega \hat{J}_x, \quad (1.6)$$

¹Throughout this and the subsequent chapter we use units in which the reduced Planck constant is $\hbar = 1$.

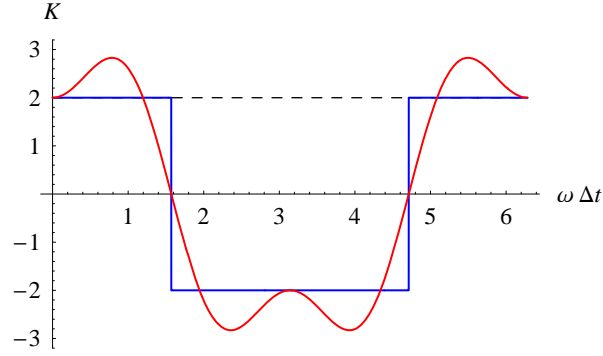


Figure 1.2: Violation of the Leggett-Garg inequality (1.4) for a rotating spin- $\frac{1}{2}$ particle with precession frequency ω . The left-hand side of the inequality, K , is shown by a red line, while the classical limit, $K = 2$, is indicated by a dashed line. If the distance Δt between the four possible equidistant measurement times is chosen as $\Delta t = \frac{\pi}{4\omega}$, then the inequality is maximally violated with $K = 2\sqrt{2}$. The blue line shows the left-hand side of the Leggett-Garg inequality for a classical rotating spin vector. Its time evolution can be understood classically and does not violate the inequality.

where $\hat{\mathbf{J}}$ is the rotor's total spin vector operator, \hat{J}_x its x -component, I the moment of inertia and ω the angular precession frequency. The constant of motion $\frac{\hat{\mathbf{J}}^2}{2I}$ can be ignored since $\hat{\mathbf{J}}^2$ commutes with the individual spin components and does not contribute to their time evolution. The solution of the Schrödinger equation produces a rotation about the x -axis, represented by the time evolution operator

$$\hat{U}_t \equiv e^{-i\omega t \hat{J}_x}. \quad (1.7)$$

We assume that individual eigenstates $|m\rangle$ can be experimentally resolved and use the parity measurement

$$\hat{A} \equiv \sum_m (-1)^{j-m} |m\rangle\langle m| = e^{i\pi(j-\hat{J}_z)} \quad (1.8)$$

with the possible dichotomic outcomes ± 1 (identifying $\pm \equiv \pm 1$). The temporal correlation function between results of the parity measurement \hat{A} at different (arbitrary) times t_i and t_j ($t_j > t_i$) is

$$C_{ij} = p_{i+} q_{j+|i+} + p_{i-} q_{j-|i-} - p_{i+} q_{j-|i+} - p_{i-} q_{j+|i-}, \quad (1.9)$$

where p_{i+} (p_{i-}) is the probability for measuring $+$ ($-$) at t_i and $q_{j|ik}$ is the probability for measuring l at t_j given that k was measured at t_i ($k, l = +, -$). Furthermore,

$$p_{i+} = 1 - p_{i-} = \frac{1}{2} (\langle \hat{A}_{t_i} \rangle + 1), \quad (1.10)$$

$$q_{j+|i\pm} = 1 - q_{j-|i\pm} = \frac{1}{2} (\langle \hat{A}_{t_j} \rangle_{\pm} + 1). \quad (1.11)$$

Here $\langle \hat{A}_{t_i} \rangle$ is the expectation value of \hat{A} at t_i and $\langle \hat{A}_{t_j} \rangle_{\pm}$ is the expectation value of \hat{A} at t_j given that \pm was the outcome at t_i . The totally mixed state is not changed until the first measurement: $\hat{\rho}(t_i) = \hat{U}_{t_i} \hat{\rho}(0) \hat{U}_{t_i}^\dagger = \hat{\rho}(0)$ and we find

$$\langle \hat{A}_{t_i} \rangle = \text{Tr}[\hat{\rho}(t_i) \hat{A}] = \frac{1}{2j+1} \sum_m (-1)^{j-m} \approx 0. \quad (1.12)$$

The approximate sign is accurate for half integer j as well as in the macroscopic limit $j \gg 1$, which is assumed from now on. Hence, we have $p_{i+} = p_{i-} = \frac{1}{2}$, which is self-evident for a totally mixed state. Depending on the measurement result \pm at t_i , the state is reduced to

$$\hat{\rho}_{\pm}(t_i) = \frac{\hat{P}_{\pm} \hat{\rho}(t_i) \hat{P}_{\pm}}{\text{Tr}[\hat{P}_{\pm} \hat{\rho}(t_i) \hat{P}_{\pm}]} = \frac{\mathbb{1} \pm \hat{A}}{2j + 1}, \quad (1.13)$$

with $\hat{P}_{\pm} \equiv \frac{1}{2}(\mathbb{1} \pm \hat{A})$ the projection operator onto positive (negative) parity states. Denoting $\theta \equiv \omega(t_j - t_i)$, the remaining expectation value $\langle \hat{A}_{t_j} \rangle_{\pm} = \text{Tr}[\hat{U}_{t_j-t_i} \hat{\rho}_{\pm}(t_i) \hat{U}_{t_j-t_i}^{\dagger} \hat{A}]$ becomes

$$\begin{aligned} \langle \hat{A}_{t_j} \rangle_{\pm} &= \pm \frac{1}{2j + 1} \text{Tr}[e^{-i\theta \hat{J}_x} e^{i\pi(j-\hat{J}_z)} e^{i\theta \hat{J}_x} e^{i\pi(j-\hat{J}_z)}] \\ &= \pm \frac{\text{Tr}[e^{2i\theta \hat{J}_x}]}{2j + 1} = \pm \frac{\sin[(2j + 1)\omega(t_j - t_i)]}{(2j + 1)\sin[\omega(t_j - t_i)]}. \end{aligned} \quad (1.14)$$

Here we used the geometrical meaning of the rotations in the first line. From $\langle \hat{A}_{t_j} \rangle_{+} = -\langle \hat{A}_{t_j} \rangle_{-}$ it follows $q_{+|+} + q_{+|-} = 1$. Using this and $p_{i+} = \frac{1}{2}$ from above, the temporal correlation function becomes

$$C_{ij} = \langle \hat{A}_{t_j} \rangle_{+}. \quad (1.15)$$

Having four possible equidistant measurements with time distance Δt , and using the abbreviation

$$x \equiv (2j + 1)\omega \Delta t \quad (1.16)$$

the Leggett–Garg inequality (1.3) now reads

$$K \approx \frac{3 \sin x}{x} - \frac{\sin 3x}{3x} \leq 2. \quad (1.17)$$

We approximated the sine function in the denominator, assuming $\frac{x}{2j+1} \ll 1$. Inequality (1.17) is violated for all positive $x \lesssim 1.656$ and maximally violated for $x \approx 1.054$ where $K \approx 2.481$ (compare with Reference [74] for the violation of local realism) as can be seen in Figure 1.3. For every spin size j , and given a precession frequency ω , it is always possible to choose the time distance Δt such that $K > 2$.

We can conclude that a violation of the Leggett-Garg inequality is possible for arbitrarily high-dimensional systems and even for initially totally mixed states.

Note, however, that the temporal precision of our measurement apparatuses, which is required for seeing the violation, increases with j , as $\omega \Delta t$ has to scale with j^{-1} in order to keep $x \approx 1$. Moreover, due to the nature of the parity measurement, consecutive values of m have to be resolved.

1.3 The quantum-to-classical transition for a spin-coherent state

In this section we will show that coarse-grained measurements not only lead to the validity of macrorealism but even to the *emergence of classical physics* for a certain class of quantum states. The generalization to arbitrary states will be done in the next section.

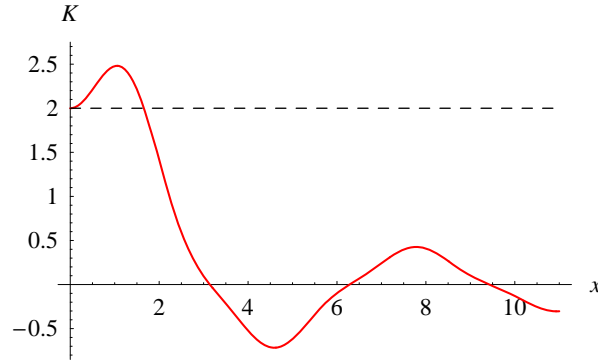


Figure 1.3: Violation of the Leggett-Garg inequality (1.17) for *arbitrarily large* spin size j . The left hand side of the inequality, K , is indicated by a red line and the classical limit is $K = 2$ (dashed line). The initial quantum state is totally mixed, eq. (1.5), and the Hamiltonian (1.6) produces a precession around the x -axis with frequency ω . The dichotomic observable is the parity in a measurement (1.8) of the spin’s z -component. For all spin sizes j and precession frequencies ω , one can always find a time distance Δt between the four possible equidistant measurement times such that the quantity $x \equiv (2j+1)\omega \Delta t$ is around the value 1 and the classical limit is violated. The maximal violation $K \approx 2.481$ is achieved for $x \approx 1.054$.

Let us start with a preliminary remark about distinguishability of states in quantum theory. Any two different eigenvalues m_1 and m_2 in a measurement of a spin’s z -component correspond to orthogonal states *without any concept of closeness or distance*. In Hilbert space the vectors $|m\rangle$ and $|m+1\rangle$ are as orthogonal as $|m\rangle$ and $|m+10^{10}\rangle$:

$$\langle m+1|m\rangle = 0, \quad (1.18)$$

$$\langle m+10^{10}|m\rangle = 0. \quad (1.19)$$

The terms “close” or “distant” only make sense in a classical context, where those eigenvalues are treated as close which correspond to neighboring outcomes in the real configuration space.

For example, the “eigenvalue labels” m and $m+1$ of a spin component observable correspond to neighboring outcomes in a Stern-Gerlach experiment. (Such observables are sometimes called classical or reasonable [101, 49, 74].) If our measurement accuracy is limited, it is those neighboring eigenvalues which we conflate to coarse-grained observables. It seems thus unavoidable that certain features of classicality have to be assumed beforehand to give the Hilbert space some structure which it does not have a priori.

In what follows, we will first consider the special case of a single spin coherent state and then generalize the transition to classicality for arbitrary states. *Spin- j coherent states* $|\Omega\rangle \equiv |\vartheta, \varphi\rangle$ [78, 6] are the eigenstates with maximal eigenvalue of a spin operator pointing into the direction $\Omega \equiv (\vartheta, \varphi)$, where ϑ and φ are the polar and azimuthal angle in spherical coordinates, respectively:

$$\hat{\mathbf{J}}_{\vartheta, \varphi} |\vartheta, \varphi\rangle = j |\vartheta, \varphi\rangle. \quad (1.20)$$

Let us consider the initial spin coherent state at time $t = 0$ pointing into the direction (ϑ_0, φ_0) . In the basis of \hat{J}_z eigenstates it reads

$$|\vartheta_0, \varphi_0\rangle = \sum_m \binom{2j}{j+m}^{1/2} \cos^{j+m} \frac{\vartheta_0}{2} \sin^{j-m} \frac{\vartheta_0}{2} e^{-im\varphi_0} |m\rangle. \quad (1.21)$$

Under time evolution $\hat{U}_t = e^{-i\omega t \hat{J}_x}$, eq. (1.7), the probability that a \hat{J}_z measurement at some later time t has the particular outcome m is given by the binomial distribution

$$p(m, t) = |\langle m | \vartheta_t, \varphi_t \rangle|^2 \quad (1.22)$$

with $\cos \vartheta_t = \sin \omega t \sin \vartheta_0 \sin \varphi_0 + \cos \omega t \cos \vartheta_0$, $\tan \varphi_t = \cos \omega t \tan \varphi_0 - \sin \omega t \tan^{-1} \vartheta_0 \cos^{-1} \varphi_0$, where ϑ_t and φ_t are the polar and azimuthal angle of the (rotated) spin coherent state $|\vartheta_t, \varphi_t\rangle = \hat{U}_t |\vartheta_0, \varphi_0\rangle$ at time t . In the macroscopic limit, $j \gg 1$, the binomial distribution (1.22) can be very well approximated by a Gaussian distribution

$$p(m, t) \approx \frac{1}{\sqrt{2\pi} \sigma} e^{-\frac{(m-\mu)^2}{2\sigma^2}} \quad (1.23)$$

with $\sigma \equiv \sqrt{j/2} \sin \vartheta_t$ the width (standard deviation) and $\mu \equiv j \cos \vartheta_t$ the mean value.

Under the ‘‘magnifying glass’’ of sharp measurements individual eigenvalues m can be distinguished and the Gaussian probability distribution $p(m, t)$ can be resolved, as shown in Figure 1.4(a), allowing a violation of the Leggett-Garg inequality. Let us now assume that, as in every-day life, the resolution of the measurement apparatus, Δm , is restricted and that it subdivides the $2j + 1$ possible different outcomes m into a much smaller number of $\frac{2j+1}{\Delta m}$ coarse-grained ‘‘slots’’ \bar{m} . If the slot size is much larger than the standard deviation $\sigma \sim \sqrt{j}$, i.e.

$$\boxed{\Delta m \gg \sqrt{j}}, \quad (1.24)$$

the sharply peaked Gaussian cannot be distinguished anymore from the discrete Kronecker delta,

$$\Delta m \gg \sqrt{j} : \quad p(m, t) \rightarrow \delta_{\bar{m}, \bar{\mu}}. \quad (1.25)$$

Here, \bar{m} is numbering the slots (from $-j + \frac{\Delta m}{2}$ to $j - \frac{\Delta m}{2}$ in steps Δm) and $\bar{\mu}$ is the number of the slot in which the center μ of the Gaussian lies. This is indicated in Figure 1.4(b).

In the *classical limit*, $j \rightarrow \infty$, one can distinguish two cases: (1) If the inaccuracy Δm scales linearly with j , i.e. $\Delta m = O(j)$, the discreteness remains. (2) If Δm scales slower than j , i.e. $\Delta m = o(j)$ but still $\Delta m \gg \sqrt{j}$, then the slots seem to become infinitely narrow. Pictorially, the *real space length* of the eigenvalue axis, representing the $2j + 1$ possible outcomes m , is limited in any laboratory, e.g., by the size of the observation screen after a Stern-Gerlach magnet, whereas the number of slots grows as $j/\Delta m$. Then, in the limit $j \rightarrow \infty$, the discrete Kronecker delta becomes the Dirac delta function,

$$\Delta m \gg \sqrt{j} \ \& \ j \rightarrow \infty : \quad p(m, t) \rightarrow \delta(\bar{m} - \bar{\mu}), \quad (1.26)$$

which is shown in Figure 1.4(c).

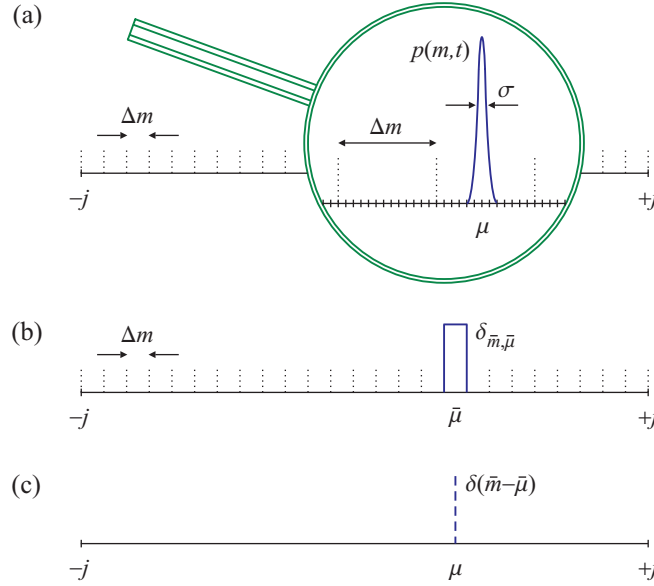


Figure 1.4: An initial spin- j coherent state $|\vartheta_0, \varphi_0\rangle$ precesses into the coherent state $|\vartheta_t, \varphi_t\rangle$ at time t under a quantum time evolution. (a) The probability $p(m, t)$ for the outcome m in a measurement of the spin's z -component is given by a Gaussian distribution with width σ and mean μ , which can be seen under the magnifying glass of sharp measurements. (b) The measurement resolution Δm is finite and subdivides the $2j + 1$ possible outcomes into a smaller number of coarse-grained “slots”. If the measurement accuracy is much poorer than the width σ , i.e., $\Delta m \gg \sqrt{j}$, the sharply peaked Gaussian cannot be distinguished anymore from the discrete Kronecker delta $\delta_{\bar{m}, \bar{\mu}}$ where \bar{m} is numbering the slots and $\bar{\mu}$ is the slot in which the center μ of the Gaussian lies. (c) In the limit $j \rightarrow \infty$ the slots *seem* to become infinitely narrow and $\delta_{\bar{m}, \bar{\mu}}$ becomes the Dirac delta function $\delta(\bar{m} - \bar{\mu})$.

Now we have to focus on the question in which sense coarse-grained von Neumann measurements disturb the spin coherent state. Let

$$\hat{P}_{\bar{m}} \equiv \sum_{m \in \{\bar{m}\}} |m\rangle\langle m| \quad (1.27)$$

denote the projector onto the slot \bar{m} with $\{\bar{m}\}$ the set of all m belonging to \bar{m} . Then $\hat{P}_{\bar{m}} |\vartheta, \varphi\rangle$ is *almost* $|\vartheta, \varphi\rangle$ (the zero vector $\mathbf{0}$) for all coherent states lying inside (outside) the slot, respectively:

$$\hat{P}_{\bar{m}} |\vartheta, \varphi\rangle \approx \begin{cases} |\vartheta, \varphi\rangle & \text{for } \bar{\mu} \text{ inside } \bar{m}, \\ \mathbf{0} & \text{for } \bar{\mu} \text{ outside } \bar{m}. \end{cases} \quad (1.28)$$

This means that the reduced (projected) state is essentially the state before the measurement or projected away. If $|\vartheta, \varphi\rangle$ is centered well inside the slot, the above relation holds with merely exponentially small deviation. Only in the cases where $|\vartheta, \varphi\rangle$ is close to the border between two slots, the measurement is invasive and disturbs the state. Presuming that the measurement times and/or slot positions chosen by the observer are statistically independent of the (initial) position of the coherent state, a significant disturbance happens merely in the fraction $\sigma/\Delta m \ll 1$ of all measurements.

This is equivalent to the already assumed condition $\sqrt{j} \ll \Delta m$. Therefore, fuzzy measurements of a spin coherent state are almost always non-invasive such as in any macrorealistic theory, in particular classical Newtonian physics. Small errors may accumulate over many measurements and eventually there might appear deviations from the classical time evolution. This, however, is unavoidable in any explanation of classicality *gradually* emerging out of quantum theory.²

Hence, at the coarse-grained level the physics of the (quantum) spin system can completely be described by a “new” formalism, utilizing an initial (classical) *spin vector* \mathbf{J} at time $t = 0$, pointing in the (ϑ_0, φ_0) -direction with length $J \equiv |\mathbf{J}| = \sqrt{j(j+1)} \approx j$, where $j \gg 1$, and a (Hamilton) function

$$H = \frac{\mathbf{J}^2}{2I} + \omega J_x. \quad (1.29)$$

At any time the probability that the spin vector’s z -component $J \cos \vartheta_t \approx j \cos \vartheta_t$ is in slot \bar{m} is given by $\delta_{\bar{m}, \bar{\mu}}$, eq. (1.25), as if the time evolution of the spin components J_i ($i = x, y, z$) is given by the Poisson brackets,

$$\dot{J}_i = [J_i, H]_{\text{PB}}, \quad (1.30)$$

and measurements are non-invasive. Only the term ωJ_x in eq. (1.29) governs the time evolution and the solutions correspond to a rotation around the x -axis. The spin vector at time t points in the (ϑ_t, φ_t) -direction where ϑ_t and φ_t are the same as for the spin coherent state and the probability of measurement outcomes is given by $\delta(\bar{m} - \bar{\mu})$, eq. (1.26).

This is classical (Newtonian) mechanics of a single spin emerging from quantum physics.

1.4 The quantum-to-classical transition for an arbitrary spin state

Now we demonstrate that the time evolution of *any* spin- j quantum state becomes classical under the restriction of coarse-grained measurements. At all times any (pure or mixed) spin- j density matrix can be written in the quasi-diagonal form [3]

$$\hat{\rho} = \iint P(\Omega) |\Omega\rangle\langle\Omega| d^2\Omega \quad (1.31)$$

with $d^2\Omega \equiv \sin \vartheta d\vartheta d\varphi$ the infinitesimal solid angle element and $P(\Omega)$ a *not necessarily positive* real function with the normalization $\iint P(\Omega) d^2\Omega = 1$.

The probability for an outcome m in a \hat{J}_z measurement in the state (1.31) is given by

$$w(m) = \text{Tr}[\hat{\rho} |m\rangle\langle m|] = \iint P(\Omega) p(m) d^2\Omega, \quad (1.32)$$

²For the general trade-off between measurement accuracy and state disturbance for the more realistic smoothed positive operator value measure (POVM) and for related approaches to classicality, see References [19, 77, 35]. A natural way of implementing coarse-grained measurements as POVM is presented in the next chapter. In contrast to von Neumann measurements, they do not allow to distinguish perfectly between two states at two sides of a slot border. But under all circumstances it is in general unavoidable that quantum measurements are invasive to some extent. Classicality arises in the sense that the effects of these deviations become negligibly small.

For fuzzy measurements with (angular) inaccuracy $\Delta\Theta \sim \vartheta_2(\bar{m}) - \vartheta_1(\bar{m}) \gg 1/\sqrt{j}$, which is equivalent to $\Delta m \gg \sqrt{j}$, the probability for having an outcome \bar{m} can now be expressed only in terms of the positive distribution Q :

$$w_{\bar{m}} \approx \iint_{\Omega_{\bar{m}}} Q(\Omega) d^2\Omega. \quad (1.37)$$

Figure 1.5 shows the integration region $\Omega_{\bar{m}}$ over which P and Q have to be integrated. The approximate equivalence of eqs. (1.34) and (1.37) is verified by substituting eq. (1.35) into (1.37) and is not accurately fulfilled for quantum states ρ directly at a slot border.³

Note that Q is a mere mathematical tool and not experimentally accessible in coarse-grained measurements. Operationally, because of $\Delta m \gg \sqrt{j}$ an averaged version of Q , denoted as R , is used by the experimenter to describe the system. Mathematically, this function R is obtained by integrating Q over solid angle elements corresponding to the actual measurement inaccuracy. In the classical limit, without the “magnifying glass”, the regions given by the experimenter’s resolution become “points” on the sphere where R is defined.

Thus, under coarse-grained measurements, a full description of an arbitrary quantum spin state is provided by an ensemble of classical spins with a positive probability distribution.

In other words, there exists a hidden variable description. The *time evolution* of the general state (1.31) is determined by (1.6). In the classical limit it can be described by an ensemble of classical spins characterized by the initial distribution Q (R), where each spin is rotating according to the Hamilton function (1.29). From eq. (1.37) one can see that for the non-invasiveness at the classical level *it is the change of the distribution Q (R) which is important and not the change of the quantum state or equivalently P itself.* In fact, upon a fuzzy \hat{J}_z measurement the state $\hat{\rho}$ is reduced to one particular state depending on the outcome \bar{m} ,

$$\hat{\rho}_{\bar{m}} = \frac{\hat{P}_{\bar{m}} \hat{\rho} \hat{P}_{\bar{m}}}{w_{\bar{m}}}, \quad (1.38)$$

with the corresponding (normalized) functions $P_{\bar{m}}$, $Q_{\bar{m}}$ and $R_{\bar{m}}$. The reduction to $\hat{\rho}_{\bar{m}}$ happens with probability $w_{\bar{m}}$, which is given by eq. (1.34) or (1.37). Whereas the P -function can change dramatically upon reduction, $Q_{\bar{m}}$ is (up to normalization) approximately the same as the original Q in the region $\Omega_{\bar{m}}$. Thus,

$$Q_{\bar{m}}(\Omega) \propto \langle \Omega | \hat{\rho}_{\bar{m}} | \Omega \rangle \propto \langle \Omega | \hat{P}_{\bar{m}} \hat{\rho} \hat{P}_{\bar{m}} | \Omega \rangle \approx \langle \Omega | \hat{\rho} | \Omega \rangle \propto \begin{cases} Q(\Omega) & \text{for } \Omega \text{ inside } \Omega_{\bar{m}}, \\ 0 & \text{for } \Omega \text{ outside } \Omega_{\bar{m}}. \end{cases} \quad (1.39)$$

Therefore, at the coarse-grained level the distribution $Q_{\bar{m}}$ ($R_{\bar{m}}$) of the reduced state after the measurement can always be understood approximately as a subensemble of the (classical) distribution Q before the measurement.

³This issue is related to the fact that our von Neumann coarse-grained measurements have sharp slot borders and will be resolved in the subsequent chapter.

Effectively, the measurement only reveals already existing properties in the mixture and does not alter the subsequent rotation of the individual classical spins.

The disturbance at the slot borders at that level is quantified by how much $Q_{\bar{m}}$ differs from a function which is (up to normalization) Q within $\Omega_{\bar{m}}$ and zero outside. One may think of dividing all quantum states and their Q -distributions into two extreme classes: The ones which show narrow pronounced regions of size comparable to individual coherent states and the ones which change smoothly over regions larger or comparable to the slot size. The former can be highly disturbed but in an extremely rare fraction of all measurements. The latter is disturbed in general in a single measurement but to very small extent, as the weight—in terms of the Q -distribution—on the slot borders ($\propto\sqrt{j}$) is small compared to the weight well inside the slot ($\propto\Delta m$). (In the intermediate cases one has a trade-off between these two scenarios.) The typical fraction of these weights is $\sqrt{j}/\Delta m \ll 1$. In any case, classicality arises with overwhelming statistical weight. In the next chapter we will introduce measurements with smooth borders (POVM) and therefore reduce the disturbance dramatically, even for states near a slot border.

Finally, we want to point out explicitly: The angular resolution which is necessary to see the quantumness, i.e. the superposition character, of a given quantum state is of the order of $1/\sqrt{j}$. In other words, it is necessary to be able to distinguish at least of the order of \sqrt{j} different measurement outcomes. For a macroscopic object, $j \sim 10^{20}$, it would be necessary to resolve $\sim 10^{10}$ different measurement outcomes. If this precision cannot be met, macrorealism emerges out of quantum physics for the rotation Hamiltonian.

1.5 An alternative derivation

For the sake of completeness we now present an alternative way to derive that classicality emerges under coarse-grained measurements. Again, we consider the totally mixed state (1.5) and the time evolution (1.7). We remind that this allows to violate the Leggett-Garg inequality if sharp measurements can be performed. Now we are interested in the probability for obtaining the results m_1 at time t_1 and m_2 at t_2 in measurements of the spin operator's z -component \hat{J}_z —in analogy to [74], where a generalized singlet state and correlations in space are considered. This probability can be written as

$$p(m_1, t_1; m_2, t_2) = p(m_1, t_1) p(m_2, t_2)_{m_1, t_1}, \quad (1.40)$$

i.e. as the probability that m_1 is obtained at t_1 times the probability that m_2 is the result at t_2 given m_1 at t_1 . Let $\hat{P}_m \equiv |m\rangle\langle m|$ denote the projector onto $|m\rangle$. Using that $\hat{\rho}(t_1) = \hat{\rho}(0)$, we have $p(m_1, t_1) = \text{Tr}[\hat{\rho}(t_1) \hat{P}_{m_1}] = \frac{1}{2j+1}$, reflecting the fact that all of the $2j+1$ eigenstates are equally probable in a maximally mixed state. If m_1 was obtained at t_1 , the state is reduced to $\hat{\rho}_{m_1}(t_1) = \hat{P}_{m_1} = |m_1\rangle\langle m_1|$. Then, with $\Delta t \equiv t_2 - t_1$ and $\theta \equiv \omega \Delta t$, we have $p(m_2, t_2)_{m_1, t_1} = \text{Tr}[\hat{U}_{t_2-t_1} \hat{P}_{m_1} \hat{U}_{t_2-t_1}^\dagger \hat{P}_{m_2}] = |\langle m_2 | e^{-i\theta \hat{J}_x} | m_1 \rangle|^2$. Therefore,

$$p(m_1, t_1; m_2, t_2) = \frac{1}{2j+1} |\langle m_2 | e^{-i\theta \hat{J}_x} | m_1 \rangle|^2. \quad (1.41)$$

To continue we perform a discrete Fourier transform with “frequencies” ξ and η :

$$\begin{aligned}\tilde{p}(\xi, \eta) &= \sum_{m_1, m_2} e^{i(\xi m_1 + \eta m_2)} p(m_1, t_1; m_2, t_2) \\ &= \frac{\text{Tr}[e^{i\eta \hat{J}_z} e^{-i\theta \hat{J}_x} e^{i\xi \hat{J}_z} e^{i\theta \hat{J}_x}]}{2j+1} = \frac{\text{Tr}[e^{-i\boldsymbol{\kappa} \cdot \hat{\mathbf{J}}}]}{2j+1} = \frac{\sin[(2j+1)\frac{\kappa}{2}]}{(2j+1)\sin\frac{\kappa}{2}},\end{aligned}\quad (1.42)$$

where the four rotations were expressed as a single rotation $e^{-i\boldsymbol{\kappa} \cdot \hat{\mathbf{J}}}$ around a vector $\boldsymbol{\kappa}$ about an angle of the size $\kappa = |\boldsymbol{\kappa}|$ and the trace was evaluated in the basis where $\boldsymbol{\kappa} \cdot \hat{\mathbf{J}}$ is diagonal. Following firmly Reference [74], it is enough to treat the rotation matrices as 2×2 as if $j = \frac{1}{2}$, since j does not affect the geometrical meaning. If one equates the product of the four matrices in (1.42) to $e^{-i\boldsymbol{\kappa} \cdot \hat{\boldsymbol{\sigma}}/2}$ (with $\hat{\boldsymbol{\sigma}}$ the vector of Pauli matrices), then one obtains the dependence of κ on ξ , η and θ :

$$\cos \frac{\kappa}{2} = \cos \frac{\xi}{2} \cos \frac{\eta}{2} - \sin \frac{\xi}{2} \sin \frac{\eta}{2} \cos \theta. \quad (1.43)$$

Due to *noise or coarse-graining of measurements*, respectively, the high frequency components ($\xi, \eta \sim 1$) are not experimentally observable. Because of $\xi, \eta \sim \frac{1}{\Delta m}$ high frequency components correspond to a sharp measurement resolution Δm . The low frequency limit ($\xi, \eta \ll 1$) of the expression for κ in the first non-trivial order reads

$$\kappa^2 \approx \xi^2 + \eta^2 + 2\xi\eta \cos \theta. \quad (1.44)$$

Now consider a *classical spin vector* \mathbf{J} at time $t = 0$ with length $J = |\mathbf{J}| = \sqrt{j(j+1)} \approx j + \frac{1}{2}$, where $j \gg 1$. In analogy to the quantum case, the probability for measuring the classical spin vector’s z -component as m_1 at t_1 and m_2 at t_2 is

$$p_{\text{cl}, \mathbf{J}}(m_1, t_1; m_2, t_2) = p_{\text{cl}, \mathbf{J}}(m_1, t_1) p_{\text{cl}, \mathbf{J}}(m_2, t_2)_{m_1, t_1}. \quad (1.45)$$

The first probability is given by $p_{\text{cl}, \mathbf{J}}(m_1, t_1) = \delta(m_1 - \mathbf{e}_z \cdot \mathbf{J}(t_1))$, where \mathbf{e}_z is the unit vector in z -direction and δ is Dirac’s delta function. The classical Newtonian time evolution of the spin components J_i ($i = x, y, z$) is given by the Poisson brackets (1.30), where the (classical) Hamilton function is given by (1.29). As $\mathbf{J}^2 = j(j+1)$ is a constant of motion, only the term ωJ_x governs the time evolution. As we already know, the solutions correspond to a rotation around the x -axis. Thus, the spin at t_1 reads $\mathbf{J}(t_1) = \hat{R}_x(\omega t_1) \mathbf{J}(0)$, with $\hat{R}_x(\gamma)$ the 3×3 rotation matrix about the x -axis by an angle γ . But for the scalar product $\mathbf{e}_z \cdot \mathbf{J}(t_1)$ in $p_{\text{cl}, \mathbf{J}}(m_1, t_1)$ it does not matter whether we rotate $\mathbf{J}(0)$ around x by ωt_1 or \mathbf{e}_z around x by $-\omega t_1$. Hence, we can write

$$p_{\text{cl}, \mathbf{J}}(m_1, t_1) = \delta(m_1 - \boldsymbol{\alpha} \cdot \mathbf{J}(0)), \quad (1.46)$$

where $\boldsymbol{\alpha} = \hat{R}_x(-\omega t_1) \mathbf{e}_z$ is the unit vector with polar angle ωt_1 and azimuthal angle $-\frac{\pi}{2}$. The remaining probability is

$$p_{\text{cl}, \mathbf{J}}(m_2, t_2)_{m_1, t_1} = \delta(m_2 - \boldsymbol{\beta} \cdot \mathbf{J}(0)), \quad (1.47)$$

i.e. it depends only on the initial spin $\mathbf{J}(0)$ and the elapsed time t_2 but not on anything that happened at t_1 because of the *non-invasiveness of classical measurements*. In other words, there is no reduction at t_1 and the condition “ m_1 was the outcome at t_1 ” is unnecessary. Here, $\boldsymbol{\beta} =$

$\hat{R}_x(-\omega t_2) \mathbf{e}_z$ is the unit vector with the polar angle ωt_2 and azimuthal angle $-\frac{\pi}{2}$. Hence, eq. (1.45) becomes

$$p_{\text{cl},\mathbf{J}}(m_1, t_1; m_2, t_2) = \delta(m_1 - \boldsymbol{\alpha} \cdot \mathbf{J}) \delta(m_2 - \boldsymbol{\beta} \cdot \mathbf{J}) \quad (1.48)$$

with $\mathbf{J} \equiv \mathbf{J}(0)$. The Fourier transform reads

$$\begin{aligned} \tilde{p}_{\text{cl},\mathbf{J}}(\xi, \eta) &= \iint e^{i(\xi m_1 + \eta m_2)} p_{\text{cl},\mathbf{J}}(m_1, t_1; m_2, t_2) dm_1 dm_2 \\ &= e^{i(\xi \boldsymbol{\alpha} \cdot \mathbf{J} + \eta \boldsymbol{\beta} \cdot \mathbf{J})} \equiv e^{i \mathbf{k} \cdot \mathbf{J}} \end{aligned} \quad (1.49)$$

with $\mathbf{k} \equiv \xi \boldsymbol{\alpha} + \eta \boldsymbol{\beta}$. This implies

$$k^2 = \mathbf{k}^2 = \xi^2 + \eta^2 + 2 \xi \eta \cos \theta, \quad (1.50)$$

where $\theta \equiv \omega(t_2 - t_1)$ is the angle between $\boldsymbol{\alpha}$ and $\boldsymbol{\beta}$, in total agreement with the low frequency limit (1.44). The classical correlation $\tilde{p}_{\text{cl},\mathbf{J}}(\xi, \eta)$ must be averaged over all possible initial directions of $\mathbf{J} = \mathbf{J}(\Omega)$. Mimicking the mixed quantum state, the distribution is isotropic and thus

$$\tilde{p}_{\text{cl}}(\xi, \eta) = \frac{1}{4\pi} \iint \tilde{p}_{\text{cl},\mathbf{J}}(\xi, \eta) d^2\Omega = \frac{\sin[(2j+1)\frac{k}{2}]}{(2j+1)\frac{k}{2}}, \quad (1.51)$$

with $d^2\Omega$ the infinitesimal solid angle element, the vector \mathbf{k} in $\tilde{p}_{\text{cl},\mathbf{J}}(\xi, \eta)$ as the polar integration axis and $J = j + \frac{1}{2}$. This is the limiting value of the quantum correlation (1.42). We note that both the quantum and the classical correlation for measurements of a rotating spin in time, eqs. (1.42) and (1.51), have a similar form as in the case of a generalized singlet state and measurements in space [74].

The quantum to classical transition. Let us now evaluate under which circumstances the quantum correlation (1.42) becomes classical (1.51), i.e.

$$\tilde{p} \rightarrow \tilde{p}_{\text{cl}}. \quad (1.52)$$

First, we note that the allowed frequencies ξ and η are independent and thus have to be small in the same order, i.e. $\xi \sim \eta$, whereas higher frequencies are cut off. In the following, for the sake of a short and intuitive notation, we consider all quantities as positive and ignore any factors of the order of 1 whenever we write ξ . Comparing the exact expression for κ^2 , obtained from eq. (1.43), with the low frequency classical limit k^2 , eq. (1.50), the leading order of the error is ξ^4 :

$$\kappa^2 = k^2 + \xi^4, \quad (1.53)$$

Since $k \sim \xi$ due to eq. (1.50), we have

$$\kappa = \sqrt{k^2 + \xi^4} = k + \xi^3. \quad (1.54)$$

Thus, $\kappa \rightarrow k$ is fulfilled if and only if $\xi^3 \ll k$, or equivalently, $\xi^2 \ll 1$. Two formal conditions—(i) for the arguments in numerators and (ii) for the denominators in eqs. (1.42) and (1.51), respectively—have to be met to guarantee $\tilde{p} \rightarrow \tilde{p}_{\text{cl}}$:

$$(2j+1) \frac{\kappa}{2} \rightarrow (2j+1) \frac{k}{2} \quad (1.55)$$

$$(2j+1) \sin \frac{\kappa}{2} \rightarrow (2j+1) \frac{k}{2} \quad (1.56)$$

Using eq. (1.54), the left-hand side of condition (1.55) becomes

$$(2j + 1) \frac{\kappa}{2} = (2j + 1) \frac{\kappa}{2} + j \xi^3. \quad (1.57)$$

As j is very large in the macroscopic limit, we have neglected the term ξ^3 compared to $j \xi^3$, which is the leading order of the error. Eq. (1.57) is a good approximation for $(2j + 1) \frac{\kappa}{2}$, i.e. the right-hand side of (1.55), if and only if the error $j \xi^3$ is much smaller than the smallest term in $(2j + 1) \frac{\kappa}{2}$, which is $\frac{\kappa}{2} \sim \xi$. Hence we have to postulate $j \xi^3 \ll \xi$, or equivalently,

$$\xi \ll \frac{1}{\sqrt{j}}, \quad (1.58)$$

and the same condition has to hold for the frequency η . The evaluation of condition (1.56), using a Taylor expansion of the sine function, leads to the same condition (1.58). This high-frequency cut-off, ensuring $\tilde{p} \rightarrow \tilde{p}_{\text{cl}}$, implies that different values of m can be experimentally distinguished only if their separation Δm fulfills

$$\Delta m \gg \sqrt{j}, \quad (1.59)$$

which is the minimum quantum uncertainty for spin coherent states and in agreement with the previous sections.

If the angular resolution of the instruments is much poorer than the intrinsic quantum uncertainty, they cannot detect the quantum features of the spin system, let alone a violation of the Leggett-Garg inequality. The temporal correlations become classical.

Chapter 2

General conditions for quantum violation of macroscopic realism

Summary:

We first show that a *violation of the Leggett-Garg inequality itself is possible for arbitrary Hamiltonians* given the ability to distinguish consecutive eigenstates in sharp quantum measurements. This is understandable because it is generally accepted that “microscopically distinct states” do not have objective existence. For testing macrorealism one needs to apply the Leggett-Garg definition referring to *macroscopically distinct states*. In our every-day life, to experience macrorealism it is usually sufficient to employ apparatus decoherence (where the system is isolated and only after a premeasurement, i.e. coupling of system and apparatus, the environment interacts irreversibly with the apparatus) or the restriction of coarse-grained measurements.

Both mechanisms usually allow to describe the time evolution of any quantum spin state by a classical time evolution of a statistical mixture. However, we demonstrate that there exist “*non-classical*” *Hamiltonians* for which the time evolution of this mixture cannot be understood classically. Despite the fact that apparatus decoherence or coarse-graining allow to describe the state merely by a classical mixture at every instance of time, a non-classical Hamiltonian builds up superpositions of macroscopically distinct states and allows to violate macrorealism. We find the necessary condition for these non-classical evolutions and illustrate it with the example of an oscillating Schrödinger cat-like state. System decoherence, i.e. the constant monitoring of the system by an environment, leads to macrorealism but a continuous spatiotemporal description of non-classical time evolutions in terms of classical laws of motion remains impossible.

In the last part we argue that non-classical Hamiltonians require interactions between a large number of particles or are computationally much more complex than classical Hamiltonians, which might be the reason why they are unlikely to appear in nature.

This chapter mainly bases on and also uses parts of References [55, 57]:

- J. Kofler and Č. Brukner
A coarse-grained Schrödinger cat
In: *Quantum Communication and Security*, ed. M. Żukowski, S. Kilin, and J. Kowalik (IOS Press 2007).
- J. Kofler and Č. Brukner
The conditions for quantum violation of macroscopic realism
Phys. Rev. Lett. (accepted); arXiv:0706.0668 [quant-ph].

2.1 Violation of the Leggett-Garg inequality for arbitrary Hamiltonians

In contrast to the Leggett-Garg inequality in the previous chapter, ineq. (1.3), with four possible measurement times t_i , we will now only use three. Then, any macrorealistic theory predicts a Leggett-Garg inequality of the Wigner type [99], where $C_{ij} \equiv \langle A_i A_j \rangle$ denotes the temporal correlation of a dichotomic quantity A at times t_i and t_j :

$$K \equiv C_{12} + C_{23} - C_{13} \leq 1. \quad (2.1)$$

We extend the approach of Peres in Reference [74] and look at the “survival probability” of the system’s initial state at time $t = 0$.¹ This state be denoted as $|\psi(0)\rangle \equiv |\psi_0\rangle$ (which must not be an energy eigenstate) and, without measurements, it evolves to

$$|\psi(t)\rangle = e^{-i\hat{H}t} |\psi_0\rangle \quad (2.2)$$

according to the Schrödinger equation in units where the reduced Planck constant is $\hbar = 1$. Our dichotomic observable is

$$\hat{A} \equiv 2|\psi_0\rangle\langle\psi_0| - \mathbf{1}, \quad (2.3)$$

i.e. we ask whether the system is (still) in the state $|\psi_0\rangle$ (outcome $+$ $\equiv +1$) or not (outcome $-$ $\equiv -1$). The temporal correlations C_{ij} , eq. (1.9), can be written as

$$C_{ij} = p_{i+} q_{j+|i+} + p_{i-} q_{j-|i-} - p_{i+} q_{j-|i+} - p_{i-} q_{j+|i-}, \quad (2.4)$$

where p_{i+} (p_{i-}) is the probability for measuring $+$ ($-$) at t_i and $q_{jl|ik}$ is the probability for measuring l at t_j given that k was measured at t_i ($k, l = +, -$). For simplicity we choose $t_1 = 0$ and equidistant possible measurement times with $\Delta t \equiv t_2 - t_1 = t_3 - t_2$ (Figure 2.1). Then the correlation C_{12} is given by $C_{12} = 2p(\Delta t) - 1$, where

$$p(t) \equiv |\langle\psi_0|\psi(t)\rangle|^2 \quad (2.5)$$

is the (survival) probability to find $|\psi_0\rangle$ given the state $|\psi(t)\rangle$. Analogously, we find $C_{13} = 2p(2\Delta t) - 1$. As $p_{2+} = 1 - p_{2-} = p(\Delta t)$, $q_{3+|2+} = 1 - q_{3-|2+} = p(\Delta t)$, and $q_{3-|2-} = 1 - q_{3+|2-}$, the only remaining unknown quantity in C_{23} is $q_{3+|2-}$. For its computation one needs the reduced state at t_2 , given that the outcome was $-$, $|\psi_-(t_2)\rangle$. It is obtained by applying the projector $\mathbf{1} - |\psi_0\rangle\langle\psi_0|$ to the state at t_2 , $|\psi(t_2)\rangle$, and normalizing: $|\psi_-(t_2)\rangle = [|\psi(t_2)\rangle - \langle\psi_0|\psi(t_2)\rangle |\psi_0\rangle] / \sqrt{1 - p(\Delta t)}$. This evolves a time Δt to t_3 , resulting in $|\psi_-(t_3)\rangle = [|\psi(t_3)\rangle - \langle\psi_0|\psi(t_2)\rangle |\psi(t_2)\rangle] / \sqrt{1 - p(\Delta t)}$, and $q_{3+|2-} = |\langle\psi_0|\psi_-(t_3)\rangle|^2$ is the probability for the outcome $+$ in that state. Plugging everything into (2.1), one ends up with the Leggett-Garg inequality

$$K = 4p(\Delta t)\sqrt{p(2\Delta t)} \cos \gamma - 4p(2\Delta t) + 1 \leq 1, \quad (2.6)$$

where $\gamma \equiv 2\alpha - \beta$ and α and β are the phases in $\langle\psi_0|\psi(t_2)\rangle = \sqrt{p(\Delta t)} \exp(i\alpha)$ and $\langle\psi_0|\psi(t_3)\rangle =$

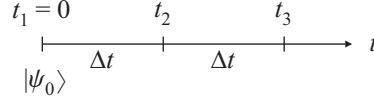


Figure 2.1: At time $t_1 = 0$ the initial state of the quantum system is $|\psi_0\rangle$. Possible later measurement times are $t_2 = \Delta t$ and $t_3 = 2\Delta t$, where the system can be asked whether it is still in its initial state or in the orthogonal subspace.

$$\sqrt{p(2\Delta t)} \exp(i\beta).$$

Now, independent of the system's dimension, it is sufficient to consider as initial state a superposition of only two energy eigenstates $|u_1\rangle$ and $|u_2\rangle$ with energy eigenvalues E_1 and E_2 , respectively: $|\psi_0\rangle = (|u_1\rangle + |u_2\rangle)/\sqrt{2}$. Ineq. (2.6) becomes

$$K = 2 \cos(\Delta E \Delta t) - \cos(2\Delta E \Delta t) \leq 1, \quad (2.7)$$

with $\Delta E \equiv E_2 - E_1$ the energy difference of the two levels.

Any non-trivial Hamiltonian leads to a violation of this inequality.

The left-hand side reaches $K = 1.5$ for $\Delta t = \frac{\pi}{3\Delta E}$ and $\Delta t = \frac{5\pi}{3\Delta E}$ and in $\frac{2\pi\hbar}{\Delta E}$ periods thereof (Figure 2.2).

2.2 Macrorealism per se

If every Hamiltonian leads to a violation of the Leggett-Garg inequality, why then do we not see this in every-day life? The possible answers *within quantum theory* are:

1. It is due to decoherence, i.e. the quantum system interacts with an uncontrollable environment such that it is driven into a statistical mixture [103, 104].
2. The fact that the resolution of our measurement apparatuses is not sharp, makes it impossible to project onto individual states and to see the above demonstrated violation that is always present for microstates [56].

For testing macrorealism—i.e. testing the Leggett-Garg inequality under the restriction of *coarse-grained measurements*—we consider again a spin- j system (with $j \gg 1$) as a model example. To keep this chapter self-contained, we briefly repeat that any spin- j state can be written in the quasi-diagonal form

$$\hat{\rho} = \iint P(\Omega) |\Omega\rangle\langle\Omega| d^2\Omega \quad (2.8)$$

¹In Reference [74], exercise 12.23 correctly claims that any non-trivial Hamiltonian is incompatible with a Leggett-Garg inequality. But the given reason is inconclusive (and no proof is presented). The survival probability, to which is referred to, is written only in form of an inequality, ineq. (12.136) in [74]. This constraint is not strong enough and does not exclude time evolutions which would not violate any Leggett-Garg inequality.

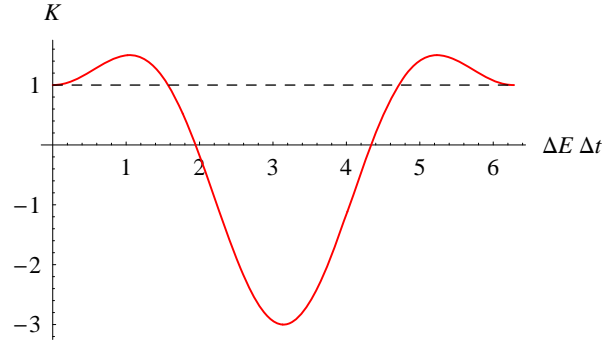


Figure 2.2: Violation of the Wigner-type Leggett-Garg inequality (2.7) for arbitrary Hamiltonian evolutions. Every non-trivial time evolution is in conflict with a classical description as long as one can project onto individual quantum states of the system.

with $d^2\Omega$ the solid angle element and P a normalized and *not necessarily positive* real function [3]. The spin coherent states $|\Omega\rangle \equiv |\vartheta, \varphi\rangle$, with ϑ and φ the polar and azimuthal angle, are the eigenstates with maximal eigenvalue of a spin operator pointing into the direction $\Omega \equiv (\vartheta, \varphi)$ [78, 6]: $\hat{\mathbf{J}}_\Omega |\Omega\rangle = j |\Omega\rangle$ in units where $\hbar = 1$.

In coarse-grained measurements our resolution is not able to resolve individual eigenvalues m of a spin component, say the z -component \hat{J}_z , but bunches together Δm *neighboring* outcomes into “slots” \bar{m} , where the measurement coarseness is much larger than the intrinsic quantum uncertainty of coherent states, i.e. $\Delta m \gg \sqrt{j}$.

The question arises whether it is problematic to use coarse-grained (projective) *von Neumann measurements* of the form

$$\sum_{m \in \{\bar{m}\}} |m\rangle\langle m|, \quad (2.9)$$

where $|m\rangle$ are the \hat{J}_z eigenstates, as “classical measurements” as we did in the previous chapter. In contrast to the *positive operator value measure* (POVM), they have sharp edges and could violate the Leggett-Garg inequality by distinguishing with certainty between microstates at two sides of a slot border. E.g., if $|m\rangle$ and $|m+1\rangle$ belong to two different slots, macrorealism could be violated by a simple microscopic time evolution, producing $\cos(\omega t) |m\rangle + \sin(\omega t) |m+1\rangle$. This is the reason why we model our coarse-grained \hat{J}_z measurements as belonging to a (spin coherent state) POVM, where the element corresponding to the outcome \bar{m} is represented by

$$\hat{P}_{\bar{m}} \equiv \frac{2j+1}{4\pi} \iint_{\Omega_{\bar{m}}} |\Omega\rangle\langle\Omega| d^2\Omega. \quad (2.10)$$

Here, $\Omega_{\bar{m}}$ is the angular region of polar angular size $\Delta\Theta_{\bar{m}} \sim \Delta m/j \gg 1/\sqrt{j}$ whose projection onto the z -axis corresponds to the slot \bar{m} (Figure 1.5). As the $\Omega_{\bar{m}}$ are mutually disjoint and form a partition of the whole angular region, we have

$$\sum_{\bar{m}} \hat{P}_{\bar{m}} = \mathbb{1}. \quad (2.11)$$

Due to overcompleteness of the spin coherent states the POVM elements are overlapping at the slot borders over the angular size $\sim 1/\sqrt{j}$ which is small compared to the angular slot size $\Delta\Theta_{\bar{m}}$.

To find out how $\hat{P}_{\bar{m}}$ looks like in the basis of \hat{J}_z eigenstates, we apply $\hat{P}_{\bar{m}}$ to an arbitrary state $|k\rangle$ and insert the identity operator $\sum_{k'} |k'\rangle\langle k'| = \mathbb{1}$:

$$\hat{P}_{\bar{m}} |k\rangle = \sum_{k'} \left(\frac{2j+1}{4\pi} \iint_{\Omega_{\bar{m}}} \langle k'|\Omega\rangle\langle\Omega|k\rangle d^2\Omega \right) |k'\rangle. \quad (2.12)$$

The scalar products in the above equation are of the form

$$\langle m|\Omega\rangle = \binom{2j}{j+m}^{1/2} \cos^{j+m} \frac{\vartheta}{2} \sin^{j-m} \frac{\vartheta}{2} e^{-im\varphi}, \quad (2.13)$$

where $\Omega \equiv (\vartheta, \varphi)$. The azimuthal integration $\int_0^{2\pi} \exp[i(k-k')\varphi] d\varphi$ gives $2\pi\delta_{kk'}$. The remaining integrand with $k = k'$ is the modulus square $|\langle k|\Omega\rangle|^2$ and independent of φ , but we can just substitute the 2π factor from the performed φ -integration by a trivial unperformed φ -integration to keep the simple writing with an integration over $\Omega_{\bar{m}}$. Thus,

$$\hat{P}_{\bar{m}} = \sum_k \left(\frac{2j+1}{4\pi} \iint_{\Omega_{\bar{m}}} |\langle k|\Omega\rangle|^2 d^2\Omega \right) |k\rangle\langle k| \quad (2.14)$$

is *diagonal* in the basis of \hat{J}_z eigenstates.

The probability for getting the outcome \bar{m} is given by

$$w_{\bar{m}} = \text{Tr}[\hat{\rho}\hat{P}_{\bar{m}}] = \frac{2j+1}{4\pi} \iint \langle\Omega|\hat{\rho}\hat{P}_{\bar{m}}|\Omega\rangle d^2\Omega. \quad (2.15)$$

Inserting $\hat{P}_{\bar{m}}$ from eq. (2.10), we obtain

$$w_{\bar{m}} = \left(\frac{2j+1}{4\pi} \right)^2 \iint d^2\Omega \iint_{\Omega_{\bar{m}}} d^2\Omega' \langle\Omega'|\Omega\rangle\langle\Omega|\hat{\rho}|\Omega'\rangle. \quad (2.16)$$

Using that $\frac{2j+1}{4\pi} \iint d^2\Omega |\Omega\rangle\langle\Omega|$ is the identity operator and renaming Ω' to Ω , we get

$$\boxed{w_{\bar{m}} = \iint_{\Omega_{\bar{m}}} Q(\Omega) d^2\Omega.} \quad (2.17)$$

This is *exactly* the integration of the *positive probability distribution*

$$Q(\Omega) \equiv \frac{2j+1}{4\pi} \langle\Omega|\hat{\rho}|\Omega\rangle \quad (2.18)$$

associated to the quantum state $\hat{\rho}$ (the well-know Q -function [1]) over the region $\Omega_{\bar{m}}$.

Given an arbitrary quantum state, under coarse-grained measurements the outcome probabilities at any time can exactly be computed from an ensemble of classical spins (i.e. there exists a hidden variable model). This is macrorealism per se.

2.3 Non-invasive measurability

Upon a coarse-grained measurement with outcome \bar{m} , the state $\hat{\rho}$ is reduced to

$$\hat{\rho}_{\bar{m}} = \frac{\hat{M}_{\bar{m}} \hat{\rho} \hat{M}_{\bar{m}}}{w_{\bar{m}}}, \quad (2.19)$$

where we have chosen a particular (optimal) implementation of the POVM with the Hermitean Kraus operators

$$\hat{M}_{\bar{m}} = \hat{M}_{\bar{m}}^\dagger = \sum_k \sqrt{\frac{2j+1}{4\pi}} \iint_{\Omega_{\bar{m}}} |k\rangle\langle\Omega|^2 d^2\Omega |k\rangle\langle k|. \quad (2.20)$$

It can be easily seen that they satisfy the necessary relation

$$\hat{M}_{\bar{m}}^2 = \hat{P}_{\bar{m}}.$$

We note that, independent of the concrete implementation, the $\hat{P}_{\bar{m}}$ (and the Kraus operators) behave almost as projectors for all states $|\Omega\rangle$ except for those near a slot border:

$$\hat{P}_{\bar{m}} |\Omega\rangle \approx \begin{cases} |\Omega\rangle & \text{for } \Omega \text{ inside } \Omega_{\bar{m}}, \\ \mathbf{0} & \text{for } \Omega \text{ outside } \Omega_{\bar{m}}. \end{cases} \quad (2.21)$$

In a proper classical limit ($\sqrt{j}/\Delta m \rightarrow 0$) the relative weight of these border Ω becomes *vanishingly small*.

We now show that the Q -distribution before the measurement is the (weighted) *mixture* of the Q -distributions

$$Q_{\bar{m}}(\Omega) = \frac{2j+1}{4\pi} \langle\Omega|\hat{\rho}_{\bar{m}}|\Omega\rangle \quad (2.22)$$

of the possible reduced states $\hat{\rho}_{\bar{m}}$:

$$Q(\Omega) \approx \sum_{\bar{m}} w_{\bar{m}} Q_{\bar{m}}(\Omega). \quad (2.23)$$

This demonstrates that a fuzzy measurement can be understood classically as reducing the previous ignorance about predetermined properties of the spin system.

The approximate sign “ \approx ” reflects that, depending on the density matrix

$$\hat{\rho} \equiv \sum_n \sum_{n'} c_{nn'} |n\rangle\langle n'|, \quad (2.24)$$

this relationship may only approximately hold for the set of those $\Omega \equiv (\vartheta, \varphi)$ near a slot border. In detail eq. (2.23) reads

$$\frac{2j+1}{4\pi} \sum_n \sum_{n'} c_{nn'} \langle\Omega|n\rangle\langle n'|\Omega\rangle \approx \frac{2j+1}{4\pi} \sum_n \sum_{n'} c_{nn'} \sum_{\bar{m}} \sqrt{g_{\bar{m}}(n) g_{\bar{m}}(n')} \langle\Omega|n\rangle\langle n'|\Omega\rangle \quad (2.25)$$

with

$$g_{\bar{m}}(k) \equiv \frac{2j+1}{4\pi} \iint_{\Omega_{\bar{m}}} |k\rangle\langle\Omega|^2 d^2\Omega \quad (2.26)$$

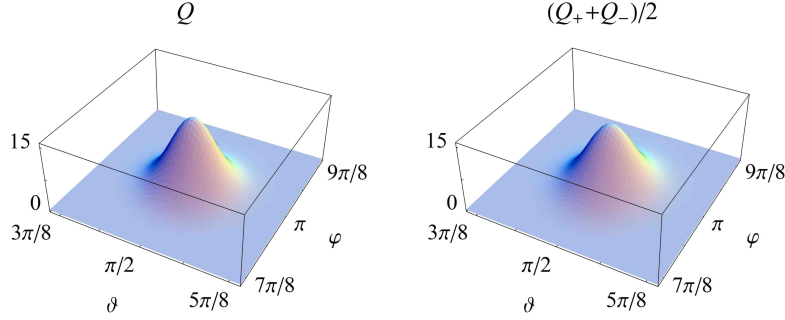


Figure 2.3: Left: The Q -distribution of the spin coherent state $|\frac{\pi}{2}, \pi\rangle$ located at the equator. Right: The mixture $\frac{1}{2}(Q_+ + Q_-)$ of the Q -distributions of the two possible reduced states in a which-hemisphere measurement. Although this is a worst-case scenario in the sense that the quantum state is located exactly at the slot border, the two distributions are very similar. The pictures are drawn for the spin size $j = 100$ but are scale invariant.

which is smaller or equal to 1. The two sides are exactly equal if $\hat{\rho}$ is diagonal as $\sum_{\bar{m}} g_{\bar{m}}(n) = 1$ for all n . Deviations only occur if n , n' and $j \cos \vartheta$ are all within a distance of order \sqrt{j} to each other and to a slot border. If they are not close to each other, the quantity $\langle \Omega | n \rangle \langle n' | \Omega \rangle$ is exponentially small and suppression by the factor $\sum_{\bar{m}} \sqrt{g_{\bar{m}}(n) g_{\bar{m}}(n')}$ is not important. If n , n' are well within a slot, $\sum_{\bar{m}} \sqrt{g_{\bar{m}}(n) g_{\bar{m}}(n')}$ is almost identical to 1.

Consider the worst-case scenario of a “which-hemisphere measurement” with only two slots $\bar{m} = +$ (northern hemisphere Ω_+) and $\bar{m} = -$ (southern hemisphere Ω_-) and an initial spin coherent state

$$\hat{\rho}_{\text{eq}} \equiv |\frac{\pi}{2}, \pi\rangle \langle \frac{\pi}{2}, \pi| \quad (2.27)$$

located exactly at the equator, i.e. the slot border. Both outcomes happen with the same probability $w_+ = w_- = \frac{1}{2}$. Figure 2.3 illustrates the unmeasured state’s Q -distribution, $Q(\Omega) = \frac{2j+1}{4\pi} \langle \Omega | \hat{\rho}_{\text{eq}} | \Omega \rangle$, and the mixture $\frac{1}{2}[Q_+(\Omega) + Q_-(\Omega)]$ of the Q -distributions

$$Q_{\pm}(\Omega) = \frac{2j+1}{4\pi} \frac{\langle \Omega | \hat{M}_{\pm} \hat{\rho}_{\text{eq}} \hat{M}_{\pm} | \Omega \rangle}{w_{\pm}} \quad (2.28)$$

of the reduced states, i.e. the left and right-hand side of eq. (2.23), respectively. Independent of the spin size j the Q -distributions with and without measurement have a very large overlap,

$$\iint \sqrt{\frac{1}{2}[Q_+(\Omega) + Q_-(\Omega)]} Q(\Omega) d^2\Omega \approx 0.997, \quad (2.29)$$

indicating the good quality of eq. (2.23). Here, the overlap between two normalized probability distributions f and g is defined by $\iint \sqrt{f(\Omega)g(\Omega)} d^2\Omega \in [0, 1]$.

However, for non-invasiveness we need more than eq. (2.23). Consider the initial distribution of classical spins, $Q(\Omega, t_0)$, corresponding to an initial quantum state $\hat{\rho}(t_0)$. We first compute the Q -distribution of the state $\hat{\rho}(t_j)$ for an undisturbed evolution without measurement until some time t_j ,

$$Q(\Omega, t_j) = \frac{2j+1}{4\pi} \langle \Omega | \hat{\rho}(t_j) | \Omega \rangle. \quad (2.30)$$

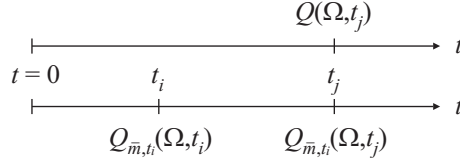


Figure 2.4: Non-invasive measurability is fulfilled if the Q -distribution at some time t_j , without any measurement before, is the same as the weighted mixture of the Q -distributions stemming from the possible reduced states from a measurement at some earlier time t_i .

This has to be compared with the *mixture* of all possible reduced distributions upon measurement at a time t_i ($t_0 \leq t_i < t_j$) with outcomes \bar{m} which evolved to t_j , denoted as

$$Q_{\bar{m}, t_i}(\Omega, t_j) = \frac{2j+1}{4\pi} \frac{\langle \Omega | \hat{U}_{t_j-t_i} \hat{M}_{\bar{m}} \hat{\rho}(t_i) \hat{M}_{\bar{m}} \hat{U}_{t_j-t_i}^\dagger | \Omega \rangle}{w_{\bar{m}, t_i}}, \quad (2.31)$$

with $w_{\bar{m}, t_i} \equiv \text{Tr}[\hat{\rho}(t_i) \hat{P}_{\bar{m}}]$ the probability for outcome \bar{m} at time t_i and $\hat{U}_t \equiv \exp(-i\hat{H}t)$ the time evolution operator (see Figure 2.4). The system evolves macrorealistically if these two quantities coincide for all t_i and t_j , i.e. if

$$Q(\Omega, t_j) \approx \sum_{\bar{m}} w_{\bar{m}, t_i} Q_{\bar{m}, t_i}(\Omega, t_j). \quad (2.32)$$

This is the condition for non-invasive measurability (together with induction).

In a dichotomic scenario, the outcomes $+$ and $-$ correspond to finding the spin system in one out of two slots $\bar{m} = \pm$. This is represented by a measurement of two complementary regions Ω_+ and Ω_- (for instance the northern and southern hemisphere in a “which hemisphere measurement”). Then, e.g., the probability for measuring $-$ at t_3 if $+$ was measured at t_1 is given by

$$q_{3-|1+} = \iint_{\Omega_-} Q_{+, t_1}(\Omega, t_3) d^2\Omega \quad (2.33)$$

with $Q_{+, t_1}(\Omega, t_3)$ the Q -distribution of the state which was reduced at t_1 with outcome $+$ and evolved to t_3 . If condition (2.32) is satisfied, it implies that the probabilities can be decomposed into “classical paths”. This means that, e.g., $q_{3-|1+}$ is just the sum of the two possible paths via $+$ and $-$ at t_2 :

$$q_{3-|1+} = q_{2+|1+} q_{3-|2+, 1+} + q_{2-|1+} q_{3-|2-, 1+}, \quad (2.34)$$

where $q_{3-|2+, 1+}$ ($q_{3-|2-, 1+}$) denotes the probability to measure $-$ at t_3 given that $+$ was measured at t_1 and $+$ ($-$) at t_2 . Thus, eq. (2.32) allows to derive Leggett-Garg inequalities such as ineq. (2.1).

2.4 The sufficient condition for macrorealism

We can now establish the sufficient condition for macrorealism that holds even for isolated systems, namely

$$\hat{P}_{\bar{m}} \hat{U}_t | \Omega \rangle \approx \begin{cases} \hat{U}_t | \Omega \rangle & \text{for one } \bar{m}, \\ \mathbf{0} & \text{for all the others,} \end{cases} \quad (2.35)$$

for all t and Ω , allowing deviations at slot borders.

This means that the time evolution does not produce superpositions of macroscopically distinct states.

Vice versa, if $\hat{U}_t |\Omega\rangle$ produced states of the form $\alpha |\Omega'\rangle + \beta |\Omega''\rangle$ where neither $|\alpha|$ nor $|\beta|$ is close to zero and with $|\Omega'\rangle$ and $|\Omega''\rangle$ belonging to macroscopically different outcomes (different slots), eq. (2.35) would not be fulfilled. Eq. (2.35) implies that $\hat{P}_{\bar{m}}$, and hence $\hat{M}_{\bar{m}}$, quasi behave as projectors and that

$$\langle \Omega | \hat{U}_{t_j - t_i} \hat{\rho}(t_i) \hat{U}_{t_j - t_i}^\dagger | \Omega \rangle \approx \sum_{\bar{m}} \langle \Omega | \hat{U}_{t_j - t_i} \hat{M}_{\bar{m}} \hat{\rho}(t_i) \hat{M}_{\bar{m}} \hat{U}_{t_j - t_i}^\dagger | \Omega \rangle \quad (2.36)$$

This directly leads to eq. (2.32). Thus, eq. (2.35) \rightarrow eq. (2.32) \rightarrow macrorealism.

2.5 An oscillating Schrödinger cat

We denote those Hamiltonians for which eq. (2.35) is satisfied under coarse-grained measurements as *classical*. An example is the rotation, say around x , $\hat{H}_{\text{rot}} = \omega \hat{J}_x$, with \hat{J}_x the spin x -component and ω the angular precession frequency, which satisfies eq. (2.35) and moreover allows a Newtonian description of the time evolution as shown in the previous chapter. But there is no *a priori* reason why all Hamiltonians should satisfy eq. (2.35).

Can one find non-classical Hamiltonians violating macrorealism despite coarse-grained measurements?

The necessary condition for such a situation is that the Hamiltonian builds up coherences between states belonging to different slots. One explicit (extreme) example is

$$\hat{H} = i\omega (|-j\rangle\langle +j| - |+j\rangle\langle -j|), \quad (2.37)$$

which, given the special initial state $|\Psi(0)\rangle = |+j\rangle$, produces a time-dependent Schrödinger cat-like superposition of two *distant* (orthogonal) spin- j coherent states $|+j\rangle$ ('north') and $|-j\rangle$ ('south'):

$$|\Psi(t)\rangle = \cos(\omega t) |+j\rangle + \sin(\omega t) |-j\rangle. \quad (2.38)$$

Under fuzzy measurements or apparatus decoherence after a premeasurement [104], the state (2.38) appears like a statistical mixture at every instance of time:

$$\hat{\rho}_{\text{mix}}(t) = \cos^2(\omega t) |+j\rangle\langle +j| + \sin^2(\omega t) |-j\rangle\langle -j|. \quad (2.39)$$

While the two states $\hat{\rho}_{\text{sup}}(t) \equiv |\Psi(t)\rangle\langle\Psi(t)|$ and $\hat{\rho}_{\text{mix}}(t)$ have dramatically different P -functions and can be distinguished by sharp measurements, they are de facto equivalent on the coarse-grained level. The Q -distributions, Q_{sup} for $\hat{\rho}_{\text{sup}}(t)$ and Q_{mix} for $\hat{\rho}_{\text{mix}}(t)$, are given by eq. (2.18). The coherence terms stemming from $\hat{\rho}_{\text{sup}}(t)$ are of the form $\langle \Omega |+j\rangle\langle -j| \Omega \rangle$ and vanish exponentially

fast with the spin length j for all Ω . For $j \gg 1$ the Q -distributions are practically identical, i.e. $Q \equiv Q_{\text{mix}} \approx Q_{\text{sup}}$:

$$Q(\Omega, t) = \frac{2j+1}{4\pi} [\cos^2(\omega t) \cos^{4j}(\frac{\Theta_1}{2}) + \sin^2(\omega t) \cos^{4j}(\frac{\Theta_2}{2})], \quad (2.40)$$

where $\Theta_1 = \vartheta$ ($\Theta_2 = \pi - \vartheta$) is the angle between $\Omega \equiv (\vartheta, \varphi)$ and $+z$ ($-z$).

In general the P -function reads [1, 2]

$$P(\Omega, t) = \sum_{k=0}^{2j} \sum_{q=-k}^k \rho_{kq} Y_{kq}(\Omega, t) \frac{(-1)^{k-q} \sqrt{(2j-k)!(2j+k+1)!}}{\sqrt{4\pi} (2j)!}. \quad (2.41)$$

Here, Y_{kq} are the spherical harmonics and

$$\rho_{kq}(t) = \sqrt{2k+1} \sum_m (-1)^{j-m} c_{m,m-q}(t) \begin{pmatrix} j & k & j \\ -m+q & -q & m \end{pmatrix}, \quad (2.42)$$

where the last bracket denotes the Wigner $3j$ symbol. The $c_{nn'}(t)$ are the coefficients in the representation (2.24) of the density matrix one is interested in.

The P and Q -functions of $\hat{\rho}_{\text{sup}}$ and $\hat{\rho}_{\text{mix}}$ at $t = \frac{\pi}{4\omega}$ are shown in Figure 2.5 for a certain choice of parameters. The P -function of the superposition is pathologically oscillating. The Q -distributions show just two peaks, corresponding to a classical mixture in which half of the spins are pointing into the north direction and the other into the south. Going to larger and larger values of j , i.e. from Schrödinger kittens to cats, makes it more and more difficult to observe the quantum nature of superposition states like (2.38). The angular resolution which is necessary to distinguish a superposition from the corresponding classical mixture is of the order of $1/\sqrt{j}$.

However, under the Hamiltonian (2.37) even simple dichotomic which-hemisphere measurements are sufficient to violate macrorealism. The temporal correlation function (for times t_i and t_j) reads

$$C_{ij} \approx \cos[\omega(t_j - t_i)] \quad (2.43)$$

with an exponentially small correction due to the tiny chance that, e.g., $|+j\rangle$ can be found in the southern hemisphere. The system effectively behaves as a spin- $\frac{1}{2}$ particle which violates the Leggett-Garg inequality. It can be easily seen that without any measurement the initial state $|+j\rangle$ evolves to the state $|-j\rangle$ at $t_2 = \frac{\pi}{2\omega}$. If, on the other hand, there is a measurement at $t_1 = \frac{\pi}{4\omega}$ in between, where we have an equal weight superposition of $|+j\rangle$ and $|-j\rangle$, the state is projected to either $|+j\rangle$ or $|-j\rangle$. Either of these reduced states will evolve to an equal weight superposition of $|+j\rangle$ and $|-j\rangle$ at t_2 . Thus, eq. (2.32) is not fulfilled for fuzzy measurements and the evolution (2.37), as shown in Figure 2.6.

Despite the fact that apparatus decoherence or coarse-graining allow to describe the state effectively by a classical mixture at every instance of time, the non-classical Hamiltonian indeed builds up superpositions of macroscopically distinct states and allows to violate macrorealism.

To get macrorealism one would have to coarse-grain always those states which are *connected by the Hamiltonian* (in time) and not necessarily in real space. In the present case it is (at least) the

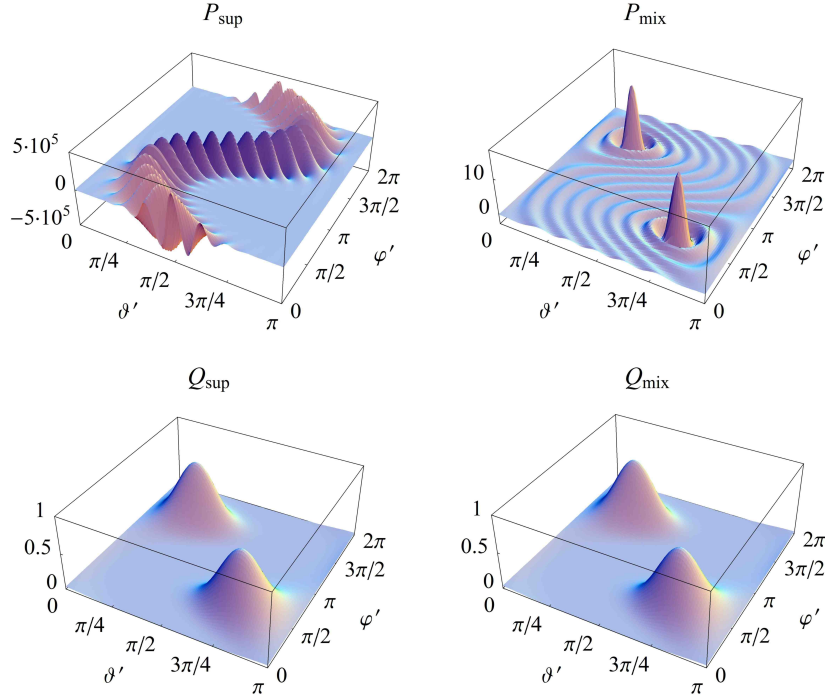


Figure 2.5: Top left: The P -function P_{sup} at time $t = \frac{\pi}{4\omega}$ of the equal-weight superposition (2.38) of two opposite spin coherent states $|+j\rangle$ and $|-j\rangle$ for spin length $j = 10$, plotted in a rotated coordinate system in which $|+j\rangle = |\frac{\pi}{4}, \frac{3\pi}{2}\rangle$. It is wildly oscillating with very large positive and negative regions. Top right: The P -function P_{mix} of the corresponding statistical mixture (2.39). Bottom: In every-day life the angular measurement resolution is much weaker than $1/\sqrt{j}$ (which is equivalent to $\Delta m \gg \sqrt{j}$ in a \hat{J}_z measurement). Then we cannot distinguish anymore between the superposition state and the classical mixture, as both effectively lead to the same (positive) Q -distribution $Q_{\text{sup}} \approx Q_{\text{mix}}$. Nevertheless, the time evolution of such a mixture can violate macrorealism even under classical coarse-grained measurements.

outcomes $+j$ and $-j$ that have to be coarse-grained into one and the same slot, which is of course highly counter-intuitive. Such a coarse-graining would lead to a different kind of macrorealistic physics than the classical laws we know, bringing systems through space and time continuously.

2.6 Continuous monitoring by an environment

Until now we have considered isolated systems. Under coarse-grained measurements or, mathematically equivalent, apparatus decoherence (where the system is isolated and only after a premeasurement of the system an uncontrollable environment couples to the apparatus), classical Hamiltonians lead to macrorealism whereas non-classical Hamiltonians allow to violate it. The question arises:

What happens if the Hamiltonian is non-classical and the system is continuously monitored by an environment?

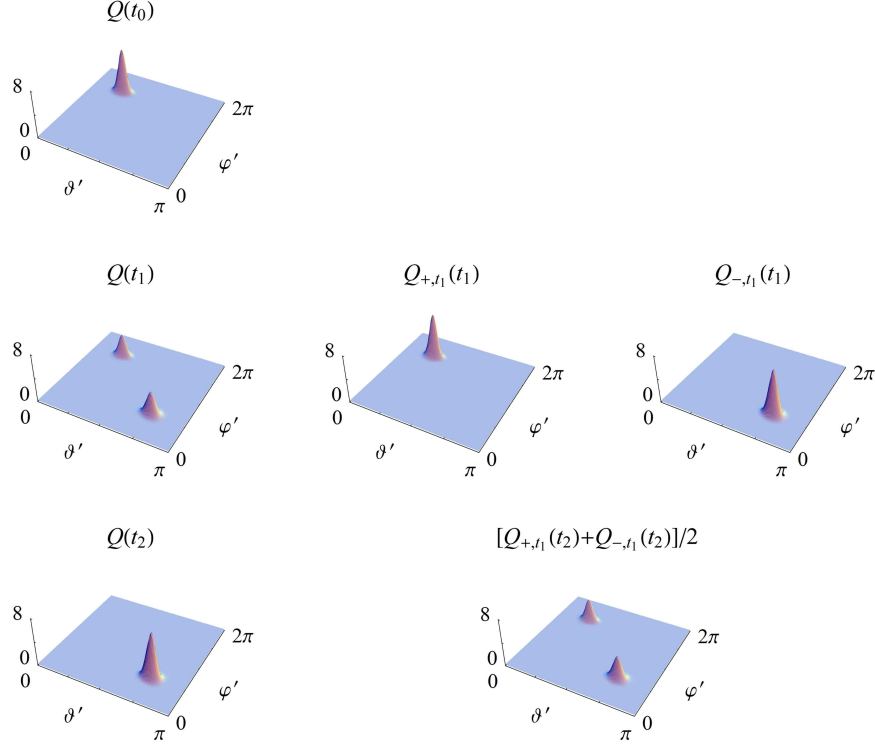


Figure 2.6: The time evolution of the Q -distribution for the non-classical (oscillating Schrödinger cat) Hamiltonian (2.37), shown for a spin $j = 100$. At time $t_0 = 0$ the quantum state is $|+j\rangle$ ('north') with the Q -distribution $Q(t_0)$. At the later time $t_1 = \frac{\pi}{4\omega}$ the spin is in an equal-weight superposition of $|+j\rangle$ and $|-j\rangle$ and the Q -distribution $Q(t_1)$ shows two peaks at north and south. If no measurement takes place, the system reaches the state $|-j\rangle$ ('south') at $t_2 = \frac{\pi}{2\omega}$, represented by $Q(t_2)$. If, on the other hand, one performs a measurement at t_1 , the state is reduced to either $|+j\rangle$ or $|-j\rangle$, with Q -distributions $Q_{+,t_1}(t_1)$ and $Q_{-,t_1}(t_1)$, respectively. Either of these two states will evolve into an equal-weight superposition until t_2 . The weighted mixture at that time, $[Q_{+,t_1}(t_2) + Q_{-,t_1}(t_2)]/2$ is different from the undisturbed evolution. Eqs. (2.35) and (2.32) are not fulfilled. Although at every instance of time the system can be described by a classical mixture, the time evolution of this mixture allows to violate the Leggett-Garg inequality and is in conflict with macrorealism.

Given the non-classical Hamiltonian (2.37) with the time evolution operator

$$\begin{aligned} \hat{U}_t = & + \cos(\omega t) (|+j\rangle\langle+j| + |-j\rangle\langle-j|) \\ & + \sin(\omega t) (|-j\rangle\langle+j| - |+j\rangle\langle-j|) + \sum_{m=-j+1}^{j-1} |m\rangle\langle m|, \end{aligned} \quad (2.44)$$

let us approximate the effects of system decoherence by the following simplified model: The initial state along north,

$$\hat{\rho}(0) = |+j\rangle\langle+j|, \quad (2.45)$$

freely evolves without decoherence a short time Δt to

$$\begin{aligned}\hat{\rho}(\Delta t) &= \hat{U}_{\Delta t} \hat{\rho}(0) \hat{U}_{\Delta t}^\dagger \\ &= \cos^2(\omega\Delta t) | +j \rangle \langle +j | + \sin^2(\omega\Delta t) | -j \rangle \langle -j | + \text{coh. terms},\end{aligned}\quad (2.46)$$

where the coherence terms are of the form $| +j \rangle \langle -j |$ and $| -j \rangle \langle +j |$. Now we assume that the macroscopic spin system decoheres very rapidly (in the standard pointer basis of $| +j \rangle$ and $| -j \rangle$), for instance due to the fact that a single qubit from the environment couples to it in a c-not manner [104], becomes inaccessible immediately afterwards, and does not interact (recohere) with it anymore. If it is impossible to make (joint) measurements on the environmental qubit (and our spin system), the partial trace over the qubit of the total density matrix has to be performed, which kills the coherence terms in eq. (2.46), leading to the decohered state of the system:

$$\hat{\rho}(\Delta t) = \cos^2(\omega\Delta t) | +j \rangle \langle +j | + \sin^2(\omega\Delta t) | -j \rangle \langle -j |. \quad (2.47)$$

Assuming again free time evolution for a duration of Δt , this decohered state will evolve to

$$\begin{aligned}\hat{\rho}(2\Delta t) &= \hat{U}_{\Delta t} \hat{\rho}(\Delta t) \hat{U}_{\Delta t}^\dagger \\ &= [\cos^4(\omega\Delta t) + \sin^4(\omega\Delta t)] | +j \rangle \langle +j | + 2 \cos^2(\omega\Delta t) \sin^2(\omega\Delta t) | -j \rangle \langle -j | + \text{coh. terms}.\end{aligned}\quad (2.48)$$

Repeating the alternating sequence of rapid decoherence and free time evolution, we obtain the general expression for the (decohered) state at time $n\Delta t$:

$$\hat{\rho}(n\Delta t) = A_n | +j \rangle \langle +j | + (1 - A_n) | -j \rangle \langle -j |. \quad (2.49)$$

The survival probability to find the state along north, A_n , can be retrieved from the recurrence relation

$$A_0 = 1, \quad (2.50)$$

$$A_n = a A_{n-1} + (1-a)(1 - A_{n-1}) \quad (2.51)$$

with integer n and

$$a \equiv \cos^2(\omega\Delta t). \quad (2.52)$$

If Δt is not too small (to avoid a quantum Zeno-like freezing of the initial state [66]) but smaller than the dynamical timescale of the Hamiltonian, $\frac{1}{\omega}$, the probability A_n decays to $A_\infty = \frac{1}{2}$ in a way which can be very well approximated by

$$A(t) = \frac{1}{2} (1 - e^{-\nu t}) \quad (2.53)$$

with $\frac{1}{\nu}$ the characteristic decay time. For $t \gg \frac{1}{\nu}$ the state becomes an equal weight statistical mixture

$$\hat{\rho}(\infty) = \frac{| +j \rangle \langle +j | + | -j \rangle \langle -j |}{2} \quad (2.54)$$

as illustrated in Figure 2.7.

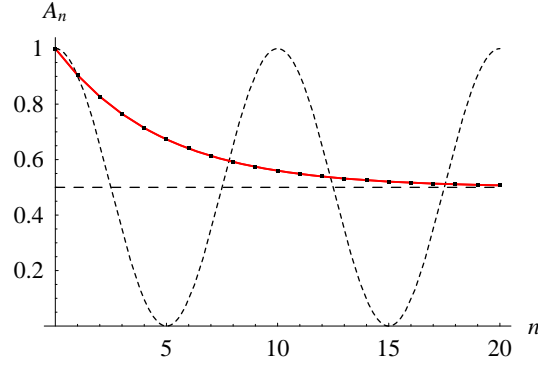


Figure 2.7: The survival probability A_n (black squares in red curve) in the decohered state $\hat{\rho}(n\Delta t)$, eq. (2.49), as a function of the number of steps, n . The free evolution time interval between instances of rapid decoherence is chosen to be $\Delta t = \frac{\pi}{10\omega}$, where ω is the angular frequency in the non-classical Hamiltonian (2.37). The state is driven into an equal weight mixture, eq. (2.54), with $A_\infty = \frac{1}{2}$ (approaching the dashed line asymptotically). For comparison, we also draw the function $\cos^2(\omega t) = \cos^2(\omega n\Delta t)$ which is the probability to find the state along north, i.e. $|+j\rangle$, at time t if no environmental decoherence takes place (dashed curve).

The conclusion of this simple and crude model of decoherence—namely that the state is driven into a mixture where half of the spins point to north and half of the spins point to south—is expected to remain valid under more realistic circumstances where one does not separate into free evolution and rapid decoherence. As long as the environmental microscopic degrees of freedom only couple to the macroscopic spin system but do not disturb its diagonal elements, the system does not leave the subspace spanned by $|+j\rangle$ and $|-j\rangle$, and never populates any of the other states $|m\rangle$.

Importantly, despite the non-classical Hamiltonian, the exponential decay of A_n due to decoherence does not allow to violate the Leggett-Garg inequality any longer. If no (coarse-grained) measurement takes place, the spin’s Q -distribution at time t_j —i.e. the left-hand side of eq. (2.32)—is given by

$$Q(t_j) = A(t_j) Q_{\text{north}} + [1 - A(t_j)] Q_{\text{south}}, \quad (2.55)$$

where Q_{north} (Q_{south}) is the Q -distribution of a spin pointing to the north (south). If a measurement takes place at the intermediate time t_i ($0 < t_i < t_j$),² the weighted mixture of the reduced and evolved Q -distributions—i.e. the right-hand side of eq. (2.32)—takes on exactly the same form for all choices of t_i and t_j , given the exponential decay $A(t) = \frac{1}{2}(1 - e^{-\nu t})$, eq. (2.53), is used.³ Hence, the system’s time evolution fulfills the condition (2.32) for non-invasive measurability, and consequently macrorealism is satisfied.

However, decoherence cannot account for a continuous spatiotemporal description of the spin system in terms of classical laws of motion.

²Note: After finding the spin along *south* at t_i , which happens with probability $1 - A(t_i)$, $A(t_j - t_i)$ is the (survival) probability to find the spin again along south at time t_j .

³It is interesting that any other form of the survival probability other than exponential decay violates the non-invasiveness condition (2.32).

To see this, it is enough to use coarse-grained measurements corresponding to only three different angular regions, one covering the northern part, one the equatorial region, and one the southern part. The initial spin along north can be found pointing to the south at some later time, *although it did not go through the equatorial region*. No classical Hamilton function can achieve such discontinuous “jumps” of a spin vector. For claiming that classicality emerges from quantum physics, it is simply not enough to show that the density matrix is driven into a diagonal form due to tracing out the environmental degrees of freedom. One must also demonstrate that the time evolution of this mixed state can be described in terms of classical laws of motion. Classical physics is within the class of macrorealistic theories but it is more restrictive than macrorealism itself.

The key point here is that in classical physics we have Newton’s or Hamilton’s *differential equations for observable quantities* such as spin directions. Under all circumstances these equations evolve the observables continuously through real space. In quantum mechanics, however, the situation is very different. The Schrödinger equation evolves the state vector continuously through Hilbert space but one cannot give a spatiotemporal description of the system’s observables independent of observation.

Figure 2.8 gives an overview of the conclusions we have reached until this point concerning the Leggett-Garg inequality, macrorealism, and classical laws of motion with respect to sharp and coarse-grained measurements as well as classical and non-classical Hamiltonians.

2.7 Non-classical Hamiltonians are complex

Finally, we suggest a possible reason why non-classical evolutions might be unlikely to be realized by nature: Such evolutions (i) either require Hamiltonians with many-particle interactions or (ii) a specific sequence of a large number of computational steps if only few-particle interactions are used. Then, they are of *high computational complexity*. In the first case the number of interacting particles, and in the second the number of computational steps has to scale linearly with the size of the Schrödinger cat state. Both cases intuitively seem to be of very low probability to happen spontaneously.

Consider our spin- j as a macroscopic ensemble of $N = 2j$ spin- $\frac{1}{2}$ particles (i.e. qubits) such as, e.g., any magnetic material is constituted by many individual microscopic spins. For violating macrorealism it is necessary to build up superpositions of two macroscopically distinct coherent states. For large j their angular separation $\Delta\theta$ can be very small and only has to obey the coarse-graining condition $\Delta\theta \gg 1/\sqrt{j}$. This guarantees quasi-orthogonality as their (modulus square) overlap is $\cos^{4j}(\Delta\theta/2) \sim e^{-j\Delta\theta^2}$. Without loss of generality we consider again the particular Hamiltonian (2.37). If $|0\rangle$ and $|1\rangle$ denote the individual qubit states ‘up’ and ‘down’ along z , then $|11\dots 1\rangle$ and $|00\dots 0\rangle$ form the total spin coherent states $|+j\rangle$ and $|-j\rangle$, respectively. The Hamiltonian represents N -particle interactions of the form

$$\hat{H} = \frac{i\omega}{2} (\hat{\sigma}_-^{\otimes N} - \hat{\sigma}_+^{\otimes N}), \quad (2.56)$$

where $\hat{\sigma}_\pm \equiv \hat{\sigma}_x \pm i\hat{\sigma}_y$ with $\hat{\sigma}_x$ and $\hat{\sigma}_y$ the Pauli operators. As an alternative one can simulate the evolution governed by this many-body interaction by means of a series of (in nature typically

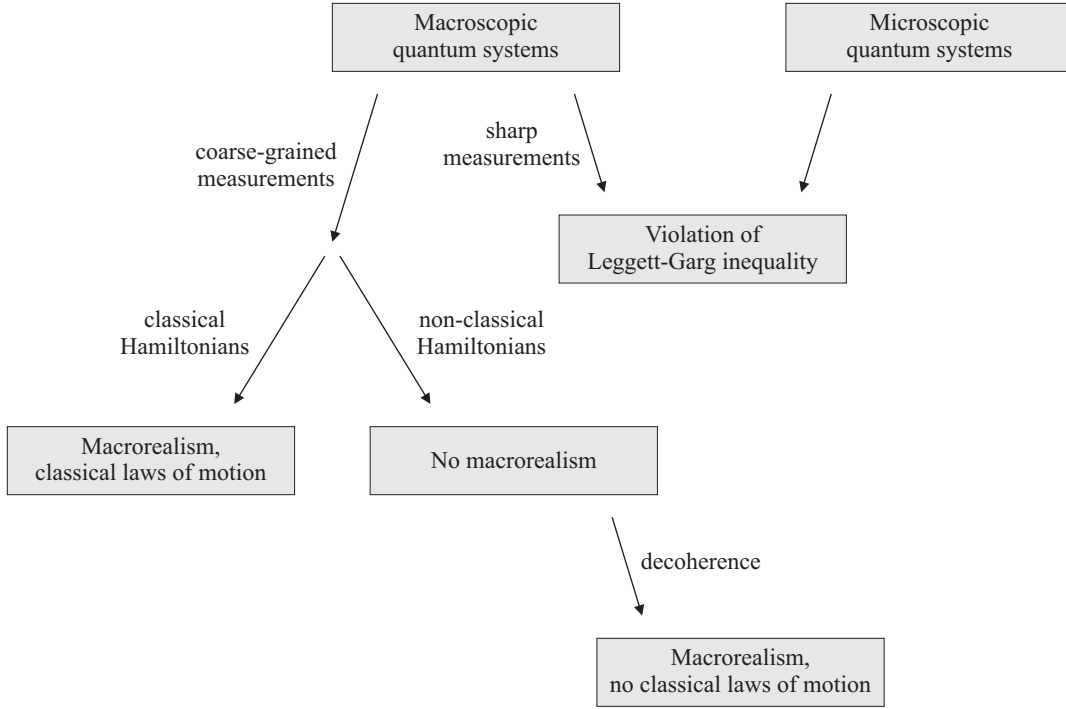


Figure 2.8: Microscopic systems as well as macroscopic systems under sharp measurements allow to violate the Leggett-Garg inequality. Since no macroscopic “classical” observables are involved, one cannot speak about a violation of macrorealism in these cases. Under coarse-grained measurements of a macroscopic system and classical Hamiltonians not only macrorealism is valid but also classical laws of motion emerge. Non-classical Hamiltonians allow to violate macrorealism even under coarse-grained measurements. Decoherence then establishes macrorealism but cannot account for a description of the system’s time evolution in terms of classical laws of motion.

appearing) few-qubit interactions (gates), using the methods of quantum computation science [67]. The task is to simulate

$$|11\dots 1\rangle \rightarrow \cos(\omega t) |11\dots 1\rangle + \sin(\omega t) |00\dots 0\rangle. \quad (2.57)$$

Assuming next-neighbor qubit interactions, we start from the state $|11\dots 1\rangle$ and rotate the first qubit ‘1’ by a small angle $\omega\Delta t$: $|1\rangle_1 \rightarrow \cos(\omega\Delta t) |1\rangle_1 + \sin(\omega\Delta t) |0\rangle_1$. Then we perform a controlled-not (c-not) gate between this qubit ‘1’ and its neighbor ‘2’ such that $|x\rangle_1|y\rangle_2 \rightarrow |x\rangle_1|x\oplus y\rangle_2$ ($x, y = 0, 1$). Afterwards c-nots between qubits are performed such that all other qubits are reached. The whole procedure is depicted in Figure 2.9(a). This procedure brings us to the state at time Δt : $|11\dots 1\rangle \rightarrow \cos(\omega\Delta t) |11\dots 1\rangle + \sin(\omega\Delta t) |00\dots 0\rangle$. To simulate the next time interval Δt , we have to undo all the c-nots, rotate the first qubit again by $\omega\Delta t$, and make all the c-nots again, leading to the correct state at time $2\Delta t$. With this procedure we get a sequence of states, simulating the evolution (2.57). One needs $O(N)$ computational steps per interval Δt . This is known to be optimal in the case where only neighboring qubits can interact [15]. Relaxing this condition and

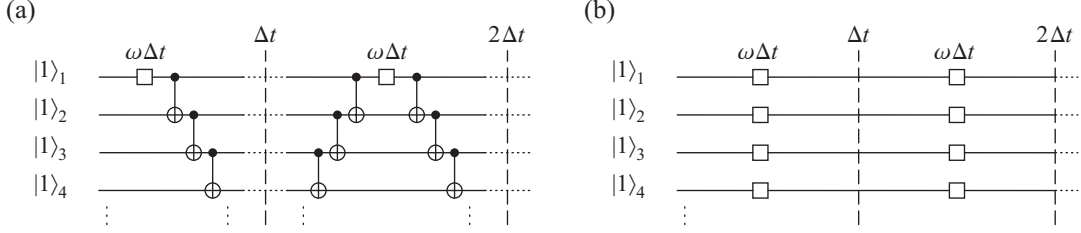


Figure 2.9: (a) In order to simulate the time evolution (2.57) of a qubit chain one has to rotate the first qubit by a small angle $\omega\Delta t$ and sequentially make c-nots. For the next time interval Δt one has to undo the c-nots, rotate the first qubit again and make all the c-nots again. With this procedure one gets a sequence of states which approximate (2.57). (b) In contrast, the simulation of an interval Δt of a spin rotation of the whole chain can be achieved in a single global transformation on all qubits simultaneously.

permitting two-qubit interactions between all possible qubits, allows to decrease the number of sequential steps but does not change the total number $O(N)$ of necessary gates per interval.

Note for comparison, however, that the rotation (say around x)

$$\hat{H}_{\text{rot}} = \frac{\omega}{2} \sum_{k=1}^N \hat{\sigma}_x^{(k)}, \quad (2.58)$$

with k labeling the qubits, does not require multi-particle interactions. Moreover, the simulation of an interval Δt of a spin rotation of the whole chain, i.e.

$$|111\dots\rangle \rightarrow [\cos(\omega\Delta t) |1\rangle + \sin(\omega\Delta t) |0\rangle]^{\otimes N}, \quad (2.59)$$

can be achieved in a *single global transformation* on all qubits simultaneously, as shown in Figure 2.9(b).

While both evolutions are rotations in Hilbert space (and require only polynomial resources), the simulation of the non-classical cosine-law between states that are distant in real space is—for macroscopically large N —computationally much more complex than the classical rotation in real space.⁴

2.8 Information and randomness

In a perfect von Neumann measurement of a spin component with sharp resolution an individual state $|m\rangle$ out of the $2j + 1 \approx 2j$ possible ones carries

$$I_{\text{sharp}} \approx \log_2(2j) = 1 + \log_2 j \quad (2.60)$$

bits of information. Coarse-grained measurements correspond to the fact that we cannot resolve individual eigenvalues m but only whole bunches of size $\Delta m \gg \sqrt{j}$. The finding that an outcome lies in a certain slot of size $\Delta m = c\sqrt{j}$ (with $c \gg 1$) carries only

$$I_{\text{c.-g.}} \approx \log_2\left(\frac{2j}{c\sqrt{j}}\right) = 1 - \log_2 c + \frac{1}{2} \log_2 j \quad (2.61)$$

⁴One should, however, mention the possibility that an *external* field may produce an effectively simple non-classical Hamiltonian for N qubits where the field interacts with the collective modes $|+j\rangle = |11\dots 1\rangle$ and $|-j\rangle = |00\dots 0\rangle$.

bits of information. For large j , i.e. $j \gg c \gg 1$, the information gain in a sharp quantum measurement is approximately $\log_2 j$ bits, whereas in the classical case it is (at most) only half of that, namely $\frac{1}{2} \log_2 j$ bits [55]:

$$I_{\text{c.-g.}} \approx \frac{1}{2} I_{\text{sharp}}. \quad (2.62)$$

Finally, we note that—given coarse-grained measurements—it is objectively random which of the two states, ‘north’ or ‘south’, one will find in a spin measurement in the Schrödinger cat state (2.38). Classical physics emerges out of the quantum world but the randomness in the classical mixture is still irreducible. Which possibility becomes factual is objectively random and does not have a causal reason, according to the Copenhagen interpretation.

In the last chapter we will address the question of quantum randomness in more detail and link it with mathematical undecidability.

Chapter 3

Entanglement between macroscopic observables

Summary:

We investigate entanglement between collective operators of two blocks of oscillators in an infinite linear harmonic chain. These operators are defined as averages over local operators (individual oscillators) in the blocks. On the one hand, this approach of “physical blocks” meets realistic experimental conditions, where measurement apparatuses do not interact with single oscillators but rather with a whole bunch of them, i.e. where in contrast to usually studied “mathematical blocks” not every possible measurement on them is allowed. On the other, this formalism naturally allows the generalization to blocks which may consist of several non-contiguous regions. We quantify entanglement between the collective operators by a measure based on the Peres-Horodecki criterion and show how it can be extracted and transferred to two qubits. Entanglement between two blocks is found even in the case where none of the oscillators from one block is entangled with an oscillator from the other, showing genuine bipartite entanglement between collective operators. Allowing the blocks to consist of a periodic sequence of subblocks, we verify that entanglement scales at most with the total boundary region. We also apply the approach of collective operators to scalar quantum field theory.

What can we learn about entanglement between individual particles in macroscopic samples by observing only the collective properties of the ensembles? Using only a few experimentally feasible collective properties, we establish an entanglement measure between two samples of spin- $\frac{1}{2}$ particles (as representatives of two-dimensional quantum systems). This is a tight lower bound for the average entanglement between all pairs of spins in general and is equal to the average entanglement for a certain class of systems. We compute the entanglement measures for explicit examples and show how to generalize the method to more than two samples and multi-partite entanglement. On the fundamental side, our method demonstrates that there is no reason in principle why purely quantum correlations could not have an effect on the global properties of objects. On the practical side, it enables us to characterize the structure of entanglement in large spin systems by performing

only a few feasible measurements of their collective properties, independently of the symmetry and mixedness of the state.

Since this analysis uses sharp measurements, it is not in disagreement with our quantum-to-classical approach resting upon coarse-grained measurements.

This chapter mainly bases on and also uses parts of References [53, 54]:

- J. Kofler, V. Vedral, M. S. Kim, and Č. Brukner
Entanglement between collective operators in a linear harmonic chain
Phys. Rev. A **73**, 052107 (2006).
- J. Kofler and Č. Brukner
Entanglement distribution revealed by macroscopic observations
Phys. Rev. A **74**, 050304(R) (2006).

3.1 The linear harmonic chain

Quantum entanglement is a physical phenomenon in which the quantum states of two or more systems can only be described with reference to each other, even though the individual systems may be spatially separated. This leads to correlations between observables of the systems that cannot be understood on the basis of classical (local realistic) theories [9]. Its importance today exceeds the realm of the foundations of quantum physics and entanglement has become an important physical resource, like energy, that allows performing communication and computation tasks with efficiency which is not achievable classically [67]. Moving to higher-dimensional entangled systems or entangling more systems with each other, will eventually push the realm of quantum physics well into the macroscopic world. It will therefore be important to investigate under which conditions entanglement within or between “macroscopic” objects, each consisting of a sample containing a large number of the constituents, can arise.

Recently, it was shown that macroscopic entanglement can arise “naturally” between constituents of various complex physical systems. Examples of such systems are chains of interacting spin systems [67, 5], harmonic oscillators [7, 85] and quantum fields [81]. Entanglement can have an effect on the macroscopic properties of these systems [37, 98, 18] and can be in principle extractable from them for quantum information processing [81, 71, 80, 27].

With the aim of better understanding macroscopic entanglement we will investigate entanglement between *collective operators*. A simple and natural system is the ground state of a linear chain of harmonic oscillators furnished with harmonic nearest-neighbor interaction. The mathematical entanglement properties of this system were extensively investigated in [7, 13, 85, 72]. Entanglement was computed in the form of logarithmic negativity for general bisections of the chain and for contiguous blocks of oscillators that do not comprise the whole chain. It was shown that the log-negativity typically decreases exponentially with the separation of the groups and that the larger the groups, the larger the maximal separation for which the log-negativity is non-zero [7]. It also was proven that an area law holds for harmonic lattice systems, stating that the amount of entanglement between two complementary regions scales with their boundary [26, 100].

In a real experimental situation, however, we are typically not able to determine the complete mathematical amount of entanglement (as measured, e.g., by log-negativity) which is non-zero even if two blocks share only one arbitrarily weak entangled pair of oscillators. Our measurement apparatuses normally cannot resolve single oscillators, but rather interact with a whole bunch of them in one way, potentially even in *non-contiguous regions*, thus measuring certain *global properties*. Here we will study entanglement between “physical blocks” of harmonic oscillators—existing only if there is entanglement between the *collective operators* defined on the entire blocks—as a function of their size, relative distance and the coupling strength. Our aim is to quantify (experimentally accessible) entanglement between global properties of two groups of harmonic oscillators. Surprisingly, we will see that such collective entanglement can be demonstrated even in the case where none of the oscillators from one block is entangled with an oscillator from the other block (i.e. it cannot be understood as a cumulative effect of entanglement between pairs of oscillators), which is in agreement with Reference [7]. This shows the existence of bipartite entanglement between

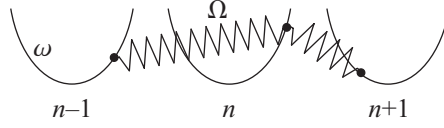


Figure 3.1: In a linear harmonic chain the oscillators are situated in a harmonic potential with frequency ω . Each oscillator, labeled with the index n , is coupled with its nearest neighbors, $n - 1$ and $n + 1$, by a harmonic potential with the coupling frequency Ω .

collective operators.

Because of the area law [26, 100] the amount of entanglement is relatively small in the first instance. We suggest a way to overcome this problem by allowing the collective blocks to consist of a *periodic sequence of subblocks*. Then the total boundary region between them is increased and we verify that indeed a larger amount of entanglement is found for periodic blocks, where the entanglement scales at most with the *total* boundary region. We give an analytical approximation of this amount of entanglement and motivate how it can in principle be extracted from the chain [81, 71, 80, 27].

Methodologically, we will quantify the entanglement between collective operators of two blocks of harmonic oscillators by using a measure for continuous variable systems based on the Peres-Horodecki criterion [75, 44, 88, 50]. The collective operators will be defined as sums over local operators for all single oscillators belonging to the block. The infinite harmonic chain is assumed to be in the ground state and since the blocks do not comprise the whole chain, they are in a mixed state.

We investigate a linear harmonic chain, where each of the N oscillators is situated in a harmonic potential with frequency ω and each oscillator is coupled with its neighbors by a harmonic potential with the coupling frequency Ω (Figure 3.1). The oscillators have mass m and their positions and momenta are denoted as \bar{q}_i and \bar{p}_i , respectively. Assuming periodic boundary conditions ($\bar{q}_{N+1} \equiv \bar{q}_1$), the Hamilton function reads [84]

$$H = \sum_{j=1}^N \left(\frac{\bar{p}_j^2}{2m} + \frac{m\omega^2 \bar{q}_j^2}{2} + \frac{m\Omega^2 (\bar{q}_j - \bar{q}_{j-1})^2}{2} \right). \quad (3.1)$$

We canonically introduce dimensionless variables: $q_j \equiv C \bar{q}_j$ and $p_j \equiv \bar{p}_j / C$, where C is given by $C \equiv \sqrt{m\omega(1 + 2\Omega^2/\omega^2)^{1/2}}$ [13]. By this means the Hamilton function becomes

$$H = \frac{E_0}{2} \sum_{j=1}^N (p_j^2 + q_j^2 - \alpha q_j q_{j+1}), \quad (3.2)$$

with the abbreviations $\alpha \equiv 2\Omega^2/(2\Omega^2 + \omega^2)$ and $E_0 \equiv \sqrt{2\Omega^2 + \omega^2}$. The (single) coupling constant is restricted to values $0 < \alpha < 1$, where $\alpha \rightarrow 0$ in the weak coupling limit ($\Omega/\omega \rightarrow 0$) and $\alpha \rightarrow 1$ in the strong coupling limit ($\Omega/\omega \rightarrow \infty$).

In the language of second quantization the positions and momenta are converted into operators ($q_j \rightarrow \hat{q}_j$, $p_j \rightarrow \hat{p}_j$) and are expanded into modes of their annihilation and creation operators, \hat{a}

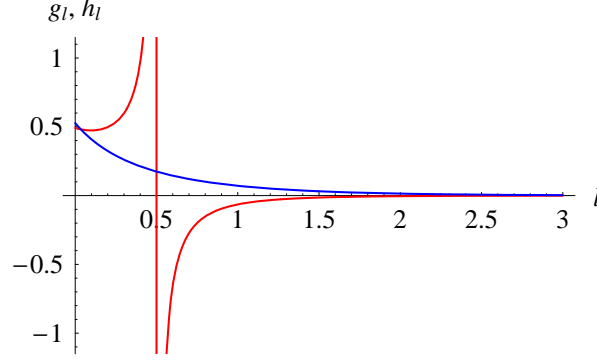


Figure 3.2: The two-point vacuum correlation functions (3.6) and (3.7) for the linear harmonic chain with coupling $\alpha = 0.5$. The blue curve shows $h_{|i-j|} \equiv \langle 0 | \hat{q}_i \hat{q}_j | 0 \rangle$, and the red curve shows $h_{|i-j|} \equiv \langle 0 | \hat{p}_i \hat{p}_j | 0 \rangle$ with $l \equiv |i-j|$. Only integer values for l are meaningful.

and \hat{a}^\dagger , respectively:

$$\hat{q}_j = \frac{1}{\sqrt{N}} \sum_{k=0}^{N-1} \frac{1}{\sqrt{2\nu(\theta_k)}} [\hat{a}(\theta_k) e^{i\theta_k j} + \text{H.c.}], \quad (3.3)$$

$$\hat{p}_j = \frac{-i}{\sqrt{N}} \sum_{k=0}^{N-1} \sqrt{\frac{\nu(\theta_k)}{2}} [\hat{a}(\theta_k) e^{i\theta_k j} - \text{H.c.}]. \quad (3.4)$$

Here $\theta_k \equiv 2\pi k/N$ (with $k = 0, 1, \dots, N-1$) is the dimensionless pseudo-momentum and

$$\nu(\theta_k) \equiv \sqrt{1 - \alpha \cos \theta_k} \quad (3.5)$$

is the dispersion relation. The annihilation and creation operators fulfil the well known commutation relation $[\hat{a}(\theta_k), \hat{a}^\dagger(\theta_{k'})] = \delta_{kk'}$, since $[\hat{q}_i, \hat{p}_j] = i\delta_{ij}$ has to be guaranteed. The ground state (vacuum), denoted as $|0\rangle$, is defined by $\hat{a}(\theta_k)|0\rangle = 0$ holding for all θ_k . The two-point vacuum correlation functions are

$$g_{|i-j|} \equiv \langle 0 | \hat{q}_i \hat{q}_j | 0 \rangle \equiv \langle \hat{q}_i \hat{q}_j \rangle = (2N)^{-1} \sum_{k=0}^{N-1} \nu^{-1}(\theta_k) \cos(l\theta_k), \quad (3.6)$$

$$h_{|i-j|} \equiv \langle 0 | \hat{p}_i \hat{p}_j | 0 \rangle \equiv \langle \hat{p}_i \hat{p}_j \rangle = (2N)^{-1} \sum_{k=0}^{N-1} \nu(\theta_k) \cos(l\theta_k), \quad (3.7)$$

where $l \equiv |i-j|$. In the limit of an infinite chain ($N \rightarrow \infty$)—which we will study below—and for $l < N/2$ they can be expressed in terms of the hypergeometric function ${}_2F_1$ [13]: $g_l = [z^l/(2\mu)] \binom{l-1/2}{l} {}_2F_1(1/2, l+1/2, l+1, z^2)$, $h_l = (\mu z^l/2) \binom{l-3/2}{l} {}_2F_1(-1/2, l-1/2, l+1, z^2)$, where $z \equiv (1 - \sqrt{1 - \alpha^2})/\alpha$ and $\mu \equiv 1/\sqrt{1 + z^2}$ (Figure 3.2).

3.1.1 Defining collective operators

In the following, we are interested in entanglement between two “physical blocks” of oscillators, where the blocks are represented by a specific form of *collective operators* which are normalized sums of individual operators. By means of such a formalism we seek to fulfil experimental conditions

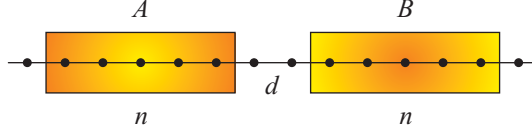


Figure 3.3: Two blocks A and B of a harmonic chain. Each block consists of n oscillators and the blocks are separated by d oscillators.

and constraints, since *finite experimental resolution implies naturally the measurement of, e.g., the average momentum of a bunch of oscillators rather than the momentum of only one*. On the other hand, this formalism can easily take account of blocks that *consist of non-contiguous regions*, leading to interesting results which will be shown below. We want to point out that this convention of the term *block* is not the same as it is normally used in the literature. In contrast to the latter, for which one allows any possible measurement, our simulation of realizable experiments already lacks some information due to the averaging.

Let us now consider two non-overlapping blocks of oscillators, A and B , within the closed harmonic chain in its ground state, where each block contains n oscillators. The blocks are separated by $d \geq 0$ oscillators (Figure 3.3). We assume $n, d \ll N$ and $N \rightarrow \infty$ for the numerical calculations of the two-point correlation functions.

By a Fourier transform we map the n oscillators of each block onto n (“orthogonal”) *frequency-dependent* collective operators

$$\hat{Q}_A^{(k)} \equiv \frac{1}{\sqrt{n}} \sum_{j \in A} \hat{q}_j e^{\frac{2\pi i j k}{n}}, \quad (3.8)$$

$$\hat{P}_A^{(k)} \equiv \frac{1}{\sqrt{n}} \sum_{j \in A} \hat{p}_j e^{-\frac{2\pi i j k}{n}}, \quad (3.9)$$

with the frequencies $k = 0, \dots, n-1$, and analogously for block B . The commutator of the collective position and momentum operators is

$$[\hat{Q}_A^{(k)}, \hat{P}_A^{(k')}] = i \delta_{kk'}. \quad (3.10)$$

This means that collective operators for different frequencies $k \neq k'$ commute. For different blocks the commutator vanishes: $[\hat{Q}_A^{(k)}, \hat{P}_B^{(k')}] = 0$.

If the individual positions and momenta of all oscillators are written into a vector

$$\hat{\mathbf{x}} \equiv (\hat{q}_1, \hat{p}_1, \hat{q}_2, \hat{p}_2, \dots, \hat{q}_N, \hat{p}_N)^T, \quad (3.11)$$

with T denoting the transpose, then there holds the commutation relation

$$[\hat{x}_i, \hat{x}_j] = i \Omega_{ij} \quad (3.12)$$

with Ω the n -fold direct sum of 2×2 symplectic matrices:

$$\Omega \equiv \bigoplus_{j=1}^n \begin{pmatrix} 0 & 1 \\ -1 & 0 \end{pmatrix}. \quad (3.13)$$

A matrix \mathbf{S} transforms $\hat{\mathbf{x}}$ into a vector of collective (and uninvolved individual) oscillators:

$$\hat{\mathbf{X}} \equiv \mathbf{S} \hat{\mathbf{x}} = (\{\hat{Q}_A^{(k)}, \hat{P}_A^{(k)}\}_k, \{\hat{Q}_B^{(k)}, \hat{P}_B^{(k)}\}_k, \{\hat{q}_j, \hat{p}_j\}_j)^T. \quad (3.14)$$

Here $\{\hat{Q}_A^{(k)}, \hat{P}_A^{(k)}\}_k = (\hat{Q}_A^{(0)}, \hat{P}_A^{(0)}, \dots, \hat{Q}_A^{(n-1)}, \hat{P}_A^{(n-1)})$ denotes all collective oscillators of block A and analogously for block B , whereas $\{\hat{q}_j, \hat{p}_j\}_j$ denotes the $2(N - 2n)$ position and momentum entries of those $N - 2n$ oscillators which are not part of one of the two blocks. The matrix \mathbf{S} corresponds to a Gaussian operation [31]. It has determinant $\det \mathbf{S} = 1$ and preserves the symplectic structure

$$\mathbf{\Omega} = \mathbf{S}^T \mathbf{\Omega} \mathbf{S}, \quad (3.15)$$

and hence

$$[\hat{X}_i, \hat{X}_j] = i\Omega_{ij} \quad (3.16)$$

for all i, j , in particular verifying eq. (3.10). This means that the Gaussianness of the ground state of the harmonic chain (i.e. the fact that the state is completely characterized by its first and second moments) is preserved by the (Fourier) transformation to the frequency-dependent collective operators.

3.1.2 Quantifying entanglement between collective operators

In reality, we are typically not capable of single particle resolution measurements but only of measuring the collective operators with one frequency, namely $k = 0$, i.e. the “average” over the individual oscillators. Note that in general the correlations of higher-frequency collective operators, e.g., $\langle (\hat{Q}_A^{(k)})^2 \rangle$ or $\langle \hat{Q}_A^{(k)} \hat{Q}_B^{(k)} \rangle$ with $k \neq 0$, are not real numbers. Therefore, as a natural choice, we denote as the collective operators

$$\boxed{\begin{aligned} \hat{Q}_A &\equiv \hat{Q}_A^{(0)} = \frac{1}{\sqrt{n}} \sum_{j \in A} \hat{q}_j, \\ \hat{P}_A &\equiv \hat{P}_A^{(0)} = \frac{1}{\sqrt{n}} \sum_{j \in A} \hat{p}_j, \end{aligned}} \quad (3.17)$$

and analogously for block B . It seems to be a very natural situation that the experimenter only has access to these collective properties and we are interested in the amount of (physical) entanglement one can extract from the system if only the collective observables $\hat{Q}_{A,B}$ and $\hat{P}_{A,B}$ are measured.

Reference [88] derives a separability criterion which is based on the Peres-Horodecki criterion [75, 44] and the fact that—in the continuous variables case—the partial transposition allows a geometric interpretation as mirror reflection in phase space. Following largely the notation in the original paper, we introduce the vector

$$\hat{\xi} \equiv (\hat{Q}_A, \hat{P}_A, \hat{Q}_B, \hat{P}_B) \quad (3.18)$$

of collective operators. The commutation relations have the compact form $[\hat{\xi}_\alpha, \hat{\xi}_\beta] = iK_{\alpha\beta}$ with $\mathbf{K} \equiv \bigoplus_{j=1}^2 \begin{pmatrix} 0 & 1 \\ -1 & 0 \end{pmatrix}$. The separability criterion bases on the covariance matrix (of first and second moments)

$$V_{\alpha\beta} \equiv \frac{1}{2} \langle \Delta \hat{\xi}_\alpha \Delta \hat{\xi}_\beta + \Delta \hat{\xi}_\beta \Delta \hat{\xi}_\alpha \rangle, \quad (3.19)$$

where $\Delta\hat{\xi}_\alpha \equiv \hat{\xi}_\alpha - \langle \hat{\xi}_\alpha \rangle$ with $\langle \hat{\xi}_\alpha \rangle = 0$ in our case (the ground state is a Gaussian with its mean at the origin of phase space).

The covariance matrix \mathbf{V} is real (which would not be the case for higher-frequency collective operators) and symmetric: $\langle \hat{Q}_A \hat{Q}_B \rangle = \langle \hat{Q}_B \hat{Q}_A \rangle$ and $\langle \hat{P}_A \hat{P}_B \rangle = \langle \hat{P}_B \hat{P}_A \rangle$, coming from the fact that the two-point correlation functions (3.6) and (3.7) only depend on the absolute value of the position index difference. On the other hand, using eqs. (3.3) and (3.4), we verify that $\langle \hat{q}_i \hat{p}_j \rangle = i(2N)^{-1} \sum_{k=0}^{N-1} \exp[i\theta_k(i-j)]$ and $\langle \hat{p}_j \hat{q}_i \rangle = -i(2N)^{-1} \sum_{k=0}^{N-1} \exp[i\theta_k(j-i)]$. For $i \neq j$ both summations vanish ($\theta_k \equiv 2\pi k/N$ and i, j integer) and for $i = j$ they are the same but with opposite sign. Thus, in all cases $\langle \hat{q}_i \hat{p}_j \rangle = -\langle \hat{p}_j \hat{q}_i \rangle$. These symmetries also hold for the collective operators and hence we obtain

$$\mathbf{V} = \begin{pmatrix} G & 0 & G_{AB} & 0 \\ 0 & H & 0 & H_{AB} \\ G_{AB} & 0 & G & 0 \\ 0 & H_{AB} & 0 & H \end{pmatrix}. \quad (3.20)$$

The matrix elements are

$$G \equiv \langle \hat{Q}_A^2 \rangle = \langle \hat{Q}_B^2 \rangle = \frac{1}{n} \sum_{j \in A} \sum_{i \in A} g_{|j-i|}, \quad (3.21)$$

$$H \equiv \langle \hat{P}_A^2 \rangle = \langle \hat{P}_B^2 \rangle = \frac{1}{n} \sum_{j \in A} \sum_{i \in A} h_{|j-i|}, \quad (3.22)$$

$$G_{AB} \equiv \langle \hat{Q}_A \hat{Q}_B \rangle = \frac{1}{n} \sum_{j \in A} \sum_{i \in B} g_{|j-i|}, \quad (3.23)$$

$$H_{AB} \equiv \langle \hat{P}_A \hat{P}_B \rangle = \frac{1}{n} \sum_{j \in A} \sum_{i \in B} h_{|j-i|}. \quad (3.24)$$

To quantify entanglement between two collective blocks we use the degree of entanglement ε , given by the absolute sum of the negative eigenvalues of the partially transposed density operator: $\varepsilon \equiv \text{Tr}|\hat{\rho}^{\text{T}B}| - 1$, i.e. by measuring how much the mirror reflected state $\hat{\rho}^{\text{T}B}$, where the momenta in block B are reversed, fails to be positive definite. This measure (proportional to the negativity) is based on the Peres-Horodecki criterion [75, 44] and was shown to be an entanglement monotone [59, 93]. For covariance matrices of the form (3.20) it reads [50]

$$\varepsilon = \max \left(0, \frac{(\delta_1 \delta_2)_0}{\delta_1 \delta_2} - 1 \right) \quad (3.25)$$

with

$$\delta_1 \equiv G - |G_{AB}|,$$

$$\delta_2 \equiv H - |H_{AB}|.$$

In general, the numerator is defined by the square of the Heisenberg uncertainty relation

$$(\delta_1 \delta_2)_0 \equiv |\langle [\hat{Q}_{A,B}, \hat{P}_{A,B}] \rangle|^2 = \frac{1}{4}, \quad (3.26)$$

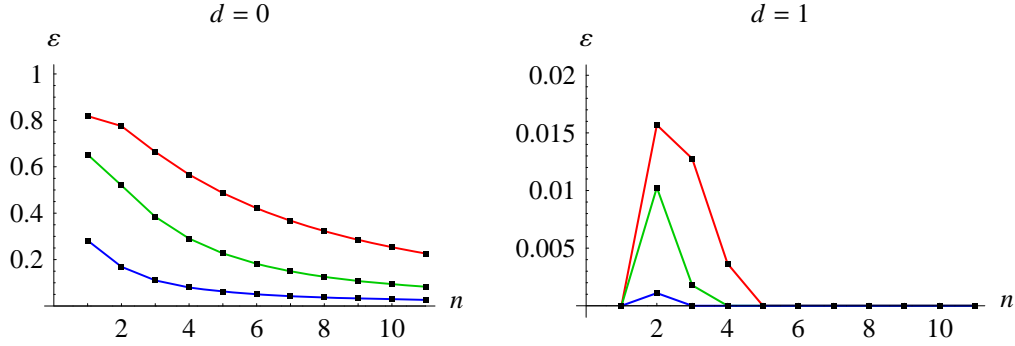


Figure 3.4: Degree of collective entanglement ε for two blocks of oscillators as a function of their size n . Left: The blocks are neighboring ($d = 0$) and entanglement exists for all n and coupling strengths α . Plotted are $\alpha = 0.99$ (red), $\alpha = 0.9$ (green) and $\alpha = 0.5$ (blue). Right: The same for two blocks which are separated by one oscillator ($d = 1$). The two blocks are unentangled for $n = 1$ but can be entangled, if one increases the block size ($n > 1$), although none of the individual pairs between the blocks is entangled.

where the last equal sign holds due to eq. (3.10). We note that ε is a *degree* of entanglement (in the sense of necessity and sufficiency) only for Gaussian states which are completely characterized by their first and second moments, as for example the ground state of the harmonic chain we are studying. However, we left out the higher-frequency collective operators (and all the oscillators which are not part of the blocks) and therefore, the entanglement ε has to be understood as the Gaussian part of the amount of entanglement which exists between (and can be extracted from) the two blocks when only the collective properties $\hat{Q}_{A,B}$ and $\hat{P}_{A,B}$, as defined in eq. (3.17), are accessible.

There also exists an entanglement witness in form of a separability criterion based on variances, where

$$\Delta \equiv \langle (\hat{Q}_A - \hat{Q}_B)^2 \rangle + \langle (\hat{P}_A + \hat{P}_B)^2 \rangle = 2(G - G_{AB} + H + H_{AB}) < 2 \quad (3.27)$$

is a sufficient condition for the state to be entangled [29]. We note that the above negativity measure (3.25) is “stronger” than this witness in the whole parameter space (α, n) . In particular, there are cases where $\varepsilon > 0$ although $\Delta \geq 2$. This is in agreement with the finding that the variance criterion is weaker than a generalized negativity criterion [86].

We further note that the amount of entanglement (3.25) is invariant under a change of potential redefinitions of the collective operators, e.g., $\hat{Q}_A \equiv \sum_{j \in A} \hat{q}_j$ or $\hat{Q}_A \equiv (1/n) \sum_{j \in A} \hat{q}_j$, as then the modified scaling in the correlations (G , G_{AB} , H , and H_{AB}) is exactly compensated by the modified scaling of the Heisenberg uncertainty in the numerator.

Figure 3.4 shows the results for $d = 0$ and $d = 1$. In the first case—if the blocks are neighboring—there exists entanglement for all possible coupling strengths α and block sizes n . In the latter case—if there is one oscillator between the blocks—due to the strongly decaying correlation functions g and h there is no entanglement between two single oscillators ($n = 1$), but there exists entanglement for larger blocks (up to $n = 4$, depending on α). The statement that entanglement can emerge by going to larger blocks was also found in [7]. But there the blocks were abstract objects, containing

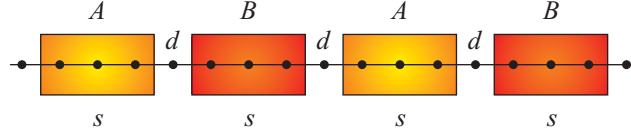


Figure 3.5: Two periodic blocks of a harmonic chain A and B . Each block can consist of m subblocks with s oscillators each, separated by d oscillators. In the picture $d = 1$, $m = 2$, $s = 3$ and the number of oscillators per block is $n = ms = 6$.

all the information of their constituents. In the case of collective operators, however, increasing the block size (averaging over more oscillators) is also connected with a loss of information. In spite of this loss and the mixedness of the state, two blocks can be entangled, although none of the individual pairs between the blocks is entangled—indicating true bipartite entanglement between collective operators (multipartite entanglement between individual oscillators). For $d \geq 2$, however, no entanglement can be found anymore.

These results are in agreement with the general statement that entanglement between a region and its complement scales with the size of the boundary [26, 100]. In the present case of two blocks in a one-dimensional chain (Figure 3.3) the boundary is constant and as the blocks are made larger, the entanglement decreases since it is distributed over more and more oscillators. We therefore propose to increase the number of boundaries by considering two non-overlapping blocks, where we allow a *periodic continuation* of the situation above, i.e. a sequence of $m \geq 1$ subblocks, separated by d oscillators and each consisting of $s \geq 1$ oscillators, where $ms = n$ (Figure 3.5).

The degree of entanglement between two periodic blocks of non-separated ($d = 0$) one-particle subblocks ($s = 1$) is larger for stronger coupling constant α and grows with the overall number of oscillators n (Figure 3.6a). For given α and n and no separation between the subblocks ($d = 0$) the entanglement is larger for the case of small subblocks, as then there are many of them, causing a large total boundary (Figure 3.6b). Entanglement can be even found for larger separation ($d = 1, 2$) with a more complicated dependence on the size s of the subblocks. There is a trade-off between having a large number of boundaries and the fact that one should have large subblocks as individual separated oscillators are not entangled (Figure 3.6c,d). For $d \geq 3$ no entanglement can be found anymore. (In a realistic experimental situation, where the separation d is not sharply defined, e.g., where there are weighted contributions for $d = 0, 1, \dots, d_{\max}$, entanglement can persist even for $d_{\max} \geq 3$, depending on the weighting factors.)

For the sake of completeness we give a rough approximation of the entanglement between two periodic blocks. Let us assume that the subblocks are directly neighbored, $d = 0$. Furthermore, we consider couplings α such that we may neglect higher than next neighbor correlations ($\alpha \lesssim 0.5$), i.e. we only take into account g_0, g_1, h_0 and h_1 . The correlations read

$$G = \frac{1}{n} \sum_{j \in A} \sum_{i \in A} g_{|j-i|} \approx g_0 + \frac{2m(s-1)}{n} g_1, \quad (3.28)$$

$$G_{AB} = \frac{1}{n} \sum_{j \in A} \sum_{i \in B} g_{|j-i|} \approx \frac{2m-1}{n} g_1, \quad (3.29)$$

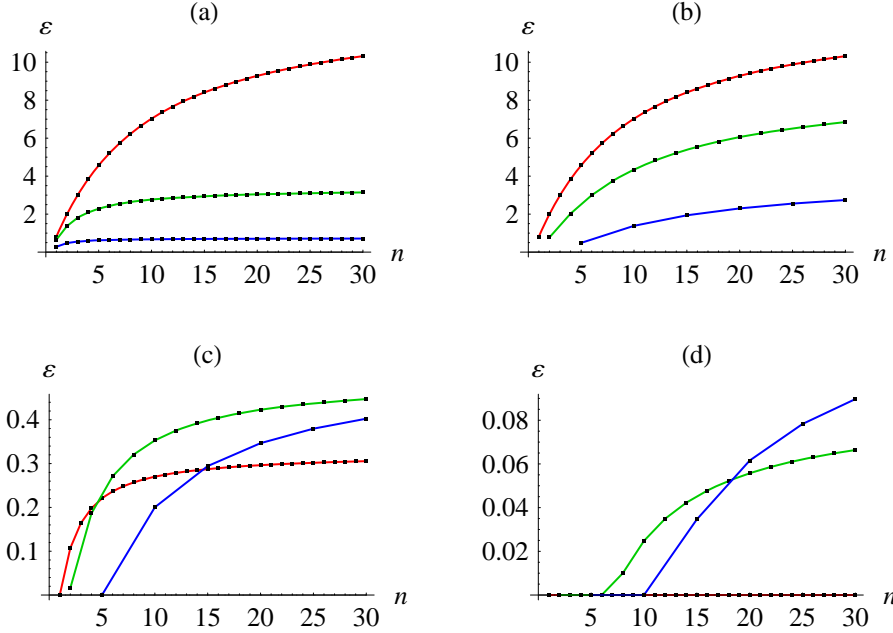


Figure 3.6: Degree of collective entanglement ε for two periodic blocks of oscillators as a function of their total size n . (a) Neighboring one-particle subblocks ($d = 0$, $s = 1$). Entanglement monotonically increases with n and becomes larger as the coupling strength α increases. Plotted are $\alpha = 0.99$ (red), $\alpha = 0.9$ (green) and $\alpha = 0.5$ (blue). (b) The coupling is fixed to $\alpha = 0.99$ for this and the subsequent graphs. There is no separation, $d = 0$. Plotted are the cases $s = 1, 2, 5$ in red, green, blue, respectively. For fixed n the entanglement is more or less proportional to the number of boundaries, i.e. inversely proportional to the subblock size s . (c) and (d) correspond to the cases $d = 1$ and $d = 2$, respectively. The dependence on the size of the subblocks is more complicated as there is a trade-off between having a large number of boundaries (i.e. small s) and the fact that one should have large subblocks as individual separated oscillators are not entangled.

and analogously for H and H_{AB} . The first equation reflects that there are n self-correlations and $m(s-1)$ nearest neighbor pairs (which are counted twice) within one block, i.e. $s-1$ pairs per subblock. The second equation represents the fact that there are $2m-1$ boundaries where blocks A and B meet. Using $s = n/m$, the entanglement (3.25) becomes (note that $g_1 > 0$ and $h_1 < 0$)

$$\varepsilon \approx \frac{1}{4 [g_0 + (2 - \frac{4m-1}{n}) g_1] [h_0 + (2 - \frac{1}{n}) h_1]} - 1. \quad (3.30)$$

For given n this approximation obviously increases with the total number of boundaries, m . It can be considered as an estimate for a situation like in Figure 3.6b, if a smaller coupling is used such that the neglect of higher correlations becomes justified.

We close this section by annotating that the entanglement (3.25) between collective blocks of oscillators—being the Gaussian part—can in principle (for sufficient control of the block separation d) be transferred to two remote qubits via a Jaynes-Cummings type interaction [81, 71, 80]. For the interaction with periodic blocks “gratings” have to be employed in the experimental setup. The

interaction Hamiltonian is of the form

$$\hat{H}_{\text{int}} \sim (e^{-i\omega_1 t} \hat{\sigma}_1^+ + e^{+i\omega_1 t} \hat{\sigma}_1^-) \hat{Q}_A + (e^{-i\omega_2 t} \hat{\sigma}_2^+ + e^{+i\omega_2 t} \hat{\sigma}_2^-) \hat{Q}_B, \quad (3.31)$$

where ω_i is the Rabi frequency and $\hat{\sigma}_i^+ = (\hat{\sigma}_i^-)^\dagger = |e\rangle_i \langle g|$ is the bosonic operator (with $|g\rangle_i$ and $|e\rangle_i$ the ground and the excited state) of the i -th qubit ($i = 1, 2$).

3.1.3 Collective operators for scalar quantum fields

The continuum limit of the linear harmonic chain is the (1+1)-dimensional Klein-Gordon field $\phi(x, t)$ with the canonical momentum field $\pi(x, t) = \dot{\phi}(x, t)$. It satisfies the Klein-Gordon equation (in natural units $\hbar = c = 1$) with mass m

$$\ddot{\phi} - \nabla^2 \phi + m^2 \phi = 0. \quad (3.32)$$

With the canonical quantization procedure ϕ and π become operators satisfying the non-trivial commutation relation $[\hat{\phi}(x, t), \hat{\pi}(x', t)] = i\delta(x - x')$. The field operator can be expanded into a Fourier integral over elementary plane wave solutions [12]

$$\hat{\phi}(x, t) = \int \frac{dk}{\sqrt{4\pi\omega_k}} [\hat{a}(k) e^{ikx - i\omega_k t} + \text{H.c.}], \quad (3.33)$$

$$\hat{\pi}(x, t) = -i \int \frac{dk \omega_k}{\sqrt{4\pi}} [\hat{a}(k) e^{ikx - i\omega_k t} - \text{H.c.}], \quad (3.34)$$

where k is the wave number and $\omega_k = +\sqrt{k^2 + m^2}$ is the dispersion relation. The annihilation and creation operators fulfil $[\hat{a}(k), \hat{a}^\dagger(k')] = \delta(k - k')$. We write the field operator as a sum of two contributions $\hat{\phi} = \hat{\phi}^{(+)} + \hat{\phi}^{(-)}$, where $\hat{\phi}^{(+)}$ ($\hat{\phi}^{(-)}$) is the contribution with positive (negative) frequency. Thus, $\hat{\phi}^{(+)}$ corresponds to the term with the annihilation operator in eq. (3.33). The vacuum correlation function is given by the (equal-time) commutator of the positive and the negative frequency part:

$$\langle 0 | \hat{\phi}(x, t) \hat{\phi}(y, t) | 0 \rangle = [\hat{\phi}^{(+)}(x, t), \hat{\phi}^{(-)}(y, t)]. \quad (3.35)$$

It is a peculiarity of the idealization of quantum field theory that for $x = y$ this propagator diverges in the ground state:

$$\langle 0 | \hat{\phi}^2(x, t) | 0 \rangle \rightarrow \infty. \quad (3.36)$$

The same is true for $\langle 0 | \hat{\pi}^2(x, t) | 0 \rangle$ and hence we cannot easily build an entanglement measure like for the harmonic chain, since the analogs of the two-point correlation functions g_0 and h_0 , eqs. (3.6) and (3.7), are divergent now. Automatically, we are motivated to study the more physical situation and consider extended space-time regions, which means that we should integrate the field (and conjugate momentum) over some spatial area. We define the collective field operators

$$\boxed{\begin{aligned} \hat{\Phi}_L(x_0, t) &\equiv \frac{1}{\sqrt{L}} \int_{-L/2}^{L/2} \hat{\phi}(x + x_0, t) dx, \\ \hat{\Pi}_L(x_0, t) &\equiv \frac{1}{\sqrt{L}} \int_{-L/2}^{L/2} \hat{\pi}(x + x_0, t) dx. \end{aligned}} \quad (3.37)$$

Therefore, $\hat{\Phi}_L(x_0, t)$ and $\hat{\Pi}_L(x_0, t)$ are equal-time operators which are spatially averaged over a length L , centered at position x_0 . The commutator is

$$[\hat{\Phi}_L(x_0, t), \hat{\Pi}_L(x_0, t)] = \frac{1}{L} \int_{-L/2}^{L/2} \int_{-L/2}^{L/2} i \delta(x - y) dx dy = i, \quad (3.38)$$

which is in complete analogy to eq. (3.10). If $\hat{\Phi}_L$ and $\hat{\Pi}_L$ correspond to separated regions without overlap, i.e. $|x_0 - y_0| > L$, then of course $[\hat{\Phi}_L(x_0, t), \hat{\Pi}_L(y_0, t)] = 0$. The spatial integration in eq. (3.37) can be carried out analytically:

$$\hat{\Phi}_L(x_0, t) = \frac{1}{\sqrt{\pi L}} \int_{-\infty}^{\infty} \frac{dk}{k\sqrt{\omega_k}} \sin\left(\frac{kL}{2}\right) [\hat{a}(k) e^{ikx_0 - i\omega_k t} + \text{H.c.}], \quad (3.39)$$

$$\hat{\Pi}_L(x_0, t) = \frac{-i}{\sqrt{\pi L}} \int_{-\infty}^{\infty} \frac{dk \sqrt{\omega_k}}{k} \sin\left(\frac{kL}{2}\right) [\hat{a}(k) e^{ikx_0 - i\omega_k t} - \text{H.c.}]. \quad (3.40)$$

The final step is to calculate the propagators of the field and the conjugate momentum. We find

$$\begin{aligned} D_{\hat{\Phi},L}(r) &\equiv \langle 0 | \hat{\Phi}_L(x_0, t) \hat{\Phi}_L(y_0, t) | 0 \rangle \\ &= \frac{1}{\pi L} \int_{-\infty}^{\infty} \frac{dk}{k^2 \sqrt{k^2 + m^2}} \sin^2\left(\frac{kL}{2}\right) \cos(kr), \end{aligned} \quad (3.41)$$

$$\begin{aligned} D_{\hat{\Pi},L}(r) &\equiv \langle 0 | \hat{\Pi}_L(x_0, t) \hat{\Pi}_L(y_0, t) | 0 \rangle \\ &= \frac{1}{\pi L} \int_{-\infty}^{\infty} \frac{dk \sqrt{k^2 + m^2}}{k^2} \sin^2\left(\frac{kL}{2}\right) \cos(kr), \end{aligned} \quad (3.42)$$

with $r \equiv |x_0 - y_0|$ the distance between the centers of the two regions, reflecting the spatial symmetry. Thus $D_{\hat{\Phi},L}(0)$ and $D_{\hat{\Pi},L}(0)$ are the analogs of $\langle \hat{Q}_{A,B}^2 \rangle$ and $\langle \hat{P}_{A,B}^2 \rangle$ (*intra*-block correlations within the same block), respectively, whereas $D_{\hat{\Phi},L}(r > L)$ and $D_{\hat{\Pi},L}(r > L)$ correspond to $\langle \hat{Q}_A \hat{Q}_B \rangle$ and $\langle \hat{P}_A \hat{P}_B \rangle$ (*inter*-block correlations between separated blocks).

The expressions (3.41) and (3.42) are finite, especially for $r = 0$. Mathematically, the integration over a finite spatial region L corresponds to a cutoff, which removes the divergence we faced in eq. (3.36). However, the expressions are ill defined for $L \rightarrow 0$.

Applying the entanglement measure (3.25) with $G = D_{\hat{\Phi},L}(0)$, $H = D_{\hat{\Pi},L}(0)$, $G_{AB} = D_{\hat{\Phi},L}(r)$, and $H_{AB} = D_{\hat{\Pi},L}(r)$ does not indicate entanglement for any choice of L and $r > L$. The same is true for the generalized case of blocks consisting of periodic subregions of space, showing an inherent difference between the harmonic chain and its continuum limit. This might be due to the fact, that any spatial integration immediately corresponds to an infinitely large block in the discrete harmonic chain and that the information loss (compared to the mathematical indeed existing exponentially small entanglement [81]) due to the collective operators already is too large. Nonetheless, defining collective operators like in eq. (3.37) and use of the measure (3.25) may reveal entanglement between spatially separated regions for other quantum field states.

3.2 Spin ensembles

Observation of quantum entanglement between increasingly larger objects is one of the most promising avenues of experimental quantum physics. Eventually, all these developments might lead to a

full understanding of the simultaneous coexistence of a macroscopic classical world and an underlying quantum realm. Macroscopic samples typically contain $N \sim 10^{20}$ particles. Because the system's Hilbert space grows exponentially with the number of constituent particles, a complete microscopic picture of entanglement in large systems seems to be in general intractable. The question arises: What can we learn about entanglement between constituent particles of macroscopic samples, if only limited experimentally accessible knowledge about the samples is available?

There is a strong motivation in addressing this question because of recent experimental progress in creating and manipulating entangled states of increasing complexity, such as spin-squeezed states of two atomic ensembles [47]. In such experiments one typically measures only expectation values of *collective operators* of two separated samples. It is known that the two samples of spins can be characterized as either entangled or separable by measuring collective spin operators [89]. Furthermore, such measurements are shown to be sufficient to determine entanglement measures of Gaussian states [87] and of a pair of particles that is extracted from a totally symmetric spin state (invariant under exchange of particles) [96]. It appears that collective operators cannot be used to fully characterize entanglement in composite systems without strong requirements on the symmetry of the state.

Here we present a general and practical method for entanglement detection between two samples of spins. It solely employs *collective spin properties of the samples* and works irrespectively of the number of spin particles constituting the samples and with no assumption about the symmetry or mixedness of the state. The method is based on an entanglement measure which is a *tight lower bound for average entanglement between all pairs of spins* belonging to the two samples. This measure is *equal* to the average entanglement for a certain class of systems which need not be totally symmetric. We generalize the method to obtain the entanglement measure between M separated spin samples based on collective measurements. The results apply for any entanglement monotone that is a convex measure on the set of density matrices (e.g., concurrence [42], negativity [105, 93], three-way tangle [24]).

3.2.1 Bipartite entanglement

Consider an ensemble of spin- $\frac{1}{2}$ particles which is separated into two ensembles A and B (Figure 3.7). Each of these ensembles contains a large number of spins which we denote as n . Because of the large dimensions,

$$d = 2^n, \tag{3.43}$$

of the samples' Hilbert spaces, the structure of entanglement between the two samples is considerably more complex than between two single spins. While there are experimentally viable methods for detecting entanglement, they still require a large number of parameters to be determined (proportional to d^2 [45]).

The problem simplifies in situations in which each of the ensembles of n spins can be treated as one large total spin of length $\frac{n}{2}$. This means that, within the ensembles, the individual spin- $\frac{1}{2}$ particles form symmetrized states (Dicke states). Though this reduces the dimension of the Hilbert

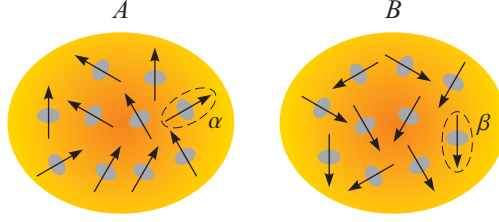


Figure 3.7: Two contiguous and non-overlapping spin subsystems A and B , each of which contains a large number n of spins. What can we learn about entanglement of a pair (α, β) of spins chosen at random where $\alpha \in A$ and $\beta \in B$, if individual spins are experimentally not accessible but only the collective properties of the samples A and B ? What can we learn about entanglement between A and B from such collective measurements?

space of A (B) to

$$d' = n + 1, \quad (3.44)$$

entanglement determination is still demanding for large n both experimentally and theoretically: Analytical solutions exist only for pure states in general and for mixed states only for small n [82].

In this section, we give a method to detect entanglement between large spin samples by measuring only a *small number of collective spin properties* (sample spin components and their correlations), which is independent of the sample size n . The collective spin operators are

$$\boxed{\begin{aligned} \hat{S}_i^A &\equiv \frac{\hbar}{2} \sum_{\alpha \in A} \hat{\sigma}_i^{(\alpha)}, \\ \hat{S}_i^B &\equiv \frac{\hbar}{2} \sum_{\beta \in B} \hat{\sigma}_i^{(\beta)}. \end{aligned}} \quad (3.45)$$

The index i denotes the spatial component of the spins: $i \in \{1 \equiv x, 2 \equiv y, 3 \equiv z\}$. The Pauli matrix of the spin at site $\alpha \in A$ is given by $\hat{\sigma}_i^{(\alpha)}$, and analogously for a spin β from subsystem B . Note that the collective operators satisfy the usual commutation relations

$$[\hat{S}_i^A, \hat{S}_j^A] = i \hbar \varepsilon_{ijk} \hat{S}_k^A, \quad (3.46)$$

since $[\hat{\sigma}_i^{(\alpha)}, \hat{\sigma}_j^{(\alpha')}] = 2i \delta_{\alpha\alpha'} \varepsilon_{ijk} \hat{\sigma}_k^{(\alpha)}$.

The spin expectation values and correlations are

$$S_i^A \equiv \langle \hat{S}_i^A \rangle = \frac{\hbar}{2} \sum_{\alpha \in A} g_i(\alpha), \quad (3.47)$$

$$T_{ij}^{AB} \equiv \langle \hat{S}_i^A \hat{S}_j^B \rangle = \frac{\hbar^2}{4} \sum_{\alpha \in A} \sum_{\beta \in B} h_{ij}(\alpha, \beta), \quad (3.48)$$

and analogously for $S_i^B \equiv \frac{\hbar}{2} \sum_{\beta \in B} g_i(\beta)$, where $S_i^A, S_i^B \in [-\frac{n\hbar}{2}, \frac{n\hbar}{2}]$, $T_{ij}^{AB} \in [-\frac{n^2\hbar^2}{4}, \frac{n^2\hbar^2}{4}]$. These are only 15 numbers. Here $g_i(\alpha)$, $g_i(\beta)$ and $h_{ij}(\alpha, \beta)$ are the (dimensionless) expectation values and

pair correlations of two single spins (α, β) to which it is assumed there is no experimental access:

$$g_i(\alpha) \equiv \langle \hat{\sigma}_i^{(\alpha)} \rangle_{\hat{\rho}_{\alpha\beta}}, \quad (3.49)$$

$$h_{ij}(\alpha, \beta) \equiv \langle \hat{\sigma}_i^{(\alpha)} \hat{\sigma}_j^{(\beta)} \rangle_{\hat{\rho}_{\alpha\beta}}. \quad (3.50)$$

They are obtained from the actual 4×4 density matrix of the two spins α and β :

$$\hat{\rho}_{\alpha\beta} \equiv \frac{1}{4} \left[\mathbb{1}^{(\alpha)} \otimes \mathbb{1}^{(\beta)} + \sum_{k=1}^3 g_k(\alpha) \hat{\sigma}_k^{(\alpha)} \otimes \mathbb{1}^{(\beta)} + \sum_{l=1}^3 \mathbb{1}^{(\alpha)} \otimes g_l(\beta) \hat{\sigma}_l^{(\beta)} + \sum_{k,l=1}^3 h_{kl}(\alpha, \beta) \hat{\sigma}_k^{(\alpha)} \otimes \hat{\sigma}_l^{(\beta)} \right] \quad (3.51)$$

with $\mathbb{1}^{(\alpha)}$ ($\mathbb{1}^{(\beta)}$) the 2×2 identity matrix in the Hilbert space of spin α (β).

Out of the experimentally accessible quantities (3.47) and (3.48) we will construct a 4×4 density matrix of *two virtual qubits* which describes the collective properties of the two spin ensembles. The *a priori* justification for this method is:

1. A general treatment of the problem between two large samples of spins is intractable because of the high dimensionality.
2. We have a fully developed theory of entanglement for two-qubit systems. Therefore, this approach is a natural way to say something about the entanglement between two spin systems if only collective observables are measured.

We first introduce the normalized (dimensionless) average subsystem expectation values (magnetization per particle) and correlations:

$$s_i^a \equiv \frac{1}{n} \sum_{\alpha \in A} g_i(\alpha) = \frac{2}{n\hbar} S_i^A, \quad (3.52)$$

$$t_{ij}^{ab} \equiv \frac{1}{n^2} \sum_{\alpha \in A} \sum_{\beta \in B} h_{ij}(\alpha, \beta) = \frac{4}{n^2 \hbar^2} T_{ij}^{AB}, \quad (3.53)$$

where $s_i^a, t_{ij}^{ab} \in [-1, 1]$. These are the coefficients of the virtual density matrix:

$$\hat{\rho}_{ab} \equiv \frac{1}{4} \left[\mathbb{1}^a \otimes \mathbb{1}^b + \sum_{k=1}^3 s_k^a \hat{\sigma}_k^a \otimes \mathbb{1}^b + \sum_{l=1}^3 \mathbb{1}^a \otimes s_l^b \hat{\sigma}_l^b + \sum_{k=1}^3 \sum_{l=1}^3 t_{kl}^{ab} \hat{\sigma}_k^a \otimes \hat{\sigma}_l^b \right] \quad (3.54)$$

with a denoting the first and b the second virtual collective qubit, associated with subsystems A and B , respectively. Here, $\mathbb{1}^a$, $\mathbb{1}^b$, $\hat{\sigma}_k^a$ and $\hat{\sigma}_l^b$ are 2×2 identity and Pauli matrices for the collective qubits a and b .

The question is whether the density matrix (3.54) is positive semi-definite, i.e. whether it is a physical state of two qubits. The answer is affirmative and the proof follows from the consideration of an equal-weight statistical mixture of *one* (virtual) qubit pair which can be in any of the n^2 states $\hat{\rho}_{\alpha\beta}$. The density matrix of this mixture is the mixture of density matrices of all possible pairs (α, β) :

$$\hat{\rho}_{\text{mix}} = \frac{1}{n^2} \sum_{\alpha, \beta} \hat{\rho}_{\alpha\beta}. \quad (3.55)$$

It can easily be seen that

$$\hat{\rho}_{\text{mix}} = \hat{\rho}_{ab} \quad (3.56)$$

for both are uniquely determined by the same expectations and correlations:

$$\langle \hat{\sigma}_i^{(\alpha)} \rangle_{\hat{\rho}_{\text{mix}}} = \langle \hat{\sigma}_i^a \rangle_{\hat{\rho}_{ab}} = s_i^a = \frac{2}{n\hbar} S_i^A, \quad (3.57)$$

$$\langle \hat{\sigma}_i^{(\alpha)} \hat{\sigma}_j^{(\beta)} \rangle_{\hat{\rho}_{\text{mix}}} = \langle \hat{\sigma}_i^a \hat{\sigma}_j^b \rangle_{\hat{\rho}_{ab}} = t_{ij}^{ab} = \frac{4}{n^2 \hbar^2} T_{ij}^{AB}. \quad (3.58)$$

Thus, $\hat{\rho}_{ab}$ is indeed a density matrix. Note that without the normalizations as given in (3.52) and (3.53), the method would not work.

Encapsulated in the following two propositions, we relate the entanglement properties of the virtual qubits to those of the spin samples.

Proposition 1. For any entanglement measure E that is convex on the set of density matrices the entanglement of the virtual density matrix $E_{ab} \equiv E(\hat{\rho}_{ab})$ is a lower bound for the average entanglement between all pairs $\bar{E}_{\alpha\beta} \equiv \frac{1}{n^2} \sum_{\alpha,\beta} E(\hat{\rho}_{\alpha\beta})$.

Proof: This is an immediate consequence of the convexity of E :

$$E_{ab} \equiv E\left(\frac{1}{n^2} \sum_{\alpha,\beta} \hat{\rho}_{\alpha\beta}\right) \leq \frac{1}{n^2} \sum_{\alpha,\beta} E(\hat{\rho}_{\alpha\beta}) \equiv \bar{E}_{\alpha\beta}. \quad (3.59)$$

Remarks: First, the result holds for entanglement measures that are convex. In certain cases this is directly implied by the definition of the entanglement measure for mixed states, which involves a convex roof $E(\hat{\rho}) \equiv \min_{p_i, \psi_i} \sum_i p_i E(|\psi_i\rangle\langle\psi_i|)$, where the minimization is taken over those probabilities p_i and pure states $|\psi_i\rangle$ that realize the density matrix $\hat{\rho} = \sum_i p_i |\psi_i\rangle\langle\psi_i|$ and $E(|\psi_i\rangle\langle\psi_i|)$ is the entanglement measure of the pure state $|\psi_i\rangle$. Second, the proposition implies that if $E_{ab} > 0$ then at least for one pair (α, β) we must have $E(\hat{\rho}_{\alpha\beta}) > 0$:

$$\hat{\rho}_{ab} \text{ entangled} \Rightarrow \exists(\alpha, \beta): \hat{\rho}_{\alpha\beta} \text{ entangled}. \quad (3.60)$$

Thus, a non-zero value of E_{ab} is a sufficient condition for entanglement between the two samples A and B . Third, the maximal pairwise concurrence [42] for symmetric states is found to be $2/n$ and is achieved for the W-state [51]. It is conjectured that this remains valid also when the symmetry constraint is removed. This suggests $E_{ab} \leq \bar{E}_{\alpha\beta} \leq 2/n$, if concurrence is used as an entanglement measure. The existence of this upper bound can be seen as a consequence of the monogamy of entanglement.

We refer to E_{ab} as *pairwise collective entanglement* as it is determined solely by the expectation and correlation values of the collective spin observables. The question arises: Under what conditions is E_{ab} equal to the average entanglement $\bar{E}_{\alpha\beta}$? Identifying systems for which the equality holds, would allow feasible experimental determination of the entanglement distribution in large samples by observation of their macroscopic properties only. It can easily be seen that, if the state is symmetric under exchange of particles *within* each of the samples, one has $E_{ab} = \bar{E}_{\alpha\beta} = E(\hat{\rho}_{\alpha\beta})$ for every pair of particles (α, β) . In what follows, we identify an important class of systems for which $E_{ab} = \bar{E}_{\alpha\beta}$ though the corresponding states need *not* be symmetric under exchange of particles.

Proposition 2. Consider a system (i) with $g_z(\alpha) = g_z^A$ for all $\alpha \in A$ and $g_z(\beta) = g_z^B$ for all $\beta \in B$ (translational invariance within the subsystems), (ii) with $h_{xx}(\alpha, \beta) = \varepsilon h_{yy}(\alpha, \beta)$ with $\varepsilon = \text{const} = +1$ or -1 (all pairs are in absolute value equally correlated in the x and y -direction, where this correlation may be different in size for different pairs), (iii) with constant sign of the z -correlations, i.e. $\text{sgn}[h_{zz}(\alpha, \beta)] = -\varepsilon$ for all (α, β) , and (iv) where all the remaining expectation values and correlations (g_x, g_y, h_{ij} with $i \neq j$) are zero. *Non-vanishing average entanglement $\bar{E}_{\alpha\beta}$ as measured by the negativity is equal to the pairwise collective entanglement E_{ab} , if and only if the correlation functions $h_{xx}(\alpha, \beta)$ and $h_{yy}(\alpha, \beta)$ are each constant for all pairs and all pairs have a non-positive eigenvalue of their partial transposed density matrix.*

Proof: The negativity [105, 93] of a density matrix $\hat{\rho}$ is defined as

$$E(\hat{\rho}) \equiv \frac{\text{Tr}|\hat{\rho}^{\text{pT}}| - 1}{2}, \quad (3.61)$$

where $\text{Tr}|\hat{\rho}^{\text{pT}}|$ stands for the trace norm of the partially transposed density matrix $\hat{\rho}^{\text{pT}}$. Hence the negativity is equal to the modulus of the sum of the negative eigenvalues of ρ^{pT} .

It is important to stress that proposition 2 holds also for states that do not need to be totally symmetric, i.e. the $h_{zz}(\alpha, \beta)$ may be different for different pairs of particles. In general, under the above symmetry, the state of the virtual qubit pair is of the form

$$\hat{\rho}_{ab} = \begin{pmatrix} u_{+++} & 0 & 0 & v_- \\ 0 & u_{+--} & v_+ & 0 \\ 0 & v_+ & u_{-+-} & 0 \\ v_- & 0 & 0 & u_{--+} \end{pmatrix}, \quad (3.62)$$

where $u_{\pm\pm\pm} \equiv \frac{1}{4}(1 \pm s_z^A \pm s_z^B \pm t_{zz}^{ab})$, $v_{\pm} \equiv \frac{1}{4}t_{xx}^{ab}(1 \pm \varepsilon)$. The state of an arbitrary pair (α, β) of particles has a similar structure. For example, the state of an arbitrary pair of particles extracted from a spin chain with xxz Heisenberg interaction has such a form.

Depending on the sign ε of the zz -correlations, only one eigenvalue of $\hat{\rho}_{\alpha\beta}^{\text{pT}}$ and $\hat{\rho}_{ab}^{\text{pT}}$, respectively, can be negative:

$$\mu_{\alpha\beta} = \frac{1}{4} \left[1 - \sqrt{(g_z^A + \varepsilon g_z^B)^2 + 4h_{xx}^2(\alpha, \beta) + \varepsilon h_{zz}(\alpha, \beta)} \right], \quad (3.63)$$

$$\nu_{ab} = \frac{1}{4} \left[1 - \sqrt{(s_z^a + \varepsilon s_z^b)^2 + 4(t_{xx}^{ab})^2 + \varepsilon t_{zz}^{ab}} \right]. \quad (3.64)$$

The corresponding negativities are given by

$$E(\hat{\rho}_{\alpha\beta}) = |\min(0, \mu_{\alpha\beta})|, \quad (3.65)$$

$$E_{ab} = |\min(0, \nu_{ab})|. \quad (3.66)$$

One can express ν_{ab} as given by

$$\nu_{ab} = \bar{\mu} + \Delta, \quad (3.67)$$

where

$$\bar{\mu} \equiv \frac{1}{n^2} \sum_{\alpha, \beta} \mu_{\alpha\beta} \quad (3.68)$$

and

$$\Delta \equiv \frac{1}{4n^2} \sum_{\alpha, \beta} \sqrt{(g_z^A + \varepsilon g_z^B)^2 + 4h_{xx}^2(\alpha, \beta)} - \frac{1}{4} \sqrt{(s_z^a + \varepsilon s_z^b)^2 + 4(t_{xx}^{ab})^2}. \quad (3.69)$$

The quantity Δ is the difference between the entanglement measures $\bar{E}_{\alpha\beta}$ and E_{ab} , i.e. $E_{ab} = \bar{E}_{\alpha\beta} - \Delta$, for the case that $\nu_{ab} \leq 0$ and $\bar{E}_{\alpha\beta} \equiv \frac{1}{n^2} \sum_{\alpha, \beta} |\min(0, \mu_{\alpha\beta})| = |\min(0, \bar{\mu})|$. This is true, if and only if $\mu_{\alpha\beta} \leq 0$ for all (α, β) , i.e. all pairs are either entangled or have eigenvalue zero. According to proposition 1, Δ is non-negative, i.e.

$$\sqrt{c^2 + 4(t_{xx}^{ab})^2} \leq \frac{1}{n^2} \sum_{\alpha, \beta} \sqrt{c^2 + 4h_{xx}^2(\alpha, \beta)}. \quad (3.70)$$

Here we abbreviated $c \equiv g_z^A + \varepsilon g_z^B = s_z^a + \varepsilon s_z^b$, where the latter equal sign is due to (3.52). Inequality (3.70) becomes an equality, i.e. $\Delta = 0$, if and only if $h_{xx}(\alpha, \beta)$ is the same for all pairs (α, β) such that $t_{xx}^{ab} = h_{xx}$. Therefore, the pairwise collective entanglement E_{ab} equals the average entanglement $\bar{E}_{\alpha\beta}$, if and only if for all individual pairs $\mu_{\alpha\beta} \leq 0$ and $h_{xx}(\alpha, \beta) = \varepsilon h_{yy}(\alpha, \beta) = \text{const}$ for all pairs. \square

We illustrate the method with some explicit examples:

1. Dicke states

We consider the Dicke state (generalized W-state)

$$|N; k\rangle \equiv \binom{N}{k}^{-1/2} \hat{P}_S | \underbrace{0 \dots 0}_{N-k} \underbrace{1 \dots 1}_k \rangle \quad (3.71)$$

with $N \geq 2$ spins, k excitations $|1\rangle$ and $N - k$ non-excited spins $|0\rangle$, where $0 \leq k \leq N$. \hat{P}_S is the symmetrization operator. Here, we identify the collective spin operators \hat{S}_i , eq. (3.45), which act on 2^n dimensional Hilbert spaces, with spin operators \hat{S}_i acting only on the $2s + 1 = n + 1$ dimensions of the (symmetric) Dicke states.

Within the system we consider two subsystems A and B each of size n . Because of the total symmetry of the state one has $E_{ab} = \bar{E}_{\alpha\beta} = E(\hat{\rho}_{\alpha\beta})$ for any size n . Only for the cases where just a single spin ($k = 0$) or all spins are excited ($k = N$), there is no entanglement between two arbitrary pairs or arbitrary sized blocks, respectively [92].

The reduced two-qubit density matrix has the form

$$\hat{\rho}_{\alpha\beta}(N; k) = d |00\rangle\langle 00| + e |11\rangle\langle 11| + 2f |\psi^+\rangle\langle \psi^+|, \quad (3.72)$$

where $|\psi^+\rangle \equiv \frac{1}{\sqrt{2}}(|01\rangle + |10\rangle)$ and

$$d = \frac{(N-k)(N-k-1)}{N(N-1)}, \quad e = \frac{k(k-1)}{N(N-1)}, \quad f = \frac{k(N-k)}{N(N-1)}, \quad (3.73)$$

with $d + e + 2f = 1$. The reduced density matrix $\hat{\rho}_{\alpha\beta}$ is the same for all pairs of spins (α, β) , independent of their position and distance from each other. We need to calculate the expectation values of the spin operator and correlations between the two sites α and β . They are independent of α and β :

$$g_z = e - d, \quad h_{xx} = h_{yy} = 2f, \quad h_{zz} = d + e - 2f. \quad (3.74)$$

All the others (g_x, g_y, h_{ij} with $i \neq j$) are zero. This is a Heisenberg xxz type situation, for which all our proofs above hold. The corresponding normalized collective values of two n -particle blocks A and B , (3.52) and (3.53), are

$$s_i = \frac{1}{n} S_i^{A,B} = \frac{1}{n} \sum_{\alpha \in A}^n g_i = g_i, \quad (3.75)$$

$$t_{ij} = \frac{1}{n^2} T_{ij}^{AB} = \frac{1}{n^2} \sum_{\alpha \in A}^n \sum_{\beta \in B}^n h_{ij} = h_{ij}, \quad (3.76)$$

i.e. the same as the actual values for two arbitrary individual spins. This means that for the W-state the averages are the values themselves, since there is no dependence at all on the position of the spins and therefore on the distance between them. Therefore, the collective block entanglement (for all block sizes $n \leq \frac{N}{2}$) equals the entanglement between two (arbitrary) spins:

$$E_{ab} = E(\hat{\rho}_{\alpha\beta}). \quad (3.77)$$

The corresponding (possibly negative) eigenvalues of the partial transposed matrices are

$$\nu_{ab} = \mu_{\alpha\beta} = \frac{1}{2} (d + e) - \frac{1}{2} \sqrt{(e - d)^2 + 4f^2}. \quad (3.78)$$

The entanglement

$$E_{ab} = |\nu_{ab}| \quad (3.79)$$

is non-zero for all excitations $1 \leq k \leq N - 1$. Only for the cases where not a single spin or where all spins are excited, $E_{ab} = 0$ and there is no entanglement between two arbitrary pairs or arbitrary sized blocks, respectively. The global maximum of the entanglement is reached for $k = \frac{N}{2}$, which is the case where half of the spins are excited (N should be even here) and its value is

$$E_{ab}^{\max} \equiv E_{ab}(k = \frac{N}{2}) = \frac{1}{2} \frac{1}{N - 1}, \quad (3.80)$$

for all block sizes n . It vanishes in the limit of an infinite chain $N \rightarrow \infty$. Figure 3.8 shows the block entanglement E_{ab} as a function of the number of excitations k .

2. Generalized singlet states

The two subsystems A and B , each forming a spin $s = \frac{n}{2}$, are in a generalized singlet state:

$$|\psi\rangle = \frac{1}{\sqrt{2s + 1}} \sum_{m=-s}^s (-1)^{s-m} |m\rangle_A |-m\rangle_B, \quad (3.81)$$

where $|m\rangle = |2s; s + m\rangle$ denotes the eigenstates of the spin operator's z -component. The collective two-qubit coefficients are $t_{ii}^{ab} = -\frac{n+2}{3n}$ and the $s_i^{a,b}$ and t_{ij}^{ab} with $i \neq j$ are all zero. The eigenvalue (3.64) of $\hat{\rho}_{ab}^{\text{pT}}$ becomes $\nu_{ab} = -\frac{1}{2n}$, and the collective entanglement (negativity) is

$$E_{ab} = \frac{1}{2n} = \frac{1}{4s}. \quad (3.82)$$

It is non-zero for all sizes n of the subsystems and vanishes only in the limit $n \rightarrow \infty$. This agrees with the statements in References [63, 74] that the generalized singlet state (3.81) can violate a Bell inequality no matter how large the spin is.

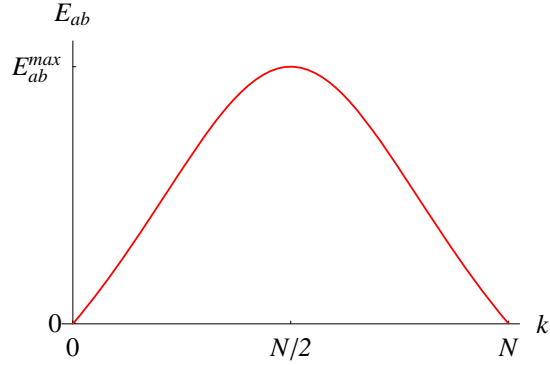


Figure 3.8: Entanglement E_{ab} between two arbitrary sized spin subensembles A and B , where the system is in a Dicke state (3.71) of N particles with k excitations. The entanglement is computed as the negativity of two virtual qubits a and b , representing the subensembles. It is non-zero except for the cases where not a single spin or where all spins are excited. The maximum entanglement $E_{ab}^{\max} = \frac{1}{2} \frac{1}{N-1}$ is reached for $k = N/2$.

3. Generalized singlet state with an admixture of non-symmetric correlations

Consider the state

$$|\psi\rangle_p = p |\psi\rangle\langle\psi| + (1-p) \bigotimes_{\alpha=1}^n \frac{1}{2} \left(|01\rangle_{\alpha,\beta=\alpha} \langle 10| + |10\rangle_{\alpha,\beta=\alpha} \langle 01| \right) \quad (3.83)$$

with $p \in [0, 1]$. This is a mixture of the generalized singlet state (3.81) and n perfectly z -correlated pairs $(\alpha, \beta = \alpha)$. This state is *not* symmetric under particle exchange in the zz -correlations. The expectation values $s_i^{a,b}$ and correlations t_{ij}^{ab} with $i \neq j$ remain zero. The correlations $t_{xx} = t_{yy}$ are reduced by a factor p compared to those of the state (3.81). The correlations in z -direction, however, are modified and read $t_{zz}^{ab} = -p \frac{n-1}{3n} - \frac{1}{n}$. Therefore, there is a critical number of particles $n_c \equiv \lceil \frac{1+p}{1-p} \rceil$, with $\lceil \cdot \rceil$ the ceiling function, beyond which there is no collective pairwise entanglement. Only for $n < n_c$ we have positive

$$E_{ab} = \frac{1+p-n(1-p)}{4n}. \quad (3.84)$$

Note that (3.83) is in accordance with proposition 2 and thus $E_{ab} = \bar{E}_{\alpha,\beta}$. Figure 3.9 shows E_{ab} as a function of the spin length $s = \frac{n}{2}$ and the mixing parameter p . E_{ab} is non-zero in regions where $p > \frac{2s-1}{2s+1}$ and decreases inversely proportionally to s .

3.2.2 Multi-partite entanglement

Our method can be generalized to define multi-partite entanglement of M collective spins belonging to M separated samples A_1, \dots, A_M , each containing a large number of spins n (Figure 3.10). The collective spin of subsystem A_p is

$$\hat{S}_{i_p}^{A_p} \equiv \frac{\hbar}{2} \sum_{\alpha_p \in A_p} \hat{\sigma}_{i_p}^{(\alpha_p)}. \quad (3.85)$$

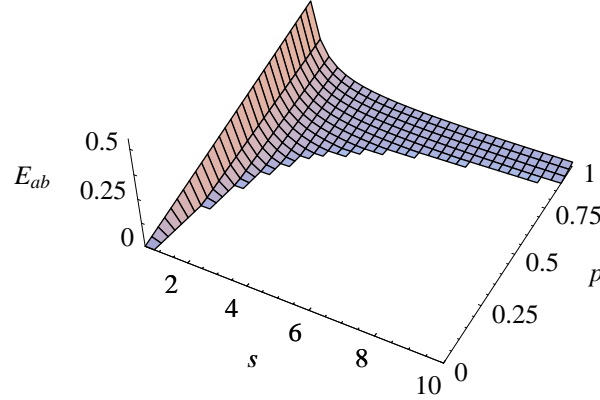


Figure 3.9: Entanglement E_{ab} between two collective spins in the generalized singlet state with an admixture of non-symmetric noise (3.83) as a function of spin length s and proportion p of the singlet state in the mixture. The entanglement is non-zero for sufficiently large p and decreases inversely proportionally to s .

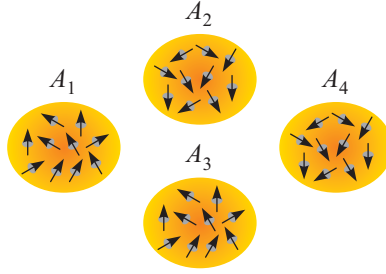


Figure 3.10: Schematic of a multi-partite scenario. There are M separated spin subensembles A_1, \dots, A_M , each containing a large number of individual spins.

Here $p = 1, \dots, M$ and $i_p \in \{0, x \equiv 1, y \equiv 2, z \equiv 3\}$ and $\hat{\sigma}_0^{(\alpha p)} = \mathbb{1}$ denotes the 2×2 identity matrix. We suppose again that the experimenter measures the collective spin components (where all i_p but one are zero) in each sample and their (higher-order) correlations (where more than one i_p is unequal to zero) $T_{i_1 \dots i_M}^{A_1 \dots A_M} \equiv \langle \hat{S}_{i_1}^{A_1} \dots \hat{S}_{i_M}^{A_M} \rangle$:

$$T_{i_1 \dots i_M}^{A_1 \dots A_M} = \frac{\hbar^M}{2^M} \sum_{\alpha_1 \in A_1} \dots \sum_{\alpha_M \in A_M} h_{i_1 \dots i_M}(\alpha_1, \dots, \alpha_M), \quad (3.86)$$

where

$$h_{i_1 \dots i_M}(\alpha_1, \dots, \alpha_M) \equiv \langle \hat{\sigma}_{i_1}^{(\alpha_1)} \dots \hat{\sigma}_{i_M}^{(\alpha_M)} \rangle_{\hat{\rho}_{\alpha_1 \dots \alpha_M}} \quad (3.87)$$

denotes the actual spin expectation values and higher-order correlations in the physical system. These are $4^M - 1$ numbers. The virtual correlations are denoted as

$$t_{i_1 \dots i_M}^{a_1 \dots a_M} \equiv \frac{2^M}{(n\hbar)^M} T_{i_1 \dots i_M}^{A_1 \dots A_M}. \quad (3.88)$$

Note that $\hat{S}_0^{A_p} = n \mathbb{1}$ is n times the 2×2 identity matrix. A normalized p -particle correlation $t_{i_1 \dots i_M}^{a_1 \dots a_M}$ with $p \leq M$ indeed scales with n^{-p} as p ($M-p$) is the number of subscripts unequal (equal) to

zero. The virtual $2^M \times 2^M$ collective M -qubit density matrix is given by

$$\hat{\rho}_{a_1 \dots a_M} \equiv \frac{1}{2^M} \sum_{i_1=0}^3 \dots \sum_{i_M=0}^3 t_{i_1 \dots i_M}^{a_1 \dots a_M} \hat{\sigma}_{i_1}^{a_1} \otimes \dots \otimes \hat{\sigma}_{i_M}^{a_M}, \quad (3.89)$$

with $\hat{\sigma}_{i_p}^{a_p}$ denoting the 2×2 Pauli or identity matrix of the p -th virtual collective qubit, associated with the n -particle subsystem A_p .

We show that the virtual matrix $\hat{\rho}_{a_1 \dots a_M}$ is a density matrix. Analogously to the two-subsystems case, we consider an equal-weight statistical mixture of *one* m -tuple of qubits $(\alpha_1, \dots, \alpha_M)$ which can be in any of the n^M (mixed) states $\hat{\rho}_{\alpha_1 \dots \alpha_M}$. The density matrix of this mixture is the mixture of density matrices of all possible m -tuples:

$$\hat{\rho}_{\text{mix}} = \frac{1}{n^M} \sum_{\alpha_1, \dots, \alpha_M} \hat{\rho}_{\alpha_1 \dots \alpha_M}.$$

We have

$$\hat{\rho}_{\text{mix}} = \hat{\rho}_{a_1 \dots a_M}$$

as both give the same expectations and correlations:

$$\langle \hat{\sigma}_{i_1}^{(\alpha_1)} \dots \hat{\sigma}_{i_M}^{(\alpha_M)} \rangle_{\hat{\rho}_{\text{mix}}} = \langle \hat{\sigma}_{i_1}^{a_1} \dots \hat{\sigma}_{i_M}^{a_M} \rangle_{\hat{\rho}_{a_1 \dots a_M}} = t_{i_1 \dots i_M}^{a_1 \dots a_M}$$

Hence, analogously to proposition 1, any convex multi-partite entanglement measure (e.g., M -way tangle) which is applied to the collective matrix, $E(\hat{\rho}_{a_1 \dots a_M})$, gives a *lower bound for the average multi-partite entanglement* $\bar{E}_{\alpha_1 \dots \alpha_M}$. For states which are symmetric within the samples equality holds: $E(\hat{\rho}_{a_1 \dots a_M}) = \bar{E}_{\alpha_1 \dots \alpha_M}$. For totally symmetric states this is also equal to the multi-particle entanglement of M extracted particles from the system. Since being a legitimate entanglement measure, the collective multi-partite entanglement $E(\hat{\rho}_{a_1 \dots a_M})$ obeys the usual constraints for entanglement sharing such as the Coffman-Kundu-Wootters inequality [24].

Importantly, in the examples considered above our entanglement measure scales at most with $1/n$ and vanishes in the limit of infinitely large subsystem sizes n . This is a generic property that follows from the commutation relation for *normalized* spins in this limit. Taking $\hat{s}_i \equiv \frac{1}{n} \hat{S}_i = \frac{\hbar}{2n} \sum_{\alpha} \hat{\sigma}_i^{(\alpha)}$ one obtains

$$\lim_{n \rightarrow \infty} [\hat{s}_x, \hat{s}_y] = \lim_{n \rightarrow \infty} i \frac{\hbar}{2n} \hat{s}_z = 0. \quad (3.90)$$

This is sometimes interpreted as suggesting that averaged collective observables, like the magnetization per particle, represent “macroscopic” or classical-like, properties of samples. Note, however, that for any n there are n^2 pairs between the subsystems so that the number of pairs multiplied by the pairwise collective entanglement can scale with n , showing the existence of entanglement for arbitrarily large n .

Chapter 4

Mathematical undecidability and quantum randomness

Summary:

The mathematics of the early twentieth century was concerned with the question whether a complete and consistent set of axioms for all of mathematics is conceivable [41]. In 1931 Gödel showed that this is fundamentally impossible [39]. In every consistent axiomatic system that is capable of expressing elementary arithmetic there are propositions which can neither be proved nor disproved within the system, i.e. they are “undecidable”. Via the halting problem Turing brought Gödel’s mathematical proof into the world of physical machines [91]. Chaitin went even one step further and argued that mathematical undecidability is not bound to self-referential statements but arises whenever a proposition to be proved and the axioms contain together more information than the set of axioms itself [21].

Here we propose a new link between mathematical undecidability and quantum physics. We demonstrate that the states of elementary quantum systems are capable of encoding mathematical axioms. Quantum mechanics imposes an upper limit on how much information can be encoded in a quantum state [43, 102], thus limiting the information content of the set of axioms. We show that quantum measurements are capable of revealing whether a given proposition is decidable or not within this set. This allows for an experimental test of mathematical undecidability by realizing in the laboratory the actual quantum states and operations required. We demonstrate experimentally both the encoding of axioms, using polarization states of photons, and that the decidability of propositions can be checked by performing suitable quantum measurements. We theoretically find and experimentally confirm that whenever a mathematical proposition is undecidable within the system of axioms encoded in the state, the measurement associated with the proposition gives random outcomes. Our results support the view that quantum randomness is irreducible [20] and a manifestation of mathematical undecidability.

Despite its overwhelming success, quantum physics is still heavily debated for its interpretation has remained to be unclear. One of the reasons is that, in contrast to all other theories, it is

lacking clear and unambiguous foundational principles. The link with pure mathematics might provide such a principle and can be seen as a novel approach towards a reconstruction of quantum theory [94].

This chapter mainly bases on and also uses parts of Reference [70]:

- T. Paterek, R. Prevedel, J. Kofler, P. Klimek, M. Aspelmeyer, A. Zeilinger, and Č. Brukner
Mathematical undecidability and quantum randomness
Submitted (2008).

4.1 Logical complementarity and mathematical undecidability

We begin our argumentation following the idea of the information-theoretical formulation of Gödel's theorem [21]: Given a set of axioms that contains a certain amount of information, it is impossible to deduce the truth value of a proposition which, together with the axioms, contains more information than the set of axioms itself. To give an example, consider Boolean functions of a single binary argument:

$$x \in \{0, 1\} \rightarrow y = f(x) \in \{0, 1\} \quad (4.1)$$

There are four such functions, y_k ($k = 0, 1, 2, 3$), shown in Figure 4.1. We shall discuss the following (binary) propositions about their properties:

- (A) “The value of $f(0)$ is ‘0’, i.e. $f(0) = 0$.”
- (B) “The value of $f(1)$ is ‘0’, i.e. $f(1) = 0$.”

These two propositions are *independent*. Knowing the truth value of one of them does not allow to infer the truth value of the other. Ascribing truth values to both propositions requires two bits of information. If one postulates only proposition (A) to be true, i.e. if we choose (A) as an “axiom”, then it is impossible to prove proposition (B) from (A). Having only axiom (A), i.e. only one bit of information, there is not enough information to know also the truth value of (B). Hence, proposition (B) is *mathematically undecidable* within the system containing the single axiom (A). Another example of an undecidable proposition within the same axiomatic system is:

- (C) “The function is constant, i.e. $f(0) = f(1)$.”

Again, this statement cannot be proved or disproved from the axiom (A) alone because (C) is independent of (A) as it involves $f(1)$.

We refer to independent propositions to which one cannot simultaneously ascribe definite truth values—given a limited amount of information resources—as *logically complementary propositions*. Knowing the truth value of one of them (i.e. having the proposition itself or its negation as an axiom) precludes any knowledge about the others. For example, given the limitation to one bit of information, the three propositions (A), (B) and (C) are logically complementary.

When the information content of the axioms and the number of independent propositions increase, more possibilities arise. Already the case of two bits as the information content is instructive.

x	y_0	y_1	y_2	y_3
0	0	0	1	1
1	0	1	0	1

Figure 4.1: The four Boolean functions $y = f(x)$ of a binary argument, i.e. $f(x) = 0, 1$ with $x = 0, 1$. The different functions are labeled by y_k with $k = 0, 1, 2, 3$.

Consider two independent Boolean functions $f_1(x)$ and $f_2(x)$ of a binary argument. The two bits can be used to define truth values of properties of the individual functions or they can define joint features of the functions. An example of the first type is the following two-bit proposition:

- (D) “The value of $f_1(0)$ is ‘0’, i.e. $f_1(0) = 0$.”
 “The value of $f_2(1)$ is ‘0’, i.e. $f_2(1) = 0$.”

An example of the second type is:

- (E) “The functions have the same values for argument ‘0’, i.e. $f_1(0) = f_2(0)$.”
 “The functions have the same values for argument ‘1’, i.e. $f_1(1) = f_2(1)$.”

Both (D) and (E) consist of two elementary (binary) propositions. Their truth values are of the form of “vectors” with two components being the truth values of their elementary propositions. The propositions (D) and (E) are logically complementary. Given (E) as a two-bit axiom, all the *individual* function values remain undefined and thus one can determine neither of the two truth values of (D).

The new aspect of multi-bit axioms is the existence of “partially” undecidable propositions, containing more than one elementary proposition only some of which are undecidable. An example of such a partially undecidable proposition within the system consisting of the two-bit axiom (D) is:

- (F) “The value of $f_1(0)$ is ‘0’, i.e. $f_1(0) = 0$.”
 “The value of $f_2(0)$ is ‘0’, i.e. $f_2(0) = 0$.”

The first elementary proposition is the same as in (D) and thus it is definitely true. The impossibility to decide the second elementary proposition leads to (partial) undecidability of the proposition (F). In a similar way, proposition (F) is partially undecidable within the axiomatic system of (E).

4.2 Physical implementation and quantum randomness

The discussion so far was purely *mathematical*. We have described axiomatic systems (of limited information content) using properties of Boolean functions. Now we show that the undecidability of mathematical propositions can be tested in quantum experiments. To this end we introduce a *physical* “black box” whose internal configuration encodes Boolean functions. The black box hence forms a bridge between mathematics and physics. Quantum systems enter it and the properties of the functions are written onto the quantum states of the systems. Finally, measurements performed on the systems extract information about the properties of the configuration of the black box and thus about the properties of the functions.

We begin with the simplest case of a spin- $\frac{1}{2}$ particle (qubit) entering the black box (see Figure 4.2 for the experimental implementation) and a single bit-to-bit function $f(x)$ implemented by the black box. Inside the black box two subsequent operations alter the state of the input spin. The first

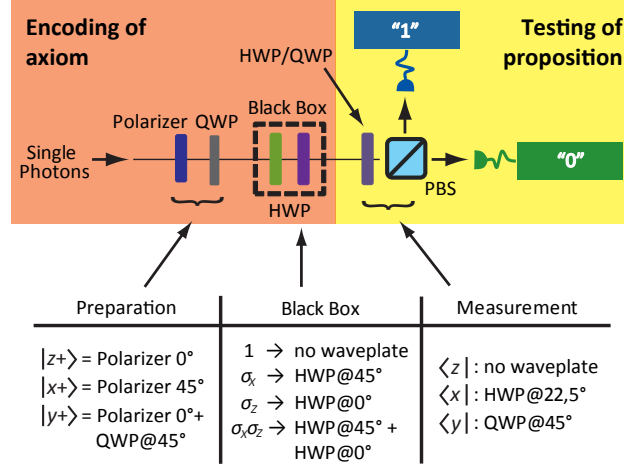


Figure 4.2: The experimental setup. We use the polarization of single photons as information carriers of binary properties encoded by the configuration in the “black box”. The photons are initialized in a definite polarization state, belonging to one of the three complementary bases z, x, y (Preparation). The Boolean functions are realized within the black box by inserting half-wave plates (HWPs) which implement the product of Pauli operators $\hat{\sigma}_x^{f(0)} \hat{\sigma}_z^{f(1)}$, eq. (4.2). The measurement apparatus consists of a quarter-wave plate (QWP) or HWP, followed by a polarizing beam-splitter (PBS) and two fibre-coupled single-photon detector modules. In this way, measurements in all complementary bases (z, x, y) can be realized.

operation encodes the value of $f(1)$ via application of $\hat{\sigma}_z^{f(1)}$, i.e. the Pauli z -operator taken to the power of $f(1)$. The second operation encodes $f(0)$ with $\hat{\sigma}_x^{f(0)}$, i.e. the Pauli x -operator taken to the power of $f(0)$. The total action of the black box is

$$\hat{U} = \hat{\sigma}_x^{f(0)} \hat{\sigma}_z^{f(1)}. \quad (4.2)$$

Consider the input spin to be in one of the eigenstates of the Pauli operator $i^{mn} \hat{\sigma}_x^m \hat{\sigma}_z^n$ (with i the imaginary unit). The three particular choices $(m, n) = (0, 1), (1, 0)$, or $(1, 1)$ correspond to the three spin operators along orthogonal directions $\hat{\sigma}_z, \hat{\sigma}_x$, or $\hat{\sigma}_y = i \hat{\sigma}_x \hat{\sigma}_z$, respectively. The input density matrix reads

$$\hat{\rho} = \frac{1}{2} [\mathbb{1} + \lambda_{mn} i^{mn} \hat{\sigma}_x^m \hat{\sigma}_z^n], \quad (4.3)$$

with $\lambda_{mn} = \pm 1$ and $\mathbb{1}$ the identity operator. It evolves under the action of the black box to

$$\hat{U} \hat{\rho} \hat{U}^\dagger = \frac{1}{2} [\mathbb{1} + \lambda_{mn} (-1)^{nf(0)+mf(1)} i^{mn} \hat{\sigma}_x^m \hat{\sigma}_z^n]. \quad (4.4)$$

Depending on the value of $nf(0) + mf(1)$ (in this chapter all sums are taken modulo 2), the state after the black box is either the same or orthogonal to the initial one. If one now performs a measurement in the basis of the initial state, i.e. the eigenbasis of the operator $i^{mn} \hat{\sigma}_x^m \hat{\sigma}_z^n$, the outcome reveals the value of $nf(0) + mf(1)$ and hence the measurement can be considered as *checking the truth value of the proposition*

$$(G) \quad “nf(0) + mf(1) = 0.”$$

Mathematics/Logic		Quantum Physics
Question about proposition	\leftrightarrow	Quantum measurement
Axioms of limited information content	\leftrightarrow	Quantum states
Decidability/Undecidability	\leftrightarrow	Definiteness/Randomness of outcomes

Figure 4.3: The link between mathematical undecidability and quantum randomness.

Each of the three *quantum complementary* measurements $\hat{\sigma}_z$, $\hat{\sigma}_x$, or $\hat{\sigma}_y$ reveals the truth value of one of the independent propositions (A), (B), or (C), respectively.

Independent of the initial state, we now identify the quantum measurement (m, n) with the question about the truth value of the corresponding mathematical proposition (G). The states that give a definite answer in the quantum experiment encode (G) or its negation as an axiom. A measurement *quantum physically complementary* to the one identified with (G) gives random results for those states, and the corresponding *logically complementary* proposition is undecidable within the one-bit axiom.

We will show in general that *whenever* the proposition identified with the measurement is decidable (in the axiomatic system encoded by the state after the black box), the measurement outcome is definite, and whenever it is undecidable, the measurement outcome is random. This links mathematical undecidability and quantum randomness and allows to experimentally find out whether a proposition is decidable or not. The essence of this chapter is summarized in Figure 4.3.

A natural explanation of *irreducible* (objective) randomness of individual quantum outcomes arises. After leaving the black box the spin's quantum state encodes exactly one bit of information about $f(x)$, namely the truth value of the proposition (G). *In mathematical language, the system encodes a one-bit axiom.* One bit is the maximum amount of information which can be carried by a single spin- $\frac{1}{2}$ particle [43, 102]. Thus, if this bit represents the truth value of, say, proposition (A), therefore defining (A) or its negation as an axiom, the other two logically complementary propositions, (B) and (C), are undecidable. This is because there is no information left for specifying their truth values. However, the spin can nevertheless be measured in the bases corresponding to (B) or (C) and—as in any measurement—will inevitably give an outcome, e.g. a click in a detector. The clicks must not contain any information whatsoever about the truth of the undecidable proposition. Therefore, the individual quantum outcome must be random, reconciling mathematical undecidability with the fact that a quantum system always gives an “answer” when “asked” in an experiment. This provides an intuitive understanding of quantum randomness, a key quantum feature, using mathematical reasoning.

To find out whether a proposition is undecidable, it is necessary to repeat an experiment sufficiently many times, such that—even in the presence of unavoidable experimental imperfections—the two possible different outcomes occur significantly often. To reveal decidability, only one outcome has to appear again and again, but sufficiently many repetitions of the experiment are needed, because in practice the other outcome sometimes occurs due to experimental errors.

We illustrate the link between mathematical undecidability and quantum randomness in an

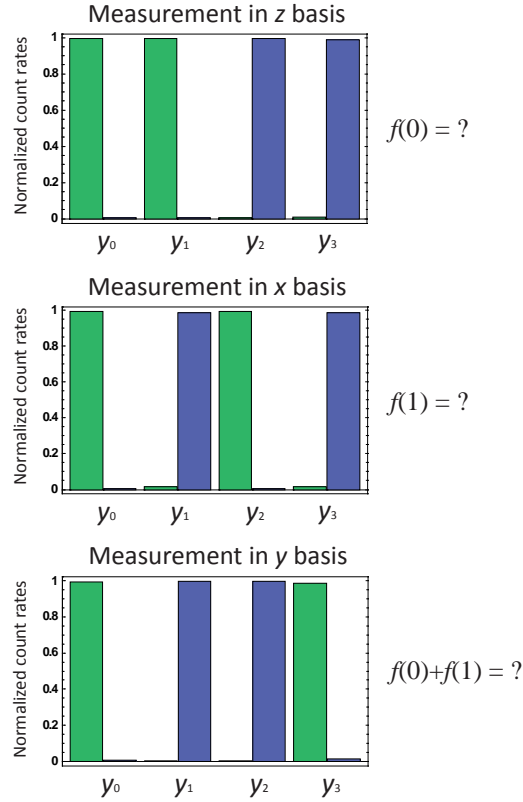


Figure 4.4: We confirm that a measurement in the z basis gives the value of $f(0)$ and similarly, measurements in x and y bases give the value of $f(1)$ and $f(0) + f(1)$, respectively. Shown are the experimental results for the cases where we prepared and measured the qubit in the *same* basis. Here, green (blue) bars represent counts in detector “0” (detector “1”), see Figure 4.2. The top graph, e.g., shows the measurement in the z basis: $f(0)$ is ‘0’ (green) for the functions y_0 and y_1 , and ‘1’ (blue) for y_2 and y_3 .

experiment. The qubit is realized by two orthogonal polarization states of a single photon generated in the process of spontaneous parametric down-conversion [58] (SPDC). This system is formally equivalent to a spin- $\frac{1}{2}$ particle. The horizontal/vertical, $+45^\circ/-45^\circ$, right/left circular polarization of the photon corresponds to eigenstates $|z\pm\rangle$, $|x\pm\rangle$, and $|y\pm\rangle$ of the spin- $\frac{1}{2}$ particle, respectively. We start by initializing the qubit in a definite polarization state by inserting a linear polarizer in the beam path (see Figure 4.2). The qubit then propagates through the black box in which the Boolean functions are encoded with the help of half-wave plates (HWP). The desired unitary transformation $\hat{\sigma}_z$ ($\hat{\sigma}_x$) on the polarization states is implemented by a HWP at an angle 0° (45°) with respect to the z -basis. Subsequently, measurements of $\hat{\sigma}_z$, $\hat{\sigma}_x$, and $\hat{\sigma}_y$, which test the truth value of a specific proposition, are performed as projective measurements in the corresponding polarization basis. Specifically, we use a polarizing beam-splitter (PBS) performing $\hat{\sigma}_z$ measurements whose output modes are fiber-coupled to single-photon detector modules and use wave plates in front of the PBS to rotate the measurement basis (see Figure 4.2). The truth value of the proposition now corresponds to photon detection in one of the two output modes of the PBS.

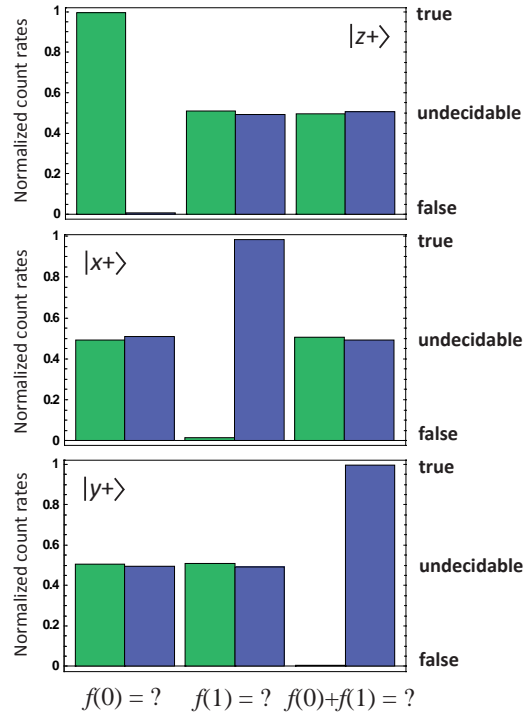


Figure 4.5: Using the setup of Figure 4.2, we input the qubit in a well-defined Pauli operator eigenstate $|z+\rangle$, $|x+\rangle$, or $|y+\rangle$ into the black box, shown from top to bottom. The black box encodes two classical bits, $f(0)$ and $f(1)$, and the choice of the initial state determines which single bit, $f(0)$, $f(1)$, or $f(0) + f(1)$, is read out. For every input state we measure in all three complementary bases, z [asking for $f(0)$], x [$f(1)$], and y [$f(0) + f(1)$], shown from left to right. The three measurements are related to three logically complementary questions (A), (B), (C) of the main text as indicated by the labels. This particular plot is the experimentally obtained data for the black box realizing the function y_1 . Similar results were obtained for the other black box configurations y_0 , y_2 , and y_3 . Again, green (blue) bars represent counts in detector “0” (detector “1”) giving the answer to the corresponding question. Each input state, after leaving the black box, reveals the truth value of one and only one of the propositions, i.e. it encodes a one-bit axiom. Given this axiom, the remaining two logically complementary propositions are undecidable. This undecidability is revealed by complete randomness of the outcomes in the other two measurement bases.

First, we confirm that complementary quantum measurements indeed reveal truth values of logically complementary propositions. To this aim we prepare the system in a state belonging to the basis in which we finally measure. The results are presented in Figure 4.4.

Next, for each of the three choices of the initial state, we ask all three logically complementary questions by measuring in all three different complementary bases. In Figure 4.5, we plot the count rate of photons measured after the PBS for a fixed configuration in the black box that encodes function y_1 . Similar results are obtained for other black box configurations (not shown). Figure 4.5 shows that for every input state one and only one question has a definite answer, as already indicated in Figure 4.4. This is the axiom encoded in the system after it leaves the black box. The remaining propositions are undecidable given that axiom, and the corresponding measurement outcomes are

completely random, i.e. evenly distributed.

4.3 Generalization to many qubits

We now generalize the above reasoning using multiple qubits. Consider a black box with N input and N output ports, one for each qubit. It encodes N Boolean functions $f_j(x)$ numbered by $j = 1, \dots, N$ by applying the operation

$$\hat{U}_N = \hat{\sigma}_x^{f_1(0)} \hat{\sigma}_z^{f_1(1)} \otimes \dots \otimes \hat{\sigma}_x^{f_N(0)} \hat{\sigma}_z^{f_N(1)}. \quad (4.5)$$

The initial N -qubit state is chosen to be a particular one of the 2^N eigenstates of *independent and mutually commuting* tensor products of Pauli operators, numbered by $p = 1, \dots, N$:

$$\hat{\Omega}_p \equiv i^{m_1(p)n_1(p)} \hat{\sigma}_x^{m_1(p)} \hat{\sigma}_z^{n_1(p)} \otimes \dots \otimes i^{m_N(p)n_N(p)} \hat{\sigma}_x^{m_N(p)} \hat{\sigma}_z^{n_N(p)}, \quad (4.6)$$

with $m_j(p), n_j(p) \in \{0, 1\}$. A broad family of such states is the family of graph states [79]. As before, the qubits propagate through the black box. After leaving it, their state encodes the truth values of the following N independent binary propositions (negating the false propositions, one has N true ones which serve as axioms):

$$(H_p) \quad \text{“}\sum_{j=1}^N [n_j(p) f_j(0) + m_j(p) f_j(1)] = 0\text{.”}$$

with $p = 1, \dots, N$. Mathematically, N binary arguments being the N truth values of the (H_p) allow to construct 2^{2^N} different Boolean functions. The statements about the values of these functions form all possible decidable (not independent) binary propositions. In suitable measurements quantum mechanics provides a way to test whether a given proposition is decidable or not. If one measures the operator

$$\hat{\Theta} \equiv i^{\alpha_1 \beta_1} \hat{\sigma}_x^{\alpha_1} \hat{\sigma}_z^{\beta_1} \otimes \dots \otimes i^{\alpha_N \beta_N} \hat{\sigma}_x^{\alpha_N} \hat{\sigma}_z^{\beta_N}, \quad (4.7)$$

with $\alpha_j, \beta_j \in \{0, 1\}$, one tests whether the proposition

$$(J) \quad \text{“}\sum_{j=1}^N [\beta_j f_j(0) + \alpha_j f_j(1)] = 0\text{.”}$$

is decidable or not. In case $\hat{\Theta}$ can be written as a product $\hat{\Omega}_1^{k_1} \dots \hat{\Omega}_N^{k_N}$ with $k_p \in \{0, 1\}$, it commutes with all the $\hat{\Omega}_p$'s and consequently the measurement of $\hat{\Theta}$ has a definite outcome. On the other hand, proposition (J) is decidable within the set of axioms (H_p) . Its truth value can be (logically) derived from the axioms in the sense that the sum in (J), $\sum_{j=1}^N [\beta_j f_j(0) + \alpha_j f_j(1)]$, is a linear combination of the sums in (H_p) with binary coefficients k_p . There are 2^N such linear combinations and therefore 2^N such $\hat{\Theta}$'s. Since in general 4^N different $\hat{\Theta}$'s exist, the remaining $4^N - 2^N = 2^N(2^N - 1)$ operators are linked with undecidable propositions and their measurement outcomes are random. Hence, there are much more undecidable propositions of the form (J) than decidable ones. The ratio between their numbers increases exponentially with the number of qubits, i.e. $\frac{2^N(2^N-1)}{2^N} = O(2^N)$.

Interestingly, in case of (J) being decidable, its truth value imposed by (classical) logic is not necessarily the same as found in the quantum measurement. This can be demonstrated for three qubits initially in the Greenberger-Horne-Zeilinger (GHZ) state [40]

$$|\text{GHZ}\rangle = \frac{1}{\sqrt{2}} (|z+\rangle_1 |z+\rangle_2 |z+\rangle_3 + |z-\rangle_1 |z-\rangle_2 |z-\rangle_3), \quad (4.8)$$

where e.g. $|z\pm\rangle_1$ denotes the eigenstate with the eigenvalue ± 1 of $\hat{\sigma}_z$ for the first qubit. We choose as axioms the propositions

$$\begin{aligned} (\text{K}_1) \quad & \text{“} f_1(0) + f_1(1) + f_2(0) + f_2(1) + f_3(1) = 1 \text{.”} \\ (\text{K}_2) \quad & \text{“} f_1(0) + f_1(1) + f_2(1) + f_3(0) + f_3(1) = 1 \text{.”} \\ (\text{K}_3) \quad & \text{“} f_1(1) + f_2(0) + f_2(1) + f_3(0) + f_3(1) = 1 \text{.”} \end{aligned}$$

linked with the operators $\hat{\sigma}_y \otimes \hat{\sigma}_y \otimes \hat{\sigma}_x$, $\hat{\sigma}_y \otimes \hat{\sigma}_x \otimes \hat{\sigma}_y$, and $\hat{\sigma}_x \otimes \hat{\sigma}_y \otimes \hat{\sigma}_y$, respectively. One can *logically* derive from (K₁) to (K₃) the true proposition

$$(\text{L}) \quad \text{“} f_1(1) + f_2(1) + f_3(1) = 1 \text{.”}$$

On the other hand, the proposition (L) is identified with the measurement of $\hat{\sigma}_x \otimes \hat{\sigma}_x \otimes \hat{\sigma}_x$. But the result imposed by quantum mechanics corresponds to the *negation* of (L), namely: “ $f_1(1) + f_2(1) + f_3(1) = 0$.” This is the heart of the experimentally confirmed GHZ argument against local realism [40, 64, 69]. In the (standard logical) derivation of (L) the individual function values are well defined and the same independently of the axiom in which they appear. Since this is equivalent to the assumptions of local realism, the truth values of decidable propositions found in quantum experiments do not necessarily have to be the same as the ones derived by logic. However, this does not change the connection between decidability (undecidability) of propositions and definiteness (randomness) of measurement outcomes.

The question arises whether one can construct a classical device to reveal the undecidability of propositions. This is possible, provided one uses $2N$ classical bits to simulate quantum complementary measurements on N qubits [90]. Since such a device satisfies local realism, it gives the truth values of decidable propositions according to classical logic. On the level of elementary physical systems, however, the world is known to be quantum. It is intriguing that nature supplies us with quantum systems which can reveal decidability but cannot be used to learn the classical truth values.

In order to illustrate the concept of partial undecidability as introduced above, we performed a two-qubit experiment. The two bits of proposition (E) described above correspond to the set of independent commuting operators $\hat{\Omega}_1 = \hat{\sigma}_z \otimes \hat{\sigma}_z$ and $\hat{\Omega}_2 = \hat{\sigma}_x \otimes \hat{\sigma}_x$. The common eigenbasis of these operators is spanned by the maximally entangled Bell states (basis b_E): $|\Phi^\pm\rangle = \frac{1}{\sqrt{2}}(|z+\rangle_1|z+\rangle_2 \pm |z-\rangle_1|z-\rangle_2)$, $|\Psi^\pm\rangle = \frac{1}{\sqrt{2}}(|z+\rangle_1|z-\rangle_2 \pm |z-\rangle_1|z+\rangle_2)$. Thus, after the black box the four Bell states encode the four possible truth values of the elementary propositions in (E) and a so-called Bell State Analyzer (i.e. an apparatus that measures in the Bell basis) reveals these values. In the same way, the truth values of the elementary propositions in (F) are encoded in the eigenstates of local $\hat{\sigma}_z$ bases, i.e. by the four states $|z\pm\rangle_1|z\pm\rangle_2$ (basis b_F). Finally, the elementary propositions in (D) are linked with the product states $|z\pm\rangle_1|x\pm\rangle_2$ (basis b_D).

The setup that was employed to generate maximally entangled Bell states via type-II SPDC is shown in Figure 4.6. We also prepared separable two-qubit states by inserting polarizers into the optical paths just before the black box. The encoding of functions within the black box as well as the polarization measurements on the individual qubits were done similarly to the single-qubit

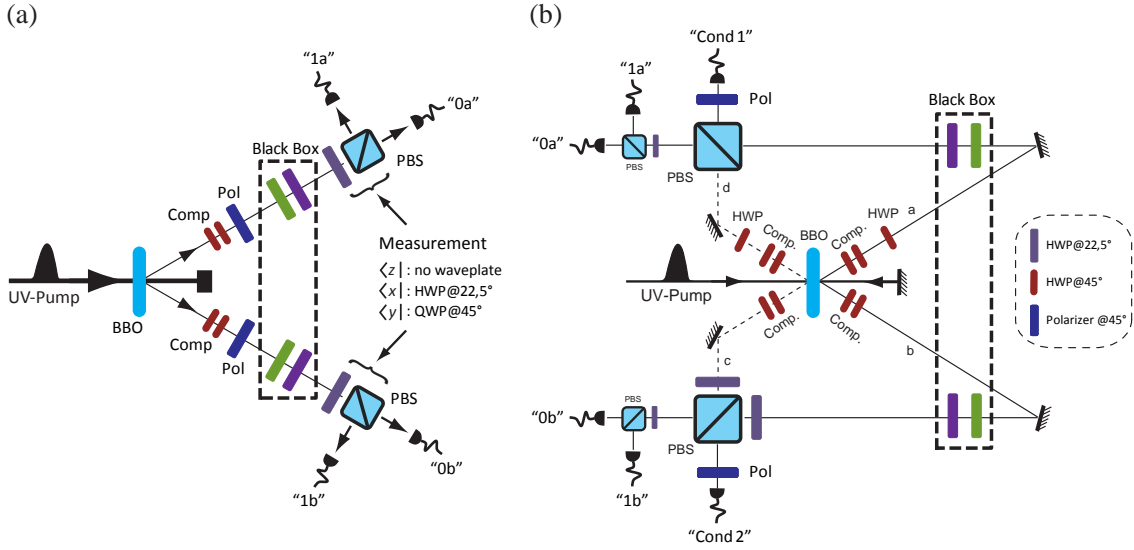


Figure 4.6: The setup in (a) allows for separable two-qubit measurements on product as well as on entangled input states. Joint two-qubit measurements require a so-called Bell State Analyzer (BSA), whose experimental realization is depicted in (b). In both cases, an ultra-violet laser pulse passes through a non-linear crystal (BBO) to produce polarization-entangled photon pairs in the process of spontaneous parametric down-conversion. Compensators (Comp), made up of half-wave plates (HWP) and BBO crystals, are used to counter walk-off effects in the down-conversion crystal. They are set such that $|\Phi^+\rangle$ states are emitted. In (a), local measurements in all complementary bases are performed with the help of HWP, QWP and PBSs. Measurements in the Bell basis, as depicted in (b), require an ancillary entangled Bell state $|\Phi^+\rangle$. Therefore the UV-laser passes twice through the crystal, emitting the input Bell state in the forward direction (modes a & b), and the ancilla pair in the backward direction (modes c & d). Coherently combining these photons on PBSs, allows the identification of all four Bell states whenever there is one photon in each output mode of the PBSs. Then, conditioned on the detection of one photon with $+45^\circ$ polarization in both detectors, “Cond 1” and “Cond 2”, the Bell state can be identified by analyzing the remaining two photons in the $+45^\circ/-45^\circ$ basis (see Reference [95] for details).

case. However, this only allows for *independent* single-qubit measurements. *Joint* measurements on both qubits in the Bell basis require conditional operations on two qubits. The heart of such a Bell State Analyzer [97, 65, 95] (BSA) is a controlled-NOT gate [8, 76, 68, 34]. In Figure 4.6 we depict the experimental setup implementing the BSA. Details of its working can be found in Reference [95].

We start our investigation by confirming that the truth values of the (elementary) propositions in (E), (F) and (D) are revealed by measurements performed in the bases b_E , b_F and b_D , respectively. As in the single-qubit case, preparation and measurement are in the same basis. The obtained results (not shown) are similar to Figure 4.4. Moreover, one can initially prepare a Bell state and measure it in the bases b_E , b_F and b_D . As can be seen in the left plot of Figure 4.7, measurements in the Bell basis, b_E , prove that the entangled state indeed encodes joint properties of the functions $f_1(x)$ and $f_2(x)$, i.e. information about (E). Measurements in other bases can then be interpreted in

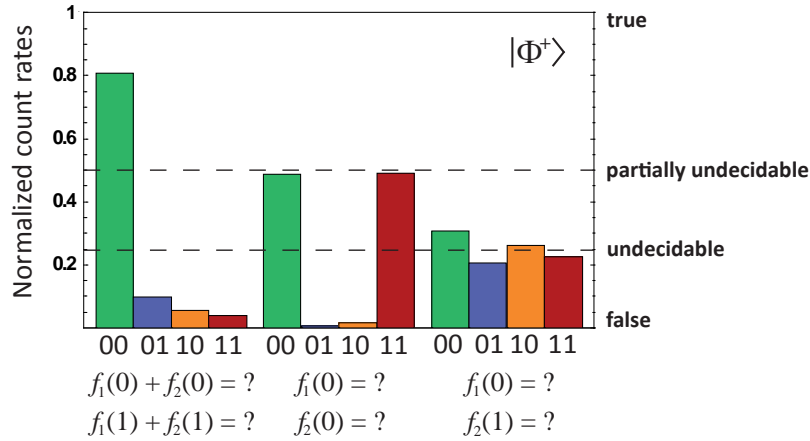


Figure 4.7: In this two-qubit experiment a $|\Phi^+\rangle$ Bell state is measured in three different bases (the Bell basis as well as $|z\pm\rangle_1|z\pm\rangle_2$ and $|z\pm\rangle_1|x\pm\rangle_2$, shown from left to right) using the setups depicted in Figure 4.6. Plotted are the count rates associated with different detector combinations for the black box encoding function y_2 on both photons. Label “00” corresponds to a coincidence event in detectors “0a” and “0b”, and similarly for the other labels. The first (second) label gives the answer to the upper (lower) question. The measurements performed in the Bell basis show that the two qubits encode proposition (E) of the main text. The data in the middle plot reveal partial undecidability of proposition (F), given (E) as an axiom, as indicated by the random outcomes in two out of four detector combinations. In contrast, the right plot presents the data corresponding to the fully undecidable proposition (D), where the outcomes are completely random. Similar results for propositions (E), (F) and (D) were obtained for other black box encodings. The reason for the fact that the Bell state in the left plot is not identified with unit fidelity stems from imperfections in the experimental setup. Unequal detector efficiencies explain the small bias in the right plot.

terms of partial and full undecidability. Proposition (D) is fully undecidable given (E) as an axiom which is encoded by $|\Phi^+\rangle$ after the black box. This can be seen from the right part in Figure 4.7, in which all four measurement outcomes occur with equal probability. On the other hand, proposition (F) is partially undecidable. This is experimentally revealed by the count distribution of the middle part in Figure 4.7. The partial undecidability is uncovered by the randomness of the two occurring outcomes, while the other two outcomes do not appear.

In conclusion, we have demonstrated how mathematical axioms can be encoded in quantum states and how decidability of mathematical propositions can be verified in quantum measurements. This extends the concept of “experimental mathematics” [22] to a new domain and sheds new light on the (mathematical) origin of quantum randomness. We have performed an experiment which showed for the first time the link between mathematical undecidability and quantum randomness. There, we found that whenever the quantum system is measured in a basis associated to an undecidable proposition, it gives random outcomes. Our results can be extended in many ways.

An interesting avenue for further research arises from the observation that in mathematical logic one usually makes a difference only between statements that are either decidable or undecid-

able within a formal system of axioms. Quantum complementarity implies that losing certainty about one of the propositions is followed by a corresponding gain of certainty in other, logically complementary, propositions [16, 17]. This opens up the possibility to quantify the *amount of undecidability* of a proposition from “impossible” to “necessary”, and to describe the continuous *trade-off* in gaining and losing knowledge about them.

Conclusions and outlook

This final part of the present work offers the room to point out some possibilities for further research, including not only conservative but also speculative thoughts.

Macroscopic realism and the quantum-to-classical transition:

- We have put forward an approach to the quantum-to-classical transition, resting solely on the idea that coarse-grained measurements give rise to the emergence of macroscopic realism. However, to offer a complementary approach to the decoherence program that also applies to isolated systems, it is necessary to *generalize the formalism to systems other than spins*. E.g., for a particle in conventional phase space with position and momentum and an arbitrary time evolution there is no quantum number that can be made larger and larger (like spin length). But Reference [74] shows how a small blurring of a particle's Wigner function makes it positive (by convoluting it with the Wigner function of a coherent state). Again, it should be possible to model coarse-grained measurements in such a way that they are non-invasive at the level of a positive probability distribution. The latter represents an ensemble of classical objects with definite positions and momenta and must be sufficient to compute probabilities for coarse-grained outcomes. It can be seen already now that the interesting issue of non-classical Hamiltonians will arise again.
- We have found that coarse-grained spin measurements are best modeled with a positive operator value measure because coarse-grained von Neumann measurements allow to distinguish microstates at two sides of a slot border. Still, under all circumstances it is unavoidable that a quantum measurement always introduces a slight disturbance of the state even on the level of the Q -distribution. Under ideal experimental conditions and sufficiently many runs, we should be able to see *tiny deviations from classical physics* even for classical Hamiltonians, macroscopic systems, and coarse-grained measurements.
- We have demonstrated that every non-trivial Hamiltonian allows to violate the Leggett-Garg inequality as long as sharp quantum measurements can be performed. This might be seen as related to the *quantum Zeno effect* [66]: Quantum measurements not only are capable of freezing the time evolution of a system but they also may influence it in such a way that it cannot be described classically anymore. Note that a perfect quantum Zeno effect itself can easily be simulated classically just by using no time evolution at all.
- We have seen that non-classical Hamiltonians can lead to a violation of macrorealism even under the restriction of coarse-grained measurements. Moreover, even environmental decoherence, though leading to macrorealism, does not resolve the problem that in principle no classical laws of motion are able to describe such time evolutions. We have tried to argue

why non-classical Hamiltonians do not appear in nature. One avenue of research would be to investigate the relation between the interactions in our measurement apparatuses and the ones governing the time evolutions of systems. The Hilbert space has no notion of closeness or distance of orthogonal states. We expect that under coarse-grained measurements which bunch together states by whatever notion of closeness or distance *quantumness can be seen only if the system Hamiltonian and the apparatus Hamiltonian connect states differently.*

- We may even conjecture that the *three-dimensionality of our real space* is a necessity under the postulate that an intersubjective classical world arises out of the quantum realm merely due to coarse-graining. This is supported by the fact that the Lie algebras $SU(2)$ and $SO(3)$ are isomorphic.

Quantum randomness and mathematical undecidability:

- In the spirit of the approach in Reference [17], one important question is whether it is possible to *derive Malus's law in the framework of propositions*, i.e. a very particular kind of continuous trade-off between gaining and losing certainty about truth values like in the quantum case. It might be that to this end the necessary number of independent binary functions immediately becomes very large and is related to the number of spatial directions that can be experimentally distinguished, or that one cannot use binary functions any longer.
- Our link between quantum physics and pure mathematics offers an intuitive understanding of randomness in which the question of decidability is more fundamental than about truth. Which other ingredients beyond mathematical undecidability are necessary to fully *reconstruct the quantum formalism* of state vectors in a Hilbert space? Is it possible to derive from this link any other physical phenomena that cannot be derived or understood from the conventional quantum postulates?
- Gödel's incompleteness theorem is known to be equivalent to Turing's halting problem. The latter can be seen as a consequence of the fact that there are more real numbers than natural numbers, or equivalently, not uncountable many Turing machines for countably many possible inputs. Chaitin's version rests on the intuitive observation that a theorem cannot be derived from axioms if the information content of theorem plus axioms is larger than the information content of the axioms itself. Thus, in both cases it is a *mismatch of "resources for answers" and "amount of possible questions"* leading to undecidability—just like in quantum mechanics where randomness is a consequence of the fact that we can measure more things than the state can definitely define. Formalizing this link between Chaitin's and Gödel's original version would strengthen the connection between quantum randomness and mathematical undecidability.

Bibliography

- [1] Agarwal, G. S., Phys. Rev. A **24**, 2889 (1981).
- [2] Agarwal, G. S., Phys. Rev. A **47**, 4608 (1993).
- [3] Arecchi, F. T., E. Courtens, R. Gilmore, and H. Thomas, Phys. Rev. A **6**, 2211 (1972).
- [4] Arndt, M., O. Nairz, J. Voss-Andreae, C. Keller, G. van der Zouw, and A. Zeilinger, Nature **401**, 680 (1999).
- [5] Arnesen, M. C., S. Bose, and V. Vedral, Phys. Rev. Lett. **87**, 017901 (2001).
- [6] Atkins, P. W., and J. C. Dobson, Proc. R. Soc. A **321**, 321 (1971).
- [7] Audenaert, K., J. Eisert, M. B. Plenio, and R. F. Werner, Phys. Rev. A **66**, 042327 (2002).
- [8] Barenco, A., C. H. Bennett, R. Cleve, D. P. DiVincenzo, N. Margolus, P. Shor, T. Sleator, J. Smolin, and H. Weinfurter, Phys. Rev. A **52**, 3457 (1995).
- [9] Bell, J. S., Physics (New York) **1**, 195 (1964).
- [10] Bennett, C. H., and G. Brassard, in: Proceedings of the IEEE International Conference on Computers, Systems, and Signal Processing, Bangalore, India, IEEE, New York, p. 175 (1984).
- [11] Bennett, C. H., G. Brassard, C. Crépeau, R. Jozsa, A. Peres, and W. K. Wootters, Phys. Rev. Lett. **70**, 1895 (1993).
- [12] Bjorken, J. D., and S. D. Drell, *Relativistic Quantum Fields* (McGraw-Hill Book Company, 1965).
- [13] Botero A., and B. Reznik, Phys. Rev. A **70**, 052329 (2004).
- [14] Bouwmeester, D., J.-W. Pan, K. Mattle, M. Eibl, H. Weinfurter, and A. Zeilinger, Nature **390**, 575 (1997).
- [15] Bravyi, S., M. B. Hastings, and F. Verstraete, Phys. Rev. Lett. **97**, 050401 (2006).
- [16] Brukner, Č., and A. Zeilinger, Phys. Rev. Lett. **83**, 3354 (1999).

-
- [17] Brukner, Č., and A. Zeilinger, in: *Time, Quantum and Information*, ed. L. Castell and O. Ischebeck (Springer Berlin, 2004).
- [18] Brukner, Č., V. Vedral, and A. Zeilinger, *Phys. Rev. A* **73**, 012110 (2006).
- [19] Busch, P., M. Grabowski, and P. J. Lahti, *Operational Quantum Physics* (Springer, 1995).
- [20] Calude, C. S., and M. A. Stay, *Int. J. Theor. Phys.* **44**, 1053 (2005).
- [21] Chaitin, G. J., *Int. J. Theor. Phys.* **21**, 941 (1982).
- [22] Chaitin, G. J., *Metamaths. The Quest for Omega* (Atlantic Books London, 2007).
- [23] Clauser, J. F., M. A. Horne, A. Shimony, and R. A. Holt, *Phys. Rev. Lett.* **23**, 880 (1969).
- [24] Coffman, V., J. Kundu, and W. K. Wootters, *Phys. Rev. A* **61**, 052306 (2000).
- [25] Collins, D., N. Gisin, N. Linden, S. Massar, and S. Popescu, *Phys. Rev. Lett.* **88**, 040404 (2002).
- [26] Cramer, M., J. Eisert, M. B. Plenio, and J. Dreißig, *Phys. Rev. A* **73**, 012309 (2006).
- [27] de Chiara, G., Č. Brukner, R. Fazio, G. M. Palma, and V. Vedral, *New. J. Phys.* **8**, 95 (2006).
- [28] Deutsch, D., *Proc. R. Soc. Lond. A* **400**, 97 (1985).
- [29] Duan, L.-M., G. Giedke, J. I. Cirac, and P. Zoller, *Phys. Rev. Lett.* **84**, 2722 (2000).
- [30] Einstein, A., B. Podolsky, and N. Rosen, *Phys. Rev.* **47**, 777 (1935).
- [31] Eisert J., and M. B. Plenio, *Int. J. Quantum Inf.* **1**, 479 (2003).
- [32] Friedman, J. R., V. Patel, W. Chen, S. K. Tolpygo, and J. E. Lukens, *Nature* **406**, 43 (2000).
- [33] Garg, A., and N. D. Mermin, *Phys. Rev. Lett.* **49**, 901 (1982).
- [34] Gasparoni, S., J.-W. Pan, P. Walther, T. Rudolph, and A. Zeilinger, *Phys. Rev. Lett.* **92**, 020504 (2004).
- [35] Gell-Mann, M., and J. B. Hartle, *Phys. Rev. A* **76**, 022104 (2007).
- [36] Ghirardi, G. C., A. Rimini, and T. Weber, *Phys. Rev. D* **34**, 470 (1986).
- [37] Ghosh, S., T. F. Rosenbaum, G. Aeppli, and S. N. Coppersmith, *Nature* **425**, 48 (2003).
- [38] Gisin, N., G. Ribordy, W. Tittel, and H. Zbinden, *Rev. Mod. Phys.* **74**, 145 (2002).
- [39] Gödel, K., *Monatsheft für Mathematik und Physik* **38**, 173 (1931).
- [40] Greenberger, D., M. A. Horne, and A. Zeilinger, in: *Bell's Theorem, Quantum Theory, and Conceptions of the Universe*, ed. M. Kafatos (Kluwer Academic Publishers 1989); electronic version: arXiv:0712.0921v1 [quant-ph].

-
- [41] Hilbert, D., *Gesammelte Abhandlungen*, Vol. 3, (Springer, 1935).
- [42] Hill, S., and W. K. Wootters, Phys. Rev. Lett. **78**, 5022 (1997).
- [43] Holevo, A. S., Probl. Inf. Transm. **9**, 177 (1973).
- [44] Horodecki, P., Phys. Lett. A **232**, 333 (1997).
- [45] Horodecki, P., and A. Ekert, Phys. Rev. Lett. **89**, 127902 (2002).
- [46] Jammer, M., *The Philosophy of Quantum Mechanics: The Interpretations of Quantum Mechanics in Historical Perspective* (John Wiley & Sons, 1974).
- [47] Julsgaard, B., A. Kozhekin, and E. S. Polzik, Nature **413**, 400 (2001).
- [48] Kaszlikowski, D., P. Gnaniński, M. Żukowski, W. Miklaszewski, and A. Zeilinger, Phys. Rev. Lett. **85**, 4418 (2000).
- [49] Kay, K. G., J. Chem. Phys. **79**, 3026 (1983).
- [50] Kim, M. S., J. Lee, and W. J. Munro, Phys. Rev. A **66**, 030301(R) (2002).
- [51] Koashi, M., V. Bužek, and N. Imoto, Phys. Rev. A **62**, 050302(R) (2000).
- [52] Kofler, J., T. Paterek, and Č. Brukner, Phys. Rev. A **73**, 022104 (2006).
- [53] Kofler, J., V. Vedral, M. S. Kim, and Č. Brukner, Phys. Rev. A **73**, 052107 (2006).
- [54] Kofler, J., and Č. Brukner, Phys. Rev. A **74**, 050304(R) (2006).
- [55] Kofler, J., and Č. Brukner, in: *Quantum Communication and Security*, ed. M. Żukowski, S. Kilin, and J. Kowalik (IOS Press 2007).
- [56] Kofler, J., and Č. Brukner, Phys. Rev. Lett. **99**, 180403 (2007).
- [57] Kofler, J., and Č. Brukner, Phys. Rev. Lett. (accepted); arXiv:0706.0668 [quant-ph].
- [58] Kwiat, P. G., K. Mattle, H. Weinfurter, A. Zeilinger, A. V. Sergienko, and Y. Shih, Phys. Rev. Lett. **75**, 4337 (1995).
- [59] Lee, J., M. S. Kim, Y. J. Park, and S. Lee, J. Mod. Opt. **47**, 2151 (2000).
- [60] Leggett, A. J., and A. Garg, Phys. Rev. Lett. **54**, 857 (1985).
- [61] Leggett, A. J., in: *Time's Arrows Today*, ed. S. F. Savitt (Cambridge University Press, 1995).
- [62] Leggett, A. J., J. Phys.: Cond. Mat. **14**, R415 (2002).
- [63] Mermin, N. D., Phys. Rev. D. **22**, 356 (1980).
- [64] Mermin, N. D., Phys. Rev. Lett. **65**, 1838 (1990).

-
- [65] Michler, M., K. Mattle, H. Weinfurter, and A. Zeilinger, *Phys. Rev. A* **72**, 1209(R) (1996).
- [66] Misra, B., and E. C. G. Sudarshan, *J. Math. Phys.* **18**, 756 (1977).
- [67] Nielsen, M. A., and I. L. Chuang, *Quantum Computation and Quantum Information* (Cambridge University Press, 2000).
- [68] O'Brien, J. L., G. J. Pryde, A. G. White, T. C. Ralph, and D. Branning, *Nature* **426**, 264 (2003).
- [69] Pan, J.-W., D. Bouwmeester, M. Daniell, H. Weinfurter, and A. Zeilinger, *Nature* **403**, 515 (2000).
- [70] Paterek, T., R. Prevedel, J. Kofler, P. Klimek, M. Aspelmeyer, A. Zeilinger, and Č. Brukner, submitted (2008).
- [71] Paternostro, M., W. Son, and M. S. Kim, *Phys. Rev. Lett.* **92**, 197901 (2004).
- [72] Paternostro, M., M. S. Kim, E. Park, and J. Lee, *Phys. Rev. A* **72**, 052307 (2005).
- [73] Penrose, R., *Gen. Rel. Grav.* **28**, 581 (1996).
- [74] Peres, A., *Quantum Theory: Concepts and Methods* (Kluwer Academic Publishers, 1995).
- [75] Peres, A., *Phys. Rev. Lett.* **77**, 1413 (1996).
- [76] Pittman, T. B., B. C. Jacobs, and J. D. Franson, *Phys. Rev. Lett.* **88**, 257902 (2002).
- [77] Poulin, D., *Phys. Rev. A* **71**, 022102 (2005).
- [78] Radcliffe, J. M., *J. Phys. A: Gen. Phys.* **4**, 313 (1971).
- [79] Raussendorf, R., D. E. Browne, and H. J. Briegel, *Phys. Rev. A* **68**, 022312 (2003).
- [80] Retzker, A., J. I. Cirac, and B. Reznik, *Phys. Rev. Lett.* **94**, 050504 (2005).
- [81] Reznik, B., *Found. of Phys.* **33**, 167 (2003).
- [82] Schliemann, J., *Phys. Rev. A* **72**, 012307 (2005).
- [83] Schrödinger, E., *Die Naturwissenschaften* **48**, 807 (1935).
- [84] Schwabl, F., *Advanced Quantum Mechanics* (Springer, 2003).
- [85] Serafini, A., G. Adesso, and F. Illuminati, *Phys. Rev. A* **71**, 032349 (2005).
- [86] Shchukin E., and W. Vogel, *Phys. Rev. Lett.* **95**, 230502 (2005).
- [87] Sherson, J., and K. Mølmer, *Phys. Rev. A* **71**, 033813 (2005).
- [88] Simon, R., *Phys. Rev. Lett.* **84**, 2726 (2000).

-
- [89] Sørensen, A., L.-M. Duan, J. Cirac, and P. Zoller, *Nature* **409**, 63 (2001).
- [90] Spekkens, R., *Phys. Rev. A* **75**, 032110 (2007).
- [91] Turing, A. M., *Proc. Lond. Math. Soc.* **42**, 230 (1936).
- [92] Vedral, V., *New J. Phys.* **6**, 102 (2004).
- [93] Vidal, G., and R. F. Werner, *Phys. Rev. A* **65**, 032314 (2002).
- [94] von Weizsäcker, C. F., *Aufbau der Physik* (Deutscher Taschenbuch Verlag, 2002); English version: von Weizsäcker, C. F., *Construction of Physics*, ed. T. Görnitz and H. Lyre (Springer Netherlands, 2007).
- [95] Walther, P., and A. Zeilinger, *Phys. Rev. A* **72**, 010302(R) (2005).
- [96] Wang, X., and K. Mølmer, *Eur. Phys. J. D* **18**, 385 (2002).
- [97] Weinfurter, H., *Europhys. Lett.* **25**, 559 (1994).
- [98] Wiesniak, M., V. Vedral, and Č. Brukner, *New J. Phys.* **7**, 258 (2005).
- [99] Wigner, E. P., *Am. J. Phys.* **38**, 1005 (1970).
- [100] Wolf, M. M., F. Verstraete, M. B. Hastings, and J. I. Cirac, *Phys. Rev. Lett.* **100**, 070502 (2008).
- [101] Yaffe, L. G., *Rev. Mod. Phys.* **54**, 407 (1982).
- [102] Zeilinger, A., *Found. Phys.* **29**, 631 (1999).
- [103] Zurek, W. H., *Phys. Today* **44**, 36 (1991).
- [104] Zurek, W. H., *Rev. Mod. Phys.* **75**, 715 (2003).
- [105] Życzkowski, K., P. Horodecki, A. Sanpera, and M. Lewenstein, *Phys. Rev. A* **58**, 883 (1998).

Curriculum vitae

Personal Information

Name	Johannes Kofler
Date and place of birth	June 16, 1980, Linz, Austria
Citizenship	Austrian

Professional History

Since 01/2007	<i>DOC Fellow</i> Austrian Academy of Sciences
01/2005 – 12/2006	<i>Research Assistant</i> Faculty of Physics, University of Vienna & Institute for Quantum Optics and Quantum Information (IQOQI), Austrian Academy of Sciences
03/2004 – 06/2004	<i>Scientific co-worker</i> Institute for Theoretical Physics & Institute for Applied Physics, University of Linz

Education

Since 03/2005	Doctoral studies of Natural Sciences (University of Vienna)
10/1999 – 11/2004	Diploma studies of Technical Physics (University of Linz)
07/1998 – 02/1999	Obligatory military service (Villach and Klagenfurt)
09/1990 – 06/1998	Grammar school (Linz and Klagenfurt)

Honors

2007	DOC Fellowship (Austrian Academy of Sciences)
2004	Wilhelm-Macke-Prize (University of Linz)
2003	Merit scholarship (University of Linz)
2002	Merit scholarship (University of Linz)
2001	Merit scholarship (University of Linz)